

PHYSICS CONFERENCE

TIM 25

**FACULTY OF PHYSICS
WEST UNIVERSITY OF TIMISOARA**

TIMISOARA, 29-31 MAY 2025

ABSTRACT BOOKLET

Contents

PL-01	5
PL-02	6
PL-03	7
PL-04	8
PL-05	10
PL-06	11
PL-07	12
PL-08	13
TCP-I01	15
TCP-I02	16
TCP-O01	17
TCP-O02	18
TCP-O03	19
TCP-O04	20
TCP-O05	21
TCP-O06	22
TCP-O07	23
TCP-O08	24
TCP-O09	26
TCP-O10	28
TCP-O11	29
TCP-O12	30
TCP-O13	31
TCP-O14	32
TCP-P01	33
TCP-P02	34
TCP-P03	35
CMP-I01	38
CMP-I02	39
CMP-O01	40
CMP-O02	41
CMP-O03	42
CMP-O04	43
CMP-O05	44
CMP-P01	46
CMP-P02	47
CMP-P03	49
CMP-P04	50
CMP-P05	51
CMP-P06	52
API-I01	54
API-I02	56

API-O01	57
AIP-O02	58
API-O03	59
API-O04	60
API-O05	61
AIP-O06	62
API-O07	64
API-O08	65
API-O09	66
API-P01	68
API-P02	69
API-P03	70
API-P04	71
API-P05	72
API-P06	73
API-P07	74
API-P08	75
API-P09	76
API-P10	77
API-P11	78
API-P12	79
API-P13	80
API-P14	81
API-P15	83
API-P16	84
API-P17	86
API-P18	87
API-P19	88
API-P20	90
API-P21	91
API-P22	92
API-P23	93
API-P24	95
API-P25	96
API-P26	97
API-P27	98
API-P28	100
EP-O01	102
EP-O02	103
EP-O03	104
EP-O04	105
EP-O05	106
EP-P01	107

PLENARY PRESENTATIONS

EXTREME LIGHT INFRASTRUCTURE – NUCLEAR PHYSICS STATUS UPDATE

For the ELI-NP team Ioan Dancus

Extreme Light Infrastructure - Nuclear Physics, IFIN-HH, 30 Reactorului Street, 077125 Magurele, Romania

The Extreme Light Infrastructure – Nuclear Physics (ELI-NP) is a state-of-the-art European research facility located in Bucharest-Măgurele, Romania. It comprises two primary high-performance systems: a high-intensity laser and a tunable, high-brilliance gamma beam source [1,2].

Since early 2020, the facility has delivered laser pulses at nominal powers of 100 TW, 1 PW, and 10 PW to experimental areas under the user access program. The High Power Laser System (HPLS) at ELI-NP currently operates as the most powerful laser system worldwide, routinely generating 10 PW pulses in experimental configurations [3,4].

IFIN-HH/ELI-NP is also managing two major initiatives: “Medical Applications of High-Power Lasers – Dr. Laser” and the Centre for High Power Optics.

This presentation will provide a technical overview of the ELI-NP infrastructure, its capabilities, and the current status of ongoing research and development activities.

Acknowledgements: This work was supported by the Extreme Light Infrastructure Nuclear Physics (ELI-NP) Phase II, a project co-financed by the Romanian Government and the European Union through the European Regional Development Fund the Competitiveness Operational Program 065208-5 (1/07.07.2016, COP, ID 1334), by the PN 23 21 01 05 and the LAS-COMB ELI-Ro contract funded by the Romanian Ministry of Research, Innovation and Digitalization and the IOSIN 2023 funds for research infrastructures of national interest. The work was partially supported by the European Union and the Romanian Government within the Romanian Health Program of the project “Medical applications of high-power lasers - Dr. Laser” Cod SMIS: 326475.

Keywords: high power lasers, ultra-high intensity lasers, scientific facilities.

References:

- [1] S. Gales, et al., The extreme light infrastructure-nuclear physics (eli-np) facility: new horizons in physics with 10 pw ultra-intense lasers and 20 mev brilliant gamma beams. *Reports on Progress in Physics*, 81(9), (2018)
- [2] K. A. Tanaka, et al., Current status and highlights of the ELI-NP research program, *Matter and Radiation at Extremes* 5(2) 024402 (2020)
- [3] F. Lureau et al., High-energy hybrid femtosecond laser system demonstrating 2×10 PW capability, *High Power Laser Science and Engineering*, 8, E43 (2020)
- [4] C. Radier, et al., 10 pw peak power femtosecond laser pulses at ELI-NP, *High Power Laser Science and Engineering*, 10, (2022)

PHYSICS-INFORMED NEURAL NETWORKS FOR PDES: A SURVEY FROM DIGITAL TO PHOTONIC APPROACHES

Péter Kovács¹

¹HUN-REN Wigner Research Centre for Physics, Konkoly-Thege Miklós út 29-33, 1121 Budapest, Hungary

Physics-Informed Neural Networks (PINNs) have emerged as a powerful class of machine learning models for solving ordinary and partial differential equations (ODEs and PDEs), integrating physical laws directly into the training process. These models have been successfully applied to a wide range of problems in physics and engineering, including heat flow, electrostatics, and fluid dynamics, using well-known equations such as the heat, Poisson, and Navier-Stokes equations. To date, most of this work has focused on classical digital neural networks.

Recently, there has been growing interest in exploring alternative computational paradigms for PINNs. In particular, continuous-variable quantum neural networks (CVQNNs) have opened the door to quantum physics-informed neural networks (QPINNs), where quantum systems are trained to respect physical constraints. At the same time, classical photonic neural networks - systems that use light instead of electricity to process information - are attracting attention for their potential for fast and energy-efficient computation. Although photonic neural networks have shown promise in tasks such as image classification, their application to solving differential equations remains largely unexplored.

This talk will review recent developments in these three approaches – digital, photonic, and quantum photonic – and discuss how each can be used to solve representative PDEs, such as the heat equation or the Burgers equation. Rather than focusing on a single result, we aim to give a broad overview of current methods and highlight how different computational architectures approach physics-informed learning.

Keywords: Physics-Informed Neural Networks, Machine Learning, Partial Differential Equations

**MODELING LASER-DRIVEN TRANSIENT PHASE
OSCILLATIONS
OBSERVED BY ULTRAFAST TEM**

Laurențiu Stoleriu and Denisa Colțuneac

Faculty of Physics and CARPATH Centre, "Alexandru Ioan Cuza" University of Iași, Romania

Ultrafast transmission electron microscopy (UTEM) was used [1, 2] to precisely probe the length changes of individual switchable spin crossover (SCO) nanoparticles induced thermally by nanosecond laser pulses. This allows revealing of the mechanisms of spin switching, leading to the macroscopic expansion of SCO materials.

After exposure to nanosecond laser pulses, the particles exhibit considerable length oscillations during and after their expansion. The vibration period of 50–100 ns is of the same order of magnitude as the time that the particles need for a transition from the low-spin to the high-spin state.

The observations are explained in the framework of the mechano-elastic model where elastic and thermal coupling between the molecules within a crystalline spin crossover particle governs the phase transition between the two spin states. The experimentally observed length oscillations are in agreement with the calculations, and it is shown that the system undergoes repeated transitions between the two spin states until relaxation in the high-spin state occurs due to energy dissipation.

Spin crossover particles are, therefore, a unique system where a resonant transition between two phases occurs in a phase transformation of first order.

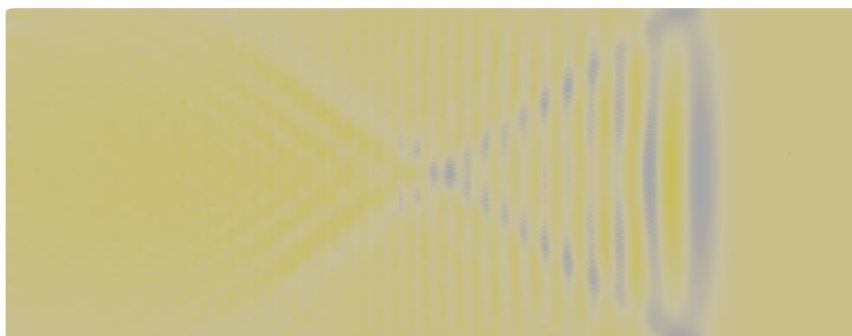


Figure 1: Phase transition induced acoustic wave propagation in a nanocrystalline SCO particle.

Keywords: spin-crossover materials, mechano-elastic model.

References:

- [1] Y. W. Hu, M. Picher, M. Palluel, N. Daro, E. Freysz, L. Stoleriu, C. Enachescu, G. Chastanet, F. Banhart, *Small* 19(39), 2303701 (2023)
- [2] Y. W. Hu, M. Picher, N. M. Tran, M. Palluel, L. Stoleriu, N. Daro, S. Mornet, C. Enachescu, E. Freysz, F. Banhart, G. Chastanet, *Adv. Mater.* 33(52), 2105586 (2021)

LUMINESCENCE AND FARADAY ROTATION PROPERTIES OF Tb₂O₃ AND Tb:Y₂O₃ SINGLE CRYSTALS

Philippe Veber¹, Grégory Gadret², Yannick Guyot³, Gabriel Bușe¹, Richard Moncorgé³
and Matias Velázquez^{4,*}

¹Faculty of Physics, West University of Timisoara, Bd. Vasile Parvan 4, Timisoara, 300223, Romania

²Laboratoire Interdisciplinaire Carnot de Bourgogne, UMR 6303 CNRS-Université de Bourgogne, Faculté des Sciences Mirande, 9 avenue Alain Savary, BP 47 870, 21078 Dijon cedex, France

³Université de Lyon, CNRS, Institut Lumière Matière, 10 rue Ada Byron, F-69622, Villeurbanne, France

⁴Univ. Grenoble Alpes, CNRS, Grenoble INP (Institute of Engineering Univ. Grenoble Alpes), SIMAP, 38000 Grenoble, France

Over the last years, many Tb-based crystals (TGG, TAG, TSLAG, TbVO₄, CALTO, STB, LTB, TbCOB, TLF, etc.), were obtained and investigated for their Faraday rotation property, noticeably in the near infrared spectral range, and their utilization in high intensity linearly polarized laser chains to protect the optics from deleterious longitudinally scattered and reflected laser lights [1–4]. Indeed, when such a transparent material is submitted to a longitudinal magnetic field and when a linearly polarized light beam is propagating forward through it, its polarization is rotated in a direction (left or right) by an angle θ_F which is proportional to the applied magnetic field H and the thickness t of the material according to the expression $\theta_F = k_V \times t \times H$, where k_V is the Verdet constant. This effect is also crucial for several high-performance photonic devices such as in telecommunications, light detection and ranging, and even quantum platforms. Crystal-based optical isolators and circulators are key components for high-performance optical systems, especially for demanding applications such as coherent telecom transceivers, optical switches for data centers, light detection and ranging (LiDAR) systems or quantum interconnects where fleeting quantum states transfer between different parts of quantum communication platforms [5]. Due to their larger transparency, as compared with 3d transition metal-based materials, Tb-based crystals are prospective materials in the visible spectral range for more compact implementations of high-performance photonic circuits, which could make their way inside integrated photonic engines.

Heavily-doped and fully concentrated 2.78 % Tb:Y₂O₃ and Tb₂O₃ single crystals with high optical quality and very low levels of impurities have been grown and studied for their luminescence and Faraday rotation properties. Absorption, emission and fluorescence decay measurements performed vs excitation wavelength and temperature and their confrontation with Judd-Ofelt and crystal-field calculations show the contributions of two types of luminescent centers: dominant ones with a ⁵D₄ emission lifetime of 23 μ s corresponding to coupled near-neighbor Tb³⁺ ions, all in C₂ symmetry sites, and minority ones with a ⁵D₄ emission lifetime of about 2 ms corresponding to coupled Tb³⁺ ions in C₂ and C_{3i} near-neighbor symmetry sites. Faraday rotation measurements confirm Tb₂O₃ as the Tb-based Faraday crystalline material with the largest ever measured Verdet constant, at all temperatures and from the visible to the near-infrared. They also show that the dominant luminescent centers contribute more particularly to this large Verdet constant thanks to a favorable crystal-field splitting of their ⁷F₆ ground multiplet and also to the contributions of both types of spin-allowed and spin-forbidden 4f-5d absorption bands.

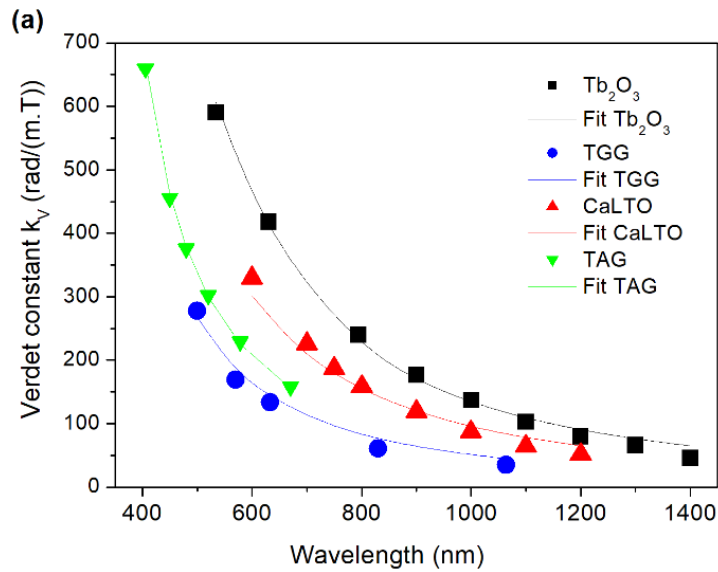


Figure 1: Absolute values of the Verdet constant versus wavelength of Tb_2O_3 , CaLTO, TGG, and TAG crystals along with fits of data values.

Keywords: Tb_2O_3 , luminescence, Faraday rotation.

References:

- [1] M. J. Weber, *Handbook of Optical Materials*, CRC Press, 2003.
- [2] D. Rytz, K. Dupré, A. Gross, Ch. Liebald, M. Peltz, P. Pues, S. Schwung, V. Wesemann, *Rare-Earth Chemistry*, De Gruyter Publ., Chap 4.4, pp. 415–438 (2020).
- [3] M. Mei, L. L. Cao, Y. He, R. R. Zhang, F. Y. Guo, N. F. Zhuang, J. Z. Chen, *Adv. Mater. Res.* **306**, 1722 (2011).
- [4] Y. Xu, M. Duan, *Phys. Rev. B* **46** (18), 11636–11641 (1992).
- [5] J. Lapointe, C. Coia, A. Dupont, *et al.*, *Nat. Photon.* **19**, 248–257 (2025).

RECOMMENDER SYSTEM FOR DISCOVERY OF NEW INORGANIC COMPOUNDS

Isao Tanaka^{1,2}

¹Office of Research Acceleration, Kyoto University (Yoshida, Sakyo, Kyoto 606-8501 JAPAN)

²Japan Fine Ceramics Center (Atsuta, Nagoya, 456-8587, Japan)

In this study, we explore the development of a recommender system designed to efficiently identify chemically relevant compositions (CRCs) of previously unknown inorganic ionic compounds [1,2]. Utilizing the Inorganic Crystal Structure Database (ICSD), our tensor-based recommender system evaluates over 23 billion chemical compositions across five-element ionic systems. Remarkably, our approach achieves high success rates without relying on prior knowledge or first-principles calculations. The recommendations generated have led to the successful synthesis of novel oxides and nitrides [3,4], highlighting the system's efficacy in accelerating materials discovery. Additionally, our recommender system predicts optimal processing conditions for these new compounds by leveraging a dataset derived from parallel synthesis experiments [5-7]. This methodology not only enhances the discovery pipeline but also sets a new standard for computational materials science, combining vast data handling with practical experimental applications.

Keywords: data-driven discovery, first principles calculations, ceramics

References:

- [1] A. Seko *et al*, *Phys. Rev. Mater.* **2**, 013805 (2018).
- [2] A. Seko *et al.*, *J Chem Phys* **148**, 7, (2018).
- [3] K. Suzuki *et al.*, *J Mater Chem A* **8**, 11582 (2020).
- [4] Y. Koyama *et al.*, *J. Chem. Phys.* **154**, 224117 (2021).
- [5] H. Hayashi *et al*, *Chem. Mater.* **31**, 9984 (2019).
- [6] H. Hayashi *et al*, *J. Am. Ceram. Soc.*, **105** 853 (2021).
- [7] H. Hayashi *et al*, *npj Comp. Mater.*, **8** 217 (2022).

PL-06

EXPLORING THE QUARK–GLUON PLASMA WITH ALICE

Alexandru Florin Dobrin (for the ALICE Collaboration)

Institute of Space Science – INFLPR Subsidiary, 409 Atomistilor Street, Magurele, Ilfov, 077125

Measurements of two- and multi-particle azimuthal correlations provide valuable information on the properties of the system created in collisions of hadrons and nuclei at high energy. In this talk, the ALICE results for inclusive and identified particle azimuthal correlations are reported in different collision systems after a brief introduction of the concepts of a heavy-ion collision.

Keywords: ALICE, azimuthal correlations

Recent theoretical predictions [1] suggest that nanometer-sized skyrmions can encode quantum information in their helicity degree of freedom, which can be controlled using electric or magnetic fields over a broad operating range, providing significant anharmonicity. These skyrmions are stabilized by competing exchange interactions, and crucially, in the absence of the Dzyaloshinskii–Moriya interaction (DMI), which would otherwise lock the helicity degree of freedom. However, traditional skyrmionic spintronic applications primarily rely on DMI mechanisms and their control within carefully designed architectures [2]. To fulfill this criterion and exploit the existing expertise in skyrmionic materials and their applications in information technologies, we explored both classic and quantum skyrmionic states stabilized by DMI. Our theoretical approach utilizes a quantum exact diagonalization framework, that can be applied to several 2D spin lattice models, geometries and symmetries.

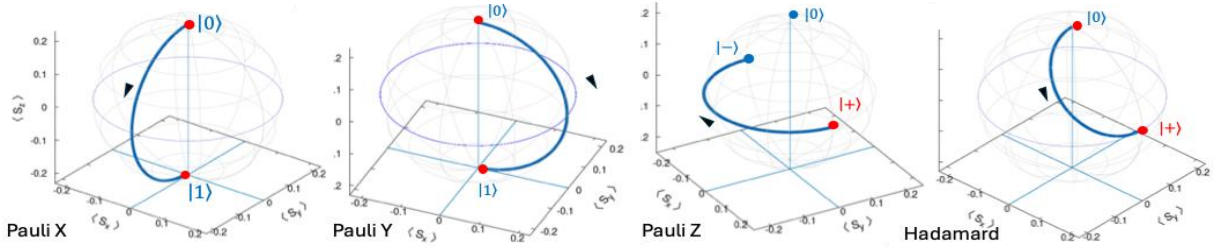


Figure 1: Quantum gates based on quantum skyrmions

We show that, under open boundary conditions, classic skyrmions emerge, similar to those described by micromagnetic tools. However, a stable and robust quantum skyrmionic phase can be realized when periodic boundary conditions are applied, within a specific region of the phase diagram determined by parameters such as DMI, direct exchange, anisotropy, and magnetic field. We demonstrate that these quantum skyrmions can be manipulated using external periodic and static field perturbations, enabling the construction of Pauli-X, Y, Z, and Hadamard-gate quantum logical gates (see Figure 1). Furthermore, by comparing the results from the 2D lattice model to those from 1D Ising spin models with DMI, we highlight the detrimental impact of DMI on the coherent precessional manipulation of quantum skyrmionic states. We also investigate the quantum quenching phenomena induced by DMI in both 2D and 1D spin lattices, under both periodic and open boundary conditions. Our findings offer promising paths for the development of new skyrmionic qubit devices for quantum spintronic applications, building on existing knowledge of DMI-controlled skyrmionic materials.

Keywords: quantum skyrmions, qubits, quantum spintronics.

References

- [1] C. Psaroudaki et al, Phys. Rev. Lett., 2021, 127, 067201.
- [2] A. Fert et al, Nature Reviews Materials, 2017, 2, 17031.

A PERSPECTIVE ON MAGNETIC INTERACTIONS IN ASSEMBLIES OF MAGNETIC NANO-OBJECTS

Victor Kuncser

National Institute of Materials Physics, Atomistilor 405A, 77125, Magurele, Ilfov, Romania

Assemblies of interacting magnetic nano-objects can be formed either in a fluid media or in a solid matrix, with the involved magnetic interactions having direct implications on the magnetic response of the system. A brief overview of different types of magnetic interactions possible to appear inside or inter magnetic nano-objects of different dimensionalities will be comparatively provided. In the first case, specific ferrofluids can be formed with wide applications from civil engineering to bio-medicine [1]. The influence of long-range magnetic dipolar interactions and possible organization of the magnetic clusters on magnetic relaxation phenomena and implicitly on the specific absorption rate of ferrofluids of different volume fractions will be discussed. In the second case, the matrix may intermediate the magnetic interactions among the magnetic nano-entities, but also influence their shape and configuration. Various examples will be provided, starting from the induced organization of magnetic nanowires in different bidimensional templates to the auto-organization of magnetic nanoclusters inside the thickness of a metallic film or on the surface of a metallic film (Figure 1). The large variety of the obtained magnetic dimensionalities and magnetic anisotropies and their influence on the electron transport properties (magnetoresistance effects) of the overall complex system will be discussed.

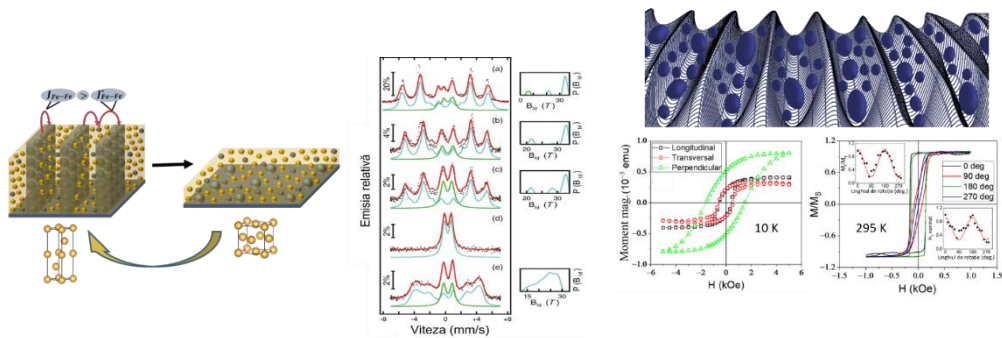


Figure 1: Organization of Fe clusters in Au 2D matrix (left side) and Fe-Co clusters on trenced Mo substrates (right side)

Keywords: magnetic interactions, assemblies of magnetic nano-objects, functionalities

References:

[1] V. Socoliuc, MV Avdeev, V. Kuncser, R. Turcu, E. Tombacz, L. Vekas, *Nanoscale* **14**(13) 4386 (2022)

**THEORETICAL AND COMPUTATIONAL
PHYSICS
(TCP)**

ARTIFICIAL INTELLIGENCE BASED AUTOMATIC ADAPTIVE QUADRATURE

Gheorghe Adam^{1,2} and Sanda Adam^{1,2}

¹*Horia Hulubei National Institute for Physics and Nuclear Engineering (IFIN-HH), 30 Reactorului, Măgurele - Bucharest, 077125, Romania*

²*Laboratory of Information Technologies, Joint Institute for Nuclear Research, 6, Joliot Curie St., 141980 Dubna, Moscow Region, Russia*

The development of a conceptual frame enabling the implementation of an *artificial intelligence* (AI) driven *automatic adaptive quadrature* (AAQ) of the one-dimensional Riemann integral (RI) is discussed.

There are two basic pillars, which drive the AI-AAQ solution:

(i) The *subrange decision tree* analysis of the RI features that are fundamental for the choice of the best conceivable quadrature rule at the initial stage of the AAQ.

(ii) Solution refinement through *Bayesian inferences*, which follow from the *local* analysis of RI features at the knots of the quadrature sum decided at the step (i).

The *inheritance* of data got over the *parental chain* of the *current subrange* enhances the reliability of the local Bayesian inference.

While the inception and refinement of the AAQ solution through subrange subdivision follows an *up-down approach*, which enables AAQ solution improvement by subrange subdivision, both AI analysis steps follow a *down-up way*, either at an *infinitesimal scale* (step (i)), or at a *finite but finer scale* (step (ii)).

The AI-AAQ method preserves all the perennial features resolved within the classical QUADPACK approach [1], as well as the features stemming from the *a priori* knowledge of the RI properties [2]. At the same time, it eliminates the *fragility* of the automatic decisions driving the path to the solution within the *state-of-the-art* QUADPACK package solutions of the Riemann integrals.

Keywords: artificial intelligence, automatic adaptive quadrature, QUADPACK package, Bayesian inferences, numerical integration, Riemann integrals.

References:

[1] R. Piessens, E. de Doncker-Kapenga, C.W. Ueberhuber, D.K. Kahaner, QUADPACK, *a subroutine package for automatic integration*, Springer, Berlin, (1983).

[2] Gh. Adam and S. Adam, *A priori* knowledge driven input to Bayesian two-rule automatic adaptive quadrature, *AIP Conf. Proc.* **3181**, 050002-1–050002-7 (2024)

<https://doi.org/10.1063/5.0215640>

CHIRAL MAGNETIC EFFECT ENHANCEMENT AT LOWER COLLISION ENERGIES

Sebastian Griener¹, Sergio Morales Tejera² and Pau G. Romeu³

¹ *Center for nuclear theory, Department of physics and astronomy, Stony Brook University, Stony Brook, New York, 11794-3800 USA*

² *Department of physics, West University of Timisoara. Bd. Vasile Parvan 4, Timisoara 300223, Romania.*

³ *Instituto de Física Teórica UAM/CSIC, c/ Nicolás Cabrera 13-15, Universidad Autónoma de Madrid, Campus de Cantoblanco, 28049 Madrid, Spain.*

The Chiral Magnetic Effect (CME) is a macroscopic transport phenomenon, whose origin lies in the anomalous chiral symmetry. It manifests itself as the generation of an electric current in a chiral plasma under a magnetic field. Such an effect can be generated in heavy ion collisions, and its measurement could serve as an indirect observation of the non-trivial topology of non-abelian gauge fields. I will review the next-to-simplest holographic model in which the chiral magnetic effect can be studied, discussing previous results as well as the most recent findings [1,2]. In particular, we extend previous holographic studies of the CME by incorporating a time-dependent magnetic field. Interestingly, the integrated chiral magnetic current can exhibit a non-monotonic dependence on the collision energy. Our results suggest that the CME signal is enhanced at collision energies below 200 GeV.

Keywords: gauge-gravity duality, anomalous transport, quark-gluon plasma.

References:

[1] J. K. Ghosh, S. Griener, K. Landsteiner, S. Morales-Tejera. Phys. Rev. D 104 (2021) 4, 046009.

[2] S. Griener, S. Morales-Tejera, P. G. Romeu. arXiv:2503.10593 [hep-ph].

SIGNATURES OF LOCAL ACCELERATION OF QUARK-GLUON PLASMA IN THE DILEPTON PRODUCTION

Victor E Ambruş¹, Aritra Bandyopadhyay¹, Maxim N Chernodub^{2,1}
and Moulindu Kundu¹

¹Department of Physics, West University of Timișoara, Bd. Vasile Pârvan 4, Timișoara
²Institut Denis Poisson, CNRS - UMR 7013, Université de Tours, 37200 France

Dilepton emissions represent a key probe for characterising the Quark-Gluon Plasma (QGP). A central role in computing dilepton yields is played by the imaginary part of the electromagnetic current-current correlation, or equivalently, of the photon polarisation tensor [1]. In this work, we investigate the influence of local acceleration on dilepton production. We compute this quantity in a thermal medium subject to acceleration. We assume the acceleration is sufficiently small so that it can be treated as a perturbation. We employ the thermal Dirac propagator in an accelerated frame, recently formulated within the imaginary-time formalism in [2]. Using a small acceleration expansion, we evaluate the imaginary part of the photon polarization tensor (see Figure 1). Our perturbative results are then compared with the case of vanishing acceleration, allowing us to clearly isolate and identify the effects introduced by local acceleration.

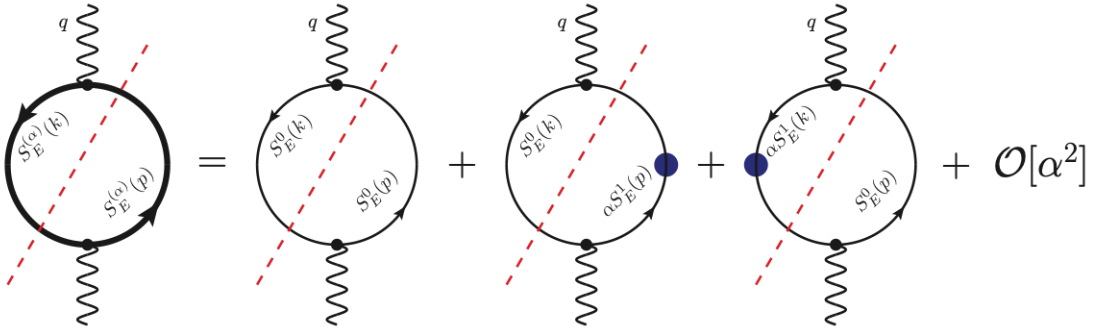


Figure 1: Imaginary part of one-loop photon polarization in a hot and weakly accelerated medium shown through the expansion of the order of the acceleration. S_E^0 denotes the Euclidean thermal Dirac propagator at vanishing acceleration and αS_E^1 denotes the first order correction in finite acceleration.

Keywords: Dilepton production rate, Accelerated medium, Quark gluon plasma.

References:

- [1] L. D. McLerran and T. Toimela, Phys. Rev. D 31, 545 (1985).
- [2] V. E. Ambruş and M. N. Chernodub, Phys. Lett. B 855, 138757 (2024).

A LATTICE BOLTZMANN MODEL USING THERMAL ENSKOG-VLASOV THEORY TO SIMULATE PHASE SEPARATION

Sergiu Busuioc¹ and Victor Sofonea²

¹West University of Timișoara, Blvd. V. Parvan 4, Timisoara 300223, Timis, Romania

²Center for Fundamental and Advanced Technical Research, Romanian Academy Bd. Mihai Viteazul 24, 300223, Timișoara, Romania

An Enskog-Vlasov finite-difference Lattice Boltzmann (EV-FDLB) for liquid-vapor systems with variable temperature is introduced. The model involves both the simplified Enskog collision operator and the self-consistent force field which accounts for the long-range interaction between the fluid particles. Full-range Gauss-Hermite quadratures were used for the discretization of the momentum space. The numerical solutions of the Enskog-Vlasov equation obtained employing the EV-FDLB model and the Direct Simulation Monte Carlo (DSMC)-like particle method (PM) are compared. Reasonable agreement is found between the two approaches when simulating the liquid-vapor phase separation and the liquid slab evaporation.

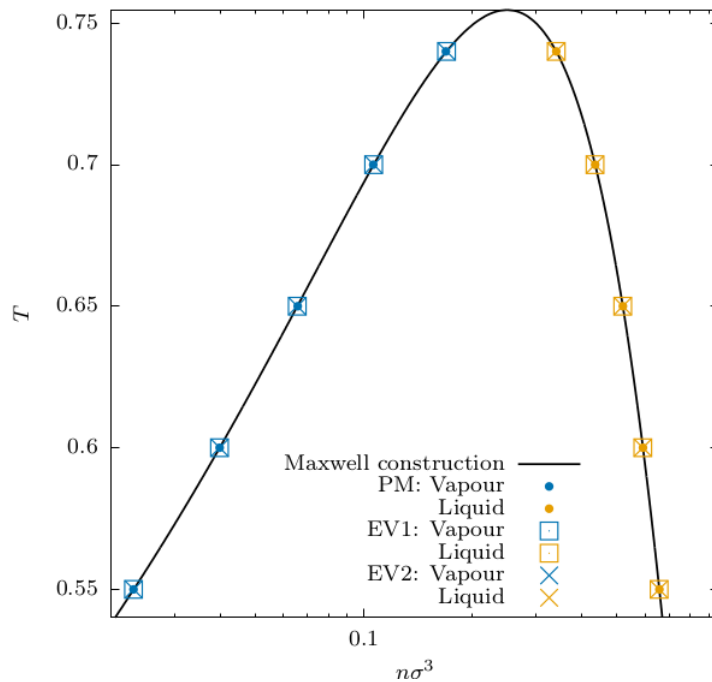


Figure 1: Phase diagram: the continuous line was traced according to the Maxwell construction, the symbols denote the values calculated numerically using the PM, as well as the EV-FDLB procedures.

Keywords: Lattice Boltzmann, Enskog-Vlasov, multiphase flow.

References:

[1] Busuioc, Sergiu, and Victor Sofonea. "Thermal Enskog-Vlasov Lattice Boltzmann model with phase separation." arXiv:2503.15187 (2025).

FIRST-PRINCIPLES CALCULATIONS OF ELECTRONIC PROPERTIES OF OPTICAL MATERIALS

Mikhail G. Brik^{1,2,3,4}, M. Piasecki⁵, N.M. Avram^{4,6}

¹ School of Optoelectronic Engineering & CQUPT-BUL Innovation Institute, Chongqing University of Posts and Telecommunications, Chongqing 400065, China

² Centre of Excellence for Photoconversion, Vinča Institute of Nuclear Sciences - National Institute of the Republic of Serbia, University of Belgrade, Belgrade, Serbia, brik@vin.bg.ac.rs

³ Institute of Physics, University of Tartu, W. Ostwald Str. 1, Tartu 50411, Estonia, mikhail.brik@ut.ee

⁴ Academy of Romanian Scientists, 3 Ilfov, 050044, Bucharest, Romania

⁵ Faculty of Science and Technology, Jan Długosz University, Armii Krajowej 13/15, PL-42200 Częstochowa, Poland

⁶ Department of Physics, West University of Timisoara, Bd.V. Parvan No. 4, 300223, Timisoara, Romania

Crystalline solid materials doped with the transition metal and rare earth ions are widely used in various optical applications. Complicated interplay of the host's structural and electronic properties, on one hand, and impurity ion's electronic properties, on the other hand, determines perspectives and limitations of performance of optical materials. Incorporation of those impurity ions into crystal lattice is accompanied by appearance of extra energy levels associated with these ions in the band gap; location of those energy levels in respect to the host's valence and conduction bands is of paramount importance for performance of optical materials and devices based on them.

In the present paper we present results of the first-principles calculations of the structural and electronic properties for several functional materials, such as $\text{Al}_2\text{O}_3:\text{Ti}^{3+}$ [1], $\text{YAlO}_3:\text{Ce}^{3+}$ [2], Rb_2MF_6 ($M=\text{Si}, \text{Ni}, \text{Pd}$) [3]. Special attention is paid to the location of the impurity ion's ground state in the host's band gap, microscopic crystal field effects and influence of hydrostatic pressure on the structural, electronic, elastic and thermodynamic properties of the above-mentioned materials.

Keywords: first-principles calculations, optical materials, transition metal and rare earth ions, electronic properties.

References:

[1] M.G. Brik, *Physica B* **532**, 178-183 (2018).

[2] M.G. Brik, C.-G. Ma, M. Piasecki, A. Suchocki, *Opt. Mater.* **113**, 110843 (2021).

[3] M.G. Brik, M. Piasecki, N.M. Avram, *Physica Status Solidi B* **259**, 2100607 (2022).

COLLECTIVE DYNAMICS IN HEAVY AND LIGHT-ION COLLISIONS

Victor E. Ambruş

*Department of physics, West university of Timisoara,
Bd. Vasile Pârvan 4, Timișoara 300223, România*

The buildup of collective flow in relativistic heavy-ion collisions is routinely described using relativistic hydrodynamics. As an effective theory for high-multiplicity, near-equilibrium fluids, the applicability of hydrodynamics in small systems is questionable. We scrutinize this by comparing event-by-event simulations in kinetic theory and viscous hydrodynamics in large (AuAu and PbPb) and small (OO) systems. As shown in the left panel of Fig. 1, hydrodynamics deviates from kinetic theory at low system opacities γ , when the system is either small, has low energy or the plasma is weakly-coupled [1].

We also demonstrate that the sensitivity to the interaction strength can be eliminated when taking ratios of certain elliptic flow cumulants (see right panel of Fig. 1). Finally, we propose an observable, denoted W , that allows to discriminate between different interaction rates, and validate it using our event-by-event kinetic theory simulations [2].

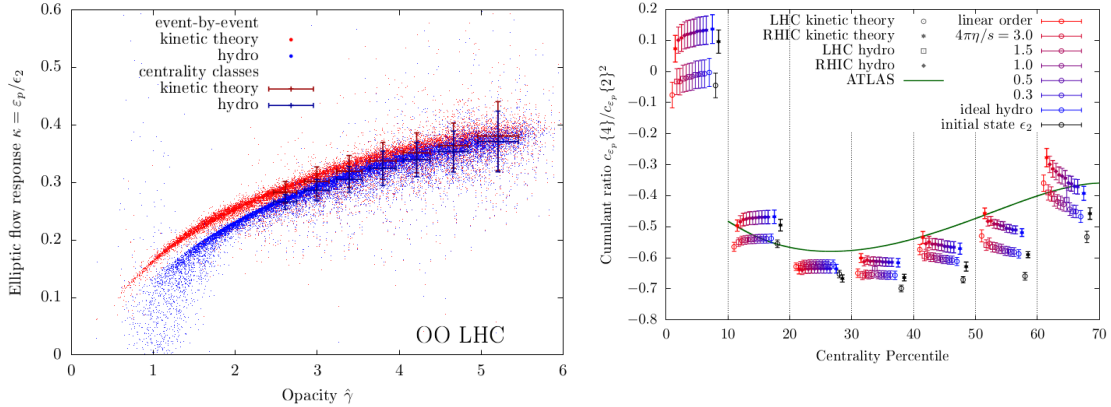


Figure 1: (left) Flow response as a function of opacity, calculated in conformal kinetic theory and viscous hydrodynamic for OO collisions at LHC energies (taken from Ref. [1]). (right) Invariance of the ratio of the fourth cumulant to the square of the second cumulant with respect to the shear viscosity to entropy density ratio, $4\pi\eta/s$, and comparison to ATLAS experimental results (taken from Ref. [1]).

Keywords: Quark-Gluon-Plasma, Elliptic flow, Relativistic kinetic theory, Relativistic hydrodynamics.

References:

- [1] V.E. Ambruş, S. Schlichting, C. Werthmann, Phys. Rev. D **111** (2025) 054024. DOI: [10.1103/PhysRevD.111.054024](https://doi.org/10.1103/PhysRevD.111.054024).
 [2] V.E. Ambruş, S. Schlichting, C. Werthmann, Phys. Rev. D **111** (2025) 054025. DOI: [10.1103/PhysRevD.111.054025](https://doi.org/10.1103/PhysRevD.111.054025).

TCP-O05

TWO DIPOLE-DIPOLE INTERACTING EMITTERS IN A LASER FIELD

Alexandr S. Cudreaşov¹ and Mihai A. Macovei¹

¹ *Institutul de Fizică Aplicată, Universitatea de Stat din Moldova, Academiei 5, MD-2028 Chişinău, Moldova*

The cooperative resonance fluorescence spectrum of a non-resonantly laser-driven dipole-dipole non-strongly coupled two-level system within the Dicke limit, i.e., the interatomic distance is much smaller compared to the emission wavelengths, and a non-trivial detuning between the laser and system transition frequencies was considered with the following approximations: the electric dipole approximation, the rotating-wave approximation, and a rotating frame of reference taken at the laser's pumping frequency [1]. The system is assumed to be driven by a moderately intense laser field. Moreover, the dipole-dipole interatomic coupling strength, while weak, is still significant and exceeds the collective spontaneous decay rate; however, it is much smaller than the Rabi frequency manifested by the system, which subsequently is much smaller than the emitter transition frequencies. We obtained the characteristic two-qubit Mollow spectrum consisting of the elastic part and, respectively, the spontaneous resonance fluorescence part of the spectrum, i.e., the central, and the left and the right spectral bands. The study discusses the elastic part of the spectrum and the vanishing dressed states dipole-dipole interaction and shows the proper analytic ratio between the non-zero detuning of the system and the doubled Rabi frequency to achieve the ensuing result [2].

Keywords: Resonance fluorescence, dicke limit, dressed states, two-qubit interaction, mollow spectrum.

References:

- [1] P. Bardetski, M. A. Macovei: Dipole-dipole-interacting two-level emitters in a moderately intense laser field. *Phys. Rev. A* **110**(4), 043720/1-9 (2024).
- [2] A. S. Cudreaşov, M. A. Macovei: *in preparation* (2025).

TCP-O06

TOWARDS A COMPACT-TIME STRING COSMOLOGY

Andrei Dogaru¹

¹University of Bucharest, Faculty of Physics, Strada Atomistilor 405, Măgurele

String gas cosmology [1] proposes to explain the dimensionality of spacetime by a decompactification scenario whereby the annihilation of winding strings/branes frees 3 large dimensions and confines the rest. However, semiclassical analysis of the coupled Einstein-Boltzmann system for a gas of branes [2] leads to fine-tuning requirements if the 6 extra dimensions are indeed to remain small. In this paper we investigate whether considering a compact-time background for the string gas addresses this issue while remaining a viable cosmological scenario itself. This approach is motivated by Gibbon's observation [3] that branes should wrap time as well if they are to avoid singularities. We present a generalized Einstein-Boltzmann system for a compact-time toroidal universe initially filled with a gas of branes winding space and time dimensions and study its late-time behaviour.

Keywords: cosmology, compactifications, string theory

References:

- [1] Robert Brandenberger, Cumrun Vafa, "Superstrings in the Early Universe", Nucl.Phys. B316 (1989) 391
- [2] R.Easther, B.R. Greene, M.G. Jackson, D. Kabat, "String Windings in the Early Universe", JCAP 0502:009,2005
- [3] G W Gibbons, "Wrapping Branes in Space and Time", arXiv:hep-th/9803206

FIREWALL BOUNDARIES FOR ROTATING QUARK MATTER IN LINEAR SIGMA MODEL

Victor E. Ambruş¹, Sergio Morales Tejera¹, Aleksandar Gecić¹

¹ *Department of Physics, West University of Timișoara, Bd. Vasile Pârvan 4, Timișoara, 300223, Romania*

Using the linear sigma model coupled with dynamical quarks, we investigate the effect of rotation on chiral restoration in strongly-interacting matter by considering a rigidly-rotating plasma in unbounded Minkowski space-time. At large distances from the rotation axis, the medium gets hotter and the sigma condensate melts, leading to the natural „firewall” boundary condition $\sigma = 0$ on the light cylinder (see Fig. 1 below), introduced in Ref. [1]. As a result, the system is either in a mixed phase, confined in the vicinity of the rotation axis and deconfined close to the light cylinder, or in a purely deconfined state. Our present study investigates the impact of quantum corrections, which become dominant close to the light cylinder [2], on the phase diagram of the system.

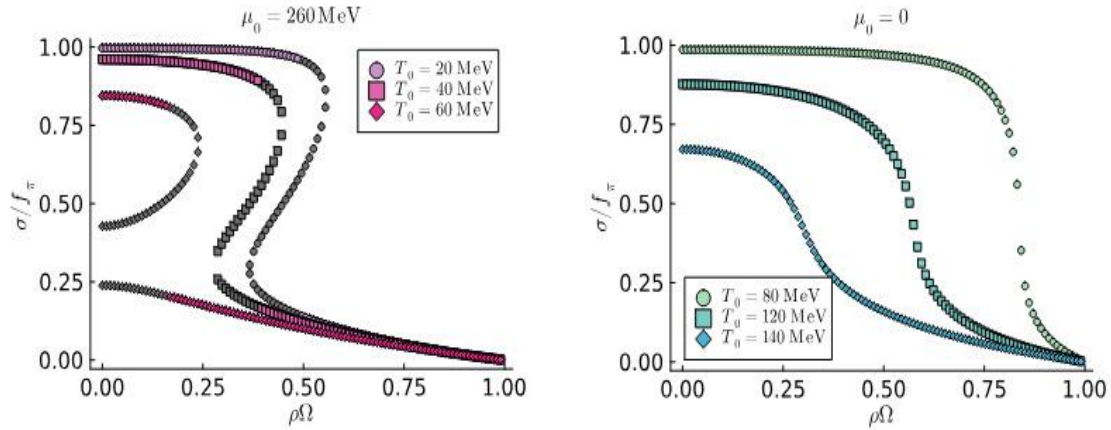


Figure 1: Normalized condensate σ as a function of the dimensionless distance $\rho\Omega$ to the rotation axis, at finite (left) and vanishing (right) on-axis baryon chemical potential, for various values of the on-axis temperature. The colored (black) points represent the thermodynamically (un)-favoured solutions [1]. The condensate vanishes on the light cylinder at $\rho\Omega=1$, confirming the firewall paradigm.

Keywords: Rotating quark-gluon plasma, chiral restoration, effective models

References:

- [1] S. Morales-Tejera, V.E. Ambruş, M.N. Chernodub, [arXiv:2502.19087 \[nucl-th\]](https://arxiv.org/abs/2502.19087).
 [2] V.E. Ambruş, Phys. Lett. B **771** (2017) 151. DOI: [10.1016/j.physletb.2017.05.038](https://doi.org/10.1016/j.physletb.2017.05.038).

CRITICAL BEHAVIOR AT THE TRANSITION TO CHAOS IN HAMILTONIAN SYSTEMS

Gabriel Majeri and Virgil Băran

University of Bucharest

Critical phenomena often occur around critical points, associated with phase transitions of physical systems [1]. Interesting behavior arises at the transition from an integrable system with regular trajectories to a chaotic one [2].

We focus on the critical behavior of a Hamiltonian system derived from a model of collective nuclear motion [3, 4, 5]. In the semiclassical limit, this system exhibits both a regular regime, where the phase space is filled with invariant tori, and a (semi)chaotic regime, in which we find pockets of the phase space with chaotic trajectories [6].

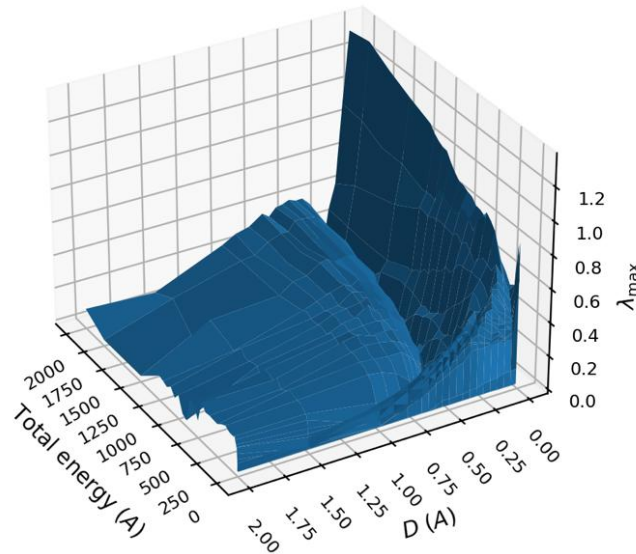


Figure 1: Maximal Lyapunov exponent for a fixed value of the parameter $B = 0.55$ A, plotted against the parameter D and the total energy of the Hamiltonian

We study the evolution of the maximum value of the Lyapunov exponents for a random, uniformly distributed sample of initial conditions, while varying the model's adiabatic parameters A , B , D and the total energy of the Hamiltonian. We find a critical value for the parameter B , from which the percentage of chaotic trajectories in the phase space starts increasing exponentially, analogous to the universal behavior of nonlinear dynamical systems, as described in [7, 8].

Keywords: critical points, phase transitions, quantum chaos, Hamiltonian mechanics, Lyapunov exponents, Feigenbaum constant.

References:

- [1] J. Ginibre, C. Domb, M. S. Green, *Phase Transitions and Critical Phenomena*, **Vol. 1: Exact Results**, 111-136 (1972)

- [2] L. Reichl, *Fundamental Theories of Physics, The Transition to Chaos: Conservative Classical and Quantum Systems*, 36-45 (2021)
- [3] A. A. Raduta, V. Baran, D. S. Delion, *Nuclear Physics A* **588** **2**, 431-462 (1995)
- [4] V. Baran, A. A. Raduta, D. S. Delion, *Physical Review E* **54** **2**, 3264-3273 (1996)
- [5] V. Baran, A. A. Raduta, *International Journal of Modern Physics E* **7** **4**, 527-551 (1998)
- [6] S. Micluta-Campeanu, M. C. Raportaru, A. I. Nicolin, V. Baran, *Romanian Reports in Physics* **70** **105** (2018)
- [7] V. Baran, M. Zus, A. Bonasera, A. Paturca, *Romanian Journal of Physics*, **60** **9-10**, 1263-1277 (2015)
- [8] M. Feigenbaum, *Journal of Statistical Physics*, **21** **6**, 669-706 (1979)

SCALE-FREE TO PARETO-TSALLIS TRANSITION IN THE WAITING TIME DISTRIBUTIONS OF ETHEREUM-USDT EXCHANGE RATE

Paul-Adrian Gogiță^{1,2*}, Mihaela-Carina Raportaru² and Alexandru Nicolin-Țaczek²

¹Faculty of Physics, University of Bucharest, Atomiștilor 405, Măgurele, România

²Institute of Space Science - Subsidiary of INFLPR, Atomiștilor 409, Măgurele, România

*Corresponding author: paul.gogita@s.unibuc.ro

This study investigates the statistical properties of waiting times derived from high-frequency Ethereum (ETH-USDT) exchange rate data spanning over several years. A waiting time is defined as the shortest time interval required for the exchange rate to increase by at least a predefined threshold, δ , following the observation of a specific exchange rate.

The Distribution of Waiting Times (or DWT for short) provides a robust statistical measure characterizing system dynamics; it is computationally tractable across a wide spectrum of hardware that ranges from low-power portable devices to large-scale data centers, accommodating analyses on both raw and privacy-preserving encrypted data.

Our analysis reveals that the DWT exhibits distinct characteristics depending on the magnitude of δ : for small values of δ the DWTs follow a scale-free (or power law) distribution, while for large values of δ the DWTs are better described by a Pareto-Tsallis distribution. We systematically analyze the transition between these two distributions by examining the goodness-of-fit indicators (Kolmogorov-Smirnov distance, D_{KS}) for both scale-free and Pareto-Tsallis fits across a range of δ values.

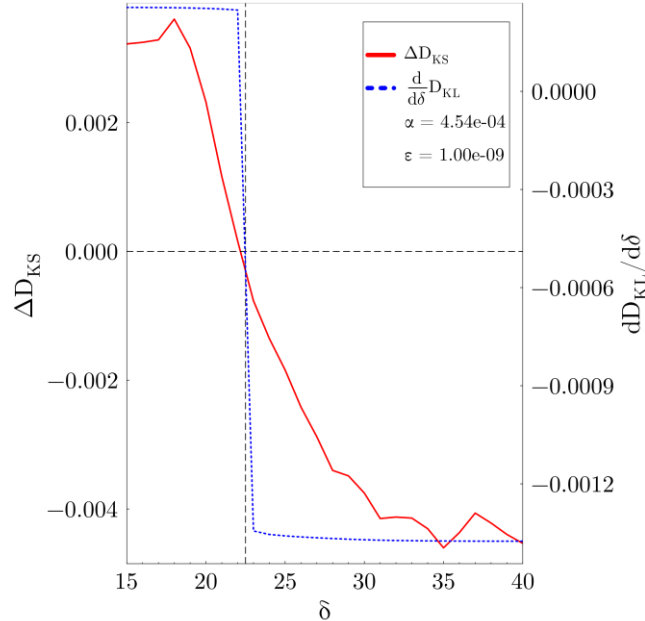


Figure 1: The scale-free to Pareto-Tsallis distribution transition in DWTs for the ETH-USDT exchange rate. The full red line shows the difference in the Kolmogorov-Smirnov quality of fit indicators (ΔD_{KS}), while the dotted blue line shows the derivative of the global Kullback-Leibler divergence ($dD_{KL}/d\delta$) obtained using a noise-robust differentiation method [3]. The jump in the derivative occurs near the zero-crossing of ΔD_{KS} , indicating the transition point.

The transition point, where the Pareto-Tsallis distribution provides a better description of the empirical DWTs than the scale-free distribution (indicated by the zero-crossing of the difference in D_{KS} values, ΔD_{KS}), is further characterized through the global Kullback-Leibler (KL) divergence. We observe a distinct jump-like structure in the derivative of the global KL divergence ($dD_{KL}/d\delta$) around this transition point, providing quantitative evidence for the shift in the underlying dynamics captured by the DWT. This transition highlights a change in the statistical nature of price fluctuations as the magnitude of the required price change increases.

Keywords: Cryptocurrency exchange, Waiting Time Distributions, Statistical Physics.

Acknowledgements: The authors were supported through the TRUSTEE Horizon Europe project, Grant Agreement ID: 101070214 and the Romanian Ministry of Research, Innovation and Digitalization under Romanian National Core Program LAPLAS VII – contract no. 30N/2023.

References:

- [1] G.T. Pană, P.-A. Gogîță, and A. Nicolin-Żaczek, Waiting times for sea level variations in the Port of Trieste: A computational data-driven study, *Romanian Journal of Physics* **69**, 111 (2024).
- [2] A. Clauset, C. R. Shalizi, and M. E. J. Newman, Power law distributions in empirical data, *SIAM Review* Vol. **51**, Iss. 4 (2009).
- [3] Rick Chartrand, Numerical Differentiation of Noisy, Nonsmooth Data, *ISRN Applied Mathematics* (2011).

FINITE SPIN DENSITY EFFECTS ON THE CHIRAL PHASE TRANSITION IN THE LINEAR SIGMA MODEL

Pracheta Singha,¹ Victor E. Ambrus,¹ Sergiu Busuioc,¹ Aritra Bandyopadhyay¹ and
Maxim N. Chernodub^{2,1}

¹*Department of physics, West university of Timisoara,
Bd. Vasile Pârvan 4, Timișoara 300223, România*

²*Institut Denis Poisson, Université de Tours, Tours 37200, France*

The experimental observation of the spin polarisation of the outgoing hadrons in non-central heavy ion collisions implies the existence of a strongly vortical QGP medium with finite spin density. We consider the effect of finite spin density on the QCD phase diagram using the Linear Sigma model coupled to quarks (LSMq). In our approach, we introduce the finite spin density via a quark spin potential (μ_s) in the canonical formulation of the spin operator, leading to a nonlinear modification of the energy dispersion relation. Besides an expected effect on the thermal fermion loop, the spin potential also enters non-trivially in the zero-point, temperature-independent part of the fermion loop. Employing renormalization techniques [1], we observe a substantial influence of this term on the phase structure of the system at non-negligible μ_s/T . Taking both the thermal and the zero-point terms into account, we find the expectation value of the sigma condensate by minimizing the thermodynamic potential of the system, as indicated by the purple dots in Fig. 1. Our findings indicate that, starting from a chiral symmetry broken phase at small T and μ_s , the minima of the thermodynamic potential moves towards lower values of σ with increasing μ_s , indicating the restoration of chiral symmetry. This behaviour is consistent with the results from the first principle lattice simulations [2].

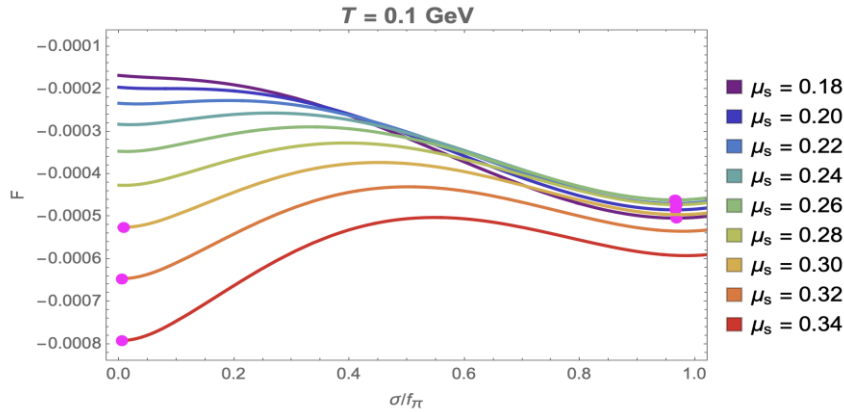


Figure 1:
*Thermodynamic potential F as a function of σ/f_π at $T = 0.1 \text{ GeV}$ for various values of μ_s .
The purple points correspond to the minima of F and indicate the expectation value of σ .*

Keywords: Quark-Gluon-Plasma, chiral phase transition, spin potential.

References:

- [1] A. Ayala, L.A. Hernandez, M. Loewe, J.C. Rojas, R. Zamora, Eur. Phys. J. A **56** (2020) 71. DOI: [10.1140/epja/s10050-020-00086-z](https://doi.org/10.1140/epja/s10050-020-00086-z).
[2] V.V. Braguta, M.N. Chernodub, A.A. Roenko, [arXiv:2503.18636](https://arxiv.org/abs/2503.18636).

TWO QUBIT SYSTEM IN A THERMAL RESERVOIR

Arthur Rotari¹ and Mihai A. Macovei¹

¹ *Institutul de Fizică Aplicată, Universitatea de Stat din Moldova, Academiei 5, MD-2028 Chişinău, Moldova*

We investigate the quantum dynamics of a system comprising two dipole-dipole coupled two-level emitters interacting via a common thermal reservoir. The analysis is conducted in the regime where the dipole-dipole interaction is appreciable—sufficiently strong to influence system dynamics, yet not exceeding the transition frequency of the individual emitters. By adopting the formalism of collective Dicke states, we derive the corresponding master equation that captures the steady-state properties of the system.

This formulation explicitly incorporates the dependence of both spontaneous emission rates and mean thermal photon numbers on the dipole-dipole coupling strength at the relevant two-qubit transitions. As a consequence, we obtain analytical expressions for the cooperative steady-state populations and the fluorescence emission spectrum of the composite system.

Our results reveal that the population ratios between adjacent transitions diverge from the canonical Boltzmann distribution, owing to the non-negligible dipole-dipole interaction within the emitter pair. The fluorescence spectrum exhibits a doublet structure, wherein the spectral lines become spectrally resolved when the dipole-dipole interaction surpasses the effective collective decay rates.

This spectral and population structure originates from the energy-level shifts induced by the dipole-dipole coupling, which lifts the degeneracy of the symmetric and antisymmetric collective states relative to the bare single-emitter transition frequency. Notably, both the magnitude and the sign of the dipole-dipole interaction play a decisive role in determining the system's spectral and dynamical characteristics.

Keywords: Fluorescence spectrum, Dicke limit, dressed states, two-qubit interaction.

TCP-012

**EARLY UNIVERSE PRODUCTION OF W BOSONS IN NEUTRINO
DECAYS**

Amalia Dariana Fodor, Cosmin Crucean and Andru Mihai Buga

Faculty of Physics, West University of Timisoara, V. Parvan Avenue 4, 300223 Timisoara, Romania

In this paper we study the rates of production of W bosons emitted in neutrino decays during the early stages of the Universe via perturbative methods. We compute the transition amplitude corresponding to the first order of de Sitter electro-weak perturbation theory and study its various limiting cases. The transition rates are derived using minimal subtraction and dimensional regularization. In the end we obtain the density number of bosons (as a function of temperature) and give an estimation of this number for different temperatures and fixed values of the particle momenta.

MOTT CRITERION IN II-VI SEMICONDUCTORS

Alexandru Varzari¹, Alexandr Cliucanov¹ and Sergiu Vatavu¹

¹ Faculty of Physics and Engineering, Moldova State University
60 A. Mateevici str., MD-2009, Chisinau, Moldova

The Mott transition (MT) of excitons into an electron-hole plasma (EHP) is characterized by a fundamental change in the radiative recombination mechanism – from radiative annihilation of excitons to direct interband transitions. The MT is driven by the screening of the Coulomb interaction between electrons and holes, with the screening parameter determined by the Debye length λ_D at high temperatures and by the Thomas-Fermi length λ_{TF} at low temperatures. The screening effect is taken into account by replacing the Coulomb potential with the Yukawa potential:

$$V_{Yukawa} = -\frac{e^2 \exp(-r/\lambda_D)}{r\epsilon_0}, \Rightarrow \frac{1}{\epsilon_0} \rightarrow \frac{1}{\epsilon_0} \frac{q^2}{q^2 + \lambda_D^{-2}}, \lambda_D^{-2} = \frac{4\pi n e^2}{\epsilon_0 k_B T_e} \quad (1)$$

The MT is experimentally observed through temperature- and excitation-power-dependent photoluminescence (PL) measurements in II–VI semiconductors. The Mott criterion (MC), expressed as the carrier density to electronic temperature ratio n/T_e , characterizes the MT and depends on the screening parameter a_B/λ_D :

$$\lambda_D^{-2} a_B^2 = \frac{4\pi n e^2}{\epsilon_0 k_B T_e} a_B^2 \Leftrightarrow \frac{n}{T_e} = \left(\frac{a_B}{\lambda_D}\right)^2 \frac{\epsilon_0 k_B a_B^{-2}}{4\pi e^2} = \left(\frac{a_B}{\lambda_D}\right)^2 \frac{k_B a_B^{-3}}{8\pi R_{exc}} \quad (2)$$

Thus, the calculation of the MC for a specific semiconductor reduces to determining the exciton Bohr radius a_B and the excitonic Rydberg energy R_{exc} . These parameters are derived from the dielectric constant ϵ_0 and the effective masses of electrons m_e and holes m_h :

$$a_B = \frac{\hbar^2 \epsilon_0}{\mu e^2}, R_{exc} = \frac{\mu e^4}{2\hbar \epsilon_0^2}, \mu = \frac{m_e m_h}{m_e + m_h} \quad (3)$$

The discrete energy spectrum of the quasiparticle bound-state is described by the Wannier–Mott equation (WME). This equation was solved using the variational method for the ground state and perturbation theory method for both the ground and excited states. The screening parameter was obtained by requiring that the exciton binding energy approaches zero.

According to the variational solution of the WME, the MT occurs at a screening parameter close to unity, i.e., $a_B/\lambda_D \approx 1$. Based on this condition and using exciton parameters specific to II–VI semiconductors, the corresponding MCs were evaluated. The resulting carrier density to electron temperature ratio n/T_e ranges from the lowest threshold for CdTe ($\sim 10^{15} \text{ cm}^{-3} \text{ K}^{-1}$) to the highest for ZnO ($\sim 10^{16} \text{ cm}^{-3} \text{ K}^{-1}$), reflecting the material dependence of exciton annihilation.

Acknowledgements: MEC subprogram 011207.

Keywords: Photoluminescence, Mott Transition, II-VI Semiconductors.

TCP-O14

ENTROPY CORRECTED GEOMETRIC BROWNIAN MOTION

Dominik Szczesniak

Jan Dlugosz University in Czestochowa, Faculty of Science and Technology, Institute of Physics

The geometric Brownian motion (GBM) is widely employed for modeling stochastic processes, yet its solutions are characterized by the log-normal distribution. This comprises predictive capabilities of GBM mainly in terms of forecasting applications. During this talk, the entropy corrections to GBM will be discussed to go beyond log-normality restrictions and better account for intricacies of real systems. It will be shown that GBM solutions can be effectively refined by arguing that entropy is reduced when deterministic content of considered data increases. Notable improvements over conventional GBM will be presented for several cases of non-log-normal distributions, ranging from a dice roll experiment to real world data.

TCP-P01

**THE HYBRID COSMOLOGY IN THE SCALAR-TENSOR
REPRESENTATION OF $f(G,T)$ GRAVITY**

Adam Zenon Kaczmarek¹ and Dominik Szczęśniak¹

¹Jan Długosz University in Częstochowa, 13/15 Armii Krajowej Ave., 42200 Częstochowa, Poland

In this work, the $f(G,T)$ theory of gravity is recast in terms of the ϕ and ψ fields within the scalar-tensor formulation, where G is the Gauss-Bonnet term and T denotes the trace of the energy-momentum tensor. The general aspects of the introduced reformulation are discussed, and the reconstruction of cosmological scenarios is presented, focusing on the so-called hybrid evolution. As a result, the scalar-tensor $f(G,T)$ theory is successfully reconstructed for the early and late-time approximations with the corresponding potentials. The procedure of recovering the $f(G,T)$ theory in the original formulation is performed for the late-time evolution and a specific quadratic potential. The scalar-tensor formulation introduced herein not only facilitates the description of various cosmic phases but also serves as a viable alternative portrayal of the $f(G,T)$ gravity, which can be viewed as an extension of the well-established scalar Einstein-Gauss-Bonnet gravity.

Keywords: modified gravity, cosmology, scalar-tensor theory

TCP-P02

BORN RATE EQUIVALENCE FOR THE KINETIC THEORY AND QUANTUM FIELD THEORY APPROACH

Moulindu Kundu, Victor E Ambruş and Aritra Bandyopadhyay

¹*Department of Physics, West University of Timișoara, Bd. Vasile Pârvan 4, Timișoara*

Dileptons are considered to be an important observable, in the context of studying the characteristics of the deconfined phase of quark gluon plasma (QGP). Historically, the dilepton production rates (DPR) from the QGP have been studied using two different approaches. In the quantum field theory (QFT) approach, the DPR is expressed in terms of the thermal expectation value of the current-current correlator [1] or the imaginary part of the photon self energy [2]. On the other hand, the kinetic theory (KT) framework assumes the QGP to be sufficiently weakly coupled, such that the quarks can be considered as quasiparticles and the DPR is computed based on a collision kernel for an inelastic scattering process (see Fig. 1). We discuss the equivalence of the two approaches at the Born level, where the QFT and KT frameworks give identical results.

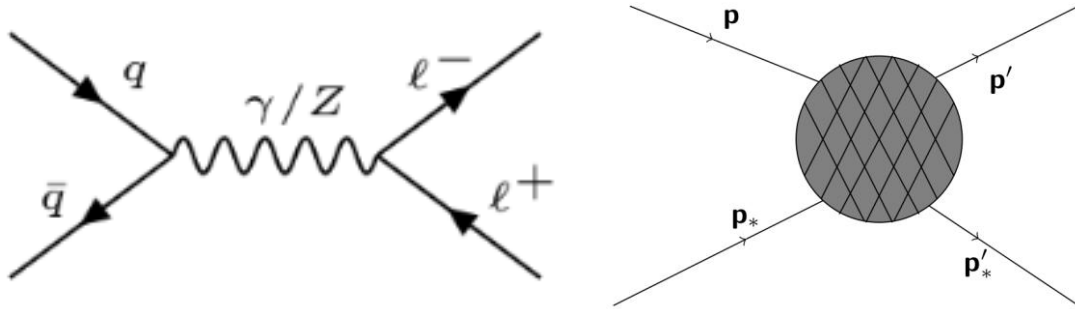


Figure 1: Illustration of dilepton production (left) via a quantum annihilation-creation process; and (right) via inelastic scatterings in kinetic theory.

Keywords: Dilepton production rate, Kinetic theory, Quark gluon plasma.

References:

- [1] D. McLerran and T. Toimela, *Phys. Rev. D* 31, 545 (1985).
- [2] H. A. Weldon, *Phys. Rev. D* 42, 2384 (1990).
- [3] K. Kajantie, J. I. Kapusta, L. D. McLerran, and A. Mekjian, *Phys. Rev. D* 34, 2746 (1986)

TCP-P03

THERMAL GRADIENT OPTIMISATION THROUGH NUMERICAL MODELING FOR OPTIMAL GROWTH OF DOUBLE DOPED SESQUIOXIDES (Y_2O_3 , Gd_2O_3 , Lu_2O_3) CRYSTALS USING THE CZOCHRALSKI METHOD

Dragos Tatomirescu¹, Philippe Veber^{1,2}, Alexandra Popescu¹, Maximilian Mangra¹,
Tiana Ile¹, Kesavan Venkatachalam¹ and Daniel Vizman¹

¹*Faculty of Physics, West University of Timisoara, 300223 Timisoara, Romania*

²*Institute for Advanced Environmental Research, West University of Timisoara, Timisoara, Romania*

Due to the good thermal and mechanical properties, Yb^{3+} -doped ceramic laser materials have attracted a lot of attention in the recent decades [1,2]. For commercial high-power continuous and mode-locking laser systems operating in the 1 μm range, Yb^{3+} -based laser materials have the potential to substitute the ones based on Nd^{3+} [3, 4].

Our study is focused on determining the ideal growth conditions for growing double doped sesquioxides (Y_2O_3 , Gd_2O_3 , Lu_2O_3) crystals. Our main concern during this study was to have a reduced longitudinal gradient within the crucible as this is the main factor that influences the growth of such materials. For this purpose, we have tested multiple configurations of the installation geometry in order to reduce the longitudinal gradient. For numerical modeling the simulation software Elmer version 9.0 [5, 6] based on the finite element method (FEM) is used. This software is mainly developed at the IT Center for Science (CSC) in Finland, and is openly available under a GPL / LGPL license.

Keywords: numerical modeling, heat transfer, thermal gradient.

References:

- [1] M. Chaika, O. Vovk, G. Mancardi, R. Tomala, W. Streck, Dynamics of Yb^{2+} to Yb^{3+} ion valence transformations in Yb:YAG ceramics used for high-power lasers, *Opt. Mater.* 101 (2020) 109774
- [2] O.V. Palashov, A.V. Starobor, E.A. Perevezentsev, I.L. Snetkov, E.A. Mironov, A.I. Yakovlev, S.S. Balabanov, D.A. Permin, A.V. Belyaev, Thermo-optical studies of laser ceramics, *Materials* 14 (2021) 3944
- [3] R.N. Maksimov, A.S. Yurovskikh, V.A. Shitov, Fabrication, microstructure, and spectroscopic properties of transparent Yb 0.118 Lu 0.464 Y 1.418 O 3 ceramics, *Phys. Status Solidi* 217 (2020) 1900883
- [4] P. Klopp, New Yb^{3+} -doped laser materials and their application in continuous-wave and mode-locked lasers, Humboldt-Universität zu Berlin, Mathematisch-Naturwissenschaftliche Fakultät I, 2006
- [5] M. Malinen and P. Råback, Elmer finite element solver for multiphysics and multiscale problems. In book: *Multiscale Modelling Methods for Applications in Material Science*, pages 101-113. Chapter: Elmer finite element solver for multiphysics and multiscale problems, Forschungszentrum Juelich, Editors: Ivan Kondov, Godehart Sutmann, 2013.
- [6] A. Enders-Seidlitz, J. Pal, K. Dadzis, Development and validation of a thermal simulation for the Czochralski crystal growth process using model experiments, *Journal of Crystal Growth*, 593 (2022) 126750

Acknowledgment

This work is funded by the European Commission within the framework of the National Recovery and Resilience Plan (PNRR) through the ESCARGOT project entitled “Enhanced Single Crystal Applications and Research in the Growth of new Optical rare earth-based compounds for sustainable and efficient Technologies” (n°: 760080/23.05.2023).

CONDENSED MATTER PHYSICS (CMP)

LUMINESCENCE IN FLUORIDE CRYSTALS DOPED WITH $M^{3+,2+}$ OR RE^{3+} IONS: PREDICTIONS FROM DENSITY FUNCTIONAL THEORY STUDY

Alexander Platonenko^{1,2}, Zafari Umar¹, Andrei Chesnokov², Mikhail Brik¹,
Vladimir Pankratov², Michal Piasecki¹

¹ Jan Długosz University, Armii Krajowej 13/15, Częstochowa, 42-201, Poland

² Institute of Solid State Physics, Kengaraga street 8, Riga, LV1063, Latvia

Radiation resistant inorganic materials emitting cross-luminescence (CL), first discovered in 1982 [1], are one of the most prospective candidates for new generation ultrafast detectors for medical tomography. The advantages of CL materials include their (i) ultrafast decay times which is typically in the range down to 500 ps – it is significantly faster than traditional doped inorganic scintillators; (ii) relatively high photon yields – up to 2,000 ph/MeV; (iii) high temperature stability – CL intensity is temperature independent; (iv) relatively high densities, which is highly desirable for the detection efficiency of ionizing radiation [2].

In current work we demonstrate results of *ab initio* calculations of undoped and doped BaF_2 by means of hybrid density functional theory [3]. As a result of the work, the density of states (DOS) for nominally pure BaF_2 and a whole series of BaF_2 doped with various trivalent ions were obtained. The positions of the core energy levels of dopant ions lying between the $Ba(5p)$ zone and the $F(2s)$ zone, as well local geometries and formation energies were calculated. Our calculations show that the $5p$ states of impurity ions can be located below the $5p$ zone of barium by several eV. This opens up opportunities for transitions from the core $5p$ Ba zone to impurity $5p$ states, which might be involved in experimentally observed appearance of an ultrafast component in doped BaF_2 [4].

Keywords: cross-luminescence, DFT, doping

References:

- [1] N.N. Ershov, N G. Zakharov and P.A. Rodnyi, Opt. Spectrosk. 53, 89 (1982)
- [2] C.W.J.van Ejik, J. Lumin. 60&61 (1994) 936-941
- [3] A. Platonenko, A. Chesnokov, K. Chernenko, V. Pankratov, Comp. Mat. Sci. 247 (2025)
- [4] R. Shendrik, E. Radzhabov, A. Myasnikova, V. Pankratova, A. Šarakovskis, A. Nepomnyashchikh, A. Bogdanov, V. Gavrilenko, V. Pankratov, arXiv preprint arXiv:2412.04303 (2024)

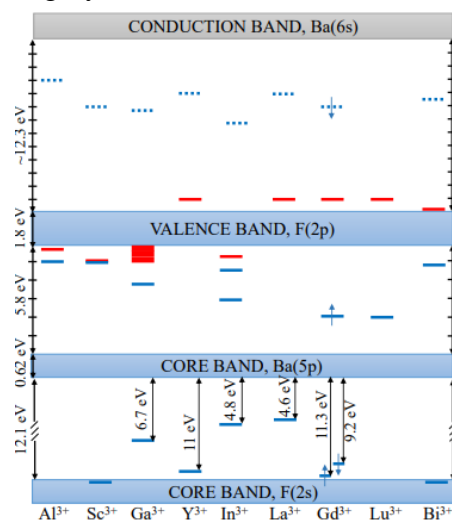


Figure 1: Schematic diagram of defect states and interstitial fluorine ion in band gap and core-valence gap. Red lines show position of energy level of F_i ; blue solid and dotted line correspond to M^{3+} filled and empty levels, respectively

DEVELOPMENT OF EFFICIENT UP-CONVERSION OXIDE PHOSPHORS

Tomoki Koikawa¹, Yuiko Shimazaki¹, Mikhail G. Brik^{2,3,4,5} and Tomoyuki Yamamoto^{1,6,7}

¹Faculty of Science and Engineering, Waseda University, Okubo, Shinjuku, Tokyo, Japan

²Institute of Physics, University of Tartu, Tartu, Estonia

³Centre of Excellence for Photoconversion, Vinca Institute of Nuclear Sciences-National Institute of the Republic of Serbia, University of Belgrade, Belgrade, Serbia

⁴Academy of Romanian Scientists, Bucharest, Romania

⁵School of Optoelectronic Engineering & CQUPT-BUL Innovation Institute, Chongqing University of Posts and Telecommunications, Chongqing, China

⁶Kagami Memorial Research Institute for Materials Science and Technology, Waseda University, Tokyo, Japan

⁷Institute of Condensed-Matter Science, Waseda University, Tokyo, Japan

Up-conversion (UC) phosphor has gained significant attention and has been widely studied because of its wide variety of applications. Among the various applications of the UC phosphors, hybridization of UC phosphors with solar cells is one of the big challenges to enhance photoconversion efficiency of the solar cells. However, luminescence efficiency of the UC phosphors is not yet so high to be applied for such application. One of the UC phosphors is realized by the doping of the rare-earth ions in the wide band gap materials such as oxides and fluorides. Among them, we have successfully enhanced the UC luminescence intensity by the addition of K₂CO₃ in Er-doped CaMoO₄ [1] and the co-doping of other rare-earth elements in Er-doped CaSnO₃ [2]. In this work, we demonstrate our recent development for the enhancement of UC luminescence intensity by the alkaline metal addition and co-doping of the rare-earth elements.

Keywords: Up-conversion phosphor, alkaline metal addition, co-doping

References:

[1] T. Koikawa and T. Yamamoto, *Opt. Mater.* **163**, 116959 (2025).

[2] Y. Shimazaki et al., *7th Int. Conf. Phys. Opt. Mater., Becici, Montenegro*, Aug. 26-30, 2024.

INFRARED SPECTRUM OF BaF₂:ErF₃-YbF₃ CRYSTALS

Emeric. C. C. Kiss¹, Michal Piasecki¹, Mikhail Brik¹, Yaroslav Zhydachevskyy²,
Andrzej Suchocki², Marius Stef³

¹Institute of Physics, Jan Dlugosz University Czestochowa, Czestochowa, Poland

²Institute of Physics, Polish Academy of Sciences, Warsaw, Poland

³Department of Physics, West University of Timisoara, Timisoara, Romania

Erbium-doped crystals exhibit remarkable emission properties in the infrared region, making them highly valuable for applications such as near-infrared lasers and mid-infrared night vision technologies [1]. In this study, we investigate three variations of barium fluoride (BaF₂) crystals doped with different concentrations of erbium fluoride (ErF₃) and ytterbium fluoride (YbF₃). The photoluminescence spectra of these samples are analyzed to determine the most suitable composition for efficient infrared emission. Furthermore, the selected crystal's spectral characteristics are examined across a temperature range from low temperatures to room temperature to assess its performance stability. The findings of this research contribute to the optimization of erbium-doped materials for advanced infrared applications.

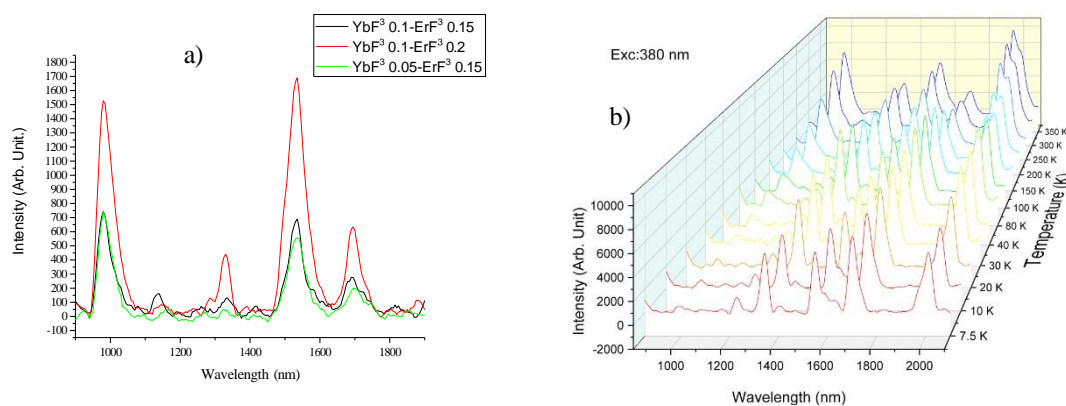


Figure 1: Photoluminescence spectra of the three BaF₂ crystals doped with different concentrations of Erbium and Ytterbium a) and the photoluminescence spectra of one crystal at different temperatures b).

Keywords: Erbium, Ytterbium, Luminescence.

References:

[1] W. Huang, H. Peng, Q. Wei, J. Wang, B. Ke, W. Liang, J. Zhao, and B. Zou Efficient Near-Infrared Luminescence with Near-Unity Photoluminescence Quantum Yield in Erbium-Doped Double Perovskites Cs₂NaYCl₆ under Green Light Excitation *Chemistry of Materials* **36** (5), 2483-2494 (2024).

MAGIC GENERATION IN SPIN CHAINS AND RANDOM CIRCUITSCătălin Pașcu Moca¹¹*Department of Physics, University of Oradea*

We explore the generation and dynamics of non-stabilizerness—also known as *magic*—in both closed and open quantum systems using the stabilizer 2-Rényi entropy M_2 . Our study begins with multi-particle quantum walks in the XXZ Heisenberg spin chain, revealing how magic spreads within a light-cone structure dictated by the system’s dynamics. Distinct behaviors emerge across interaction regimes: in the easy-plane phase, magic generation is dominated by single-particle dynamics, while in the easy-axis regime doublon propagation leads to a markedly slower growth of M_2 , which increases logarithmically in time. We further show that the Pauli spectrum displays Poissonian level statistics, independent of interaction strength or particle number, highlighting the subtle interplay between integrability and non-stabilizerness. Extending our investigation to open systems, we examine the boundary-driven XXZ chain under bulk dephasing. To access large system sizes, we develop a novel algorithm to compute M_2 efficiently within the matrix product state framework at constant bond dimension. Our results reveal universal scaling behavior $M_2(t) \sim t^{1/z}$ governed by the transport exponent z , with signatures of Kardar-Parisi-Zhang (KPZ) dynamics at the isotropic point. We identify two key timescales—dephasing and coherence—that dictate the transient enhancement and eventual suppression of magic. A mean-field decomposition further isolates the contribution of genuine quantum correlations, underscoring the utility of M_2 as a diagnostic for transport and decoherence. Our findings position magic as a versatile probe of quantum dynamics in both isolated and open many-body systems.

Keywords: Non-stabilizer entropy, spin chains.

References:

- [1] E. Grumbling and M. A. Horowitz, eds., *Quantum computing: Progress and prospects*, A consensus study report of the National Academies of Sciences, Engineering, Medicine (The National Academies Press, Washington, DC, 2019).
- [2] S. F. E. Oliviero, L. Leone, A. Hamma, and S. Lloyd, Measuring magic on a quantum processor, *Quantum Inf.* 8, 148 (2022).
- [3] X. Turkeshi, E. Tirrito, and P. Sierant, Magic spreading in random quantum circuits (2025), arXiv:2407.03929 [quant-ph].
- [4] S. Bera and M. Schir`o, Non-stabilizerness of Sachdev-YeKitaev model (2025), arXiv:2502.01582 [quant-ph].
- [5] L. Aolita, F. de Melo, and L. Davidovich, Open-system dynamics of entanglement: A key issues review, *Rep. Prog. Phys.* 78, 042001 (2015).

CMP-O03

SEMICLASSICAL ANALYSIS OF SPIN DYNAMICS IN THE NON-HERMITIAN HUBBARD MODEL

Doru Sticlet

National Institute for R&D of Isotopic and Molecular Technologies, 67-103 Donat, 400293 Cluj-Napoca, Romania

We study the one-dimensional non-Hermitian Hubbard model with complex interactions, mapped onto a spin ladder with coupled XY chains via Ising ZZ interactions. The spin ladder model is then examined within the semiclassical limit using a spin-coherent state basis, in which the dynamics is governed by a set of coupled Landau-Lifshitz-Gilbert equations. We find that non-Hermitian interactions generate a spin torque term that drives the system to several potential steady states. In the infinite-temperature limit, we show that the favored steady state is that of decoupled ladder rungs in which pairs of spins are locked in a ferro- or antiferromagnetic configuration. Nevertheless, the interactions within each of rails of the spin ladder lead to the formation of ferromagnetic domains in each chain in the steady state. Additionally, we investigate the time-dependent spin correlation functions and identify signatures of anomalous spin dynamics.

Keywords: Non-Hermitian quantum mechanics, spin chains, spin torque

References:

[1] Doru Sticlet, Cătălin Pașcu Moca, Balázs Dóra, Phys. Rev. B 110, 224433 (2024).

EVALUATION OF NONLINEAR OPTICAL PROPERTIES OF MATERIALS BASED ON SPECTROSCOPIC DATA ANALYSIS

M. Piasecki, *^{a,b} O. Y. Khyzhun^c, M.G.Brik^{a,d,e,f}

^{a)} Jan Dlugosz University in Częstochowa, Poland, m.piasecki@ujd.edu.pl

^{b)} Uzhhorod National University, Uzhhorod, Ukraine

^{c)} Frantsevych Institute for Problems of Materials Science, National Academy of Sciences of Ukraine, Kyiv, Ukraine

^{d)} School of Optoelectronic Engineering & CQUPT-BUL Innovation Institute, Chongqing University of Posts and Telecommunications, Chongqing, People's Republic of China

^{e)} Institute of Physics, University of Tartu, Estonia

^{f)} Centre of Excellence for Photoconversion, Vinca Institute of Nuclear Sciences, University of Belgrade, Serbia

^{g)} Academy of Romanian Scientists, Bucharest, Romania

We show how is possible evaluate (predict) nonlinear optical properties of materials based on spectroscopic data analysis. We focus on the connection of emission properties and electronic structure parameters with the possibility of generating the second harmonic of light. As examples, we will analyze oxide phosphors (RE-activated) on the one hand and chalcogenide crystals on the other. In these first ones, the influence of orbital hybridization on the intensity of the hypersensitive transition in isostructural vanadate, arsenide and phosphate systems is discussed. We show the same mechanism is also responsible for the efficiency of second harmonic generation (SHG). Is well-known that SHG is a nonlinear process in which a crystal converts lower frequency radiation to higher frequency. The bonding covalence within the acentric anionic groups, that are the basic structural moiety of the crystal framework (such as PO₄, AsO₄, VO₄, SiO₄, GeO₄, etc.), is chiefly responsible for the SHG activity. The importance of orbital hybridization on the SHG efficiency is exemplified by the striking difference in optical nonlinearity between isostructural titled compounds. While the vanadate is efficient, the phosphate shows no SHG activity, although the calculated SHG coefficients (pm/V) for both compounds are non-zero. The difference in the SHG efficiency has been clarified by examining the electronic band structure of these compounds. Our analysis supports the polarizability of (XO₄)₃₋ (X = P, As, V) over local site distortion effects as the intensity enhancing mechanism of the ⁵D₀→⁷F₂ transition. The connection between the mechanism of hypersensitivity and second harmonic generation (SHG) is discussed. Then we will show how the complexity of the crystallographic structure of chalcogenide crystals and the size of the energy gap affect the SHG intensity. In this case the SHG intensity increases with a decrease in the bandgap width Ag₂In₂SiSe₆ (1,68 eV), Ag₂In₂GeSe₆ (1,55 eV), Ag₂In₂SiS₆ (2,0 eV), Ag₂In₂GeS₆ (1,96 eV), which effect is characteristic of multi-component chalcogenide crystals.

References:

- [1] A M Srivastava, M G Brik, W W Beers, Chong-Geng Ma, M Piasecki, W E Cohen (2023) J.Lumin. 257, 119709.
- [2] A. M. Srivastava, M G Brik, B. Lou, W W Beers, Chong-Geng Ma, M Piasecki, W E Cohen (2023) ECS J. Solid State Sci. Technol. 12 066001
- [3] Alok M Srivastava, Mikhail G Brik, Chong-Geng Ma, William W Beers, William E Cohen, Michal Piasecki The Journal of Physical Chemistry Letters (2004) 15, 4175-4184
- [4] Michał Piasecki, G Myronchuk, OY Khyzhun, A Fedorchuk, B Andryievsky, I Barchyi, M Brik, , Journal of Alloys and Compounds, (2022) 909, 164636

INTERPLAY BETWEEN SURFACE CHARGE AND SURFACE FERROMAGNETISM: FOUR RECENT EXAMPLESCristian Mihail Teodorescu¹¹*National Institute of Materials Physics, Atomiștilor 405A, 077125 Măgurele–Ilfov, Romania*

Two simple criteria were proposed for the occurrence of ferromagnetism: the first one is the Stoner criterion $g(\varepsilon_F)U > 1$, where $g(\varepsilon)$ is the (paramagnetic) density of states (DOS), ε_F is the Fermi level and U the Hubbard on-site electronic repulsion term [1]. This criterion was established by comparing the increase of kinetic energy associated with electron transfer from minority towards majority spin partial DOS with the decrease (stabilization) induced by the on-site repulsion between electrons with opposite spin. In another work, the *total* (i. e. kinetic + potential) energy was taken into account and not only the kinetic energy, and another criterion emerged relying only on the shape of the paramagnetic DOS, $g'(\varepsilon_F) \int_0^{\varepsilon_F} g(\varepsilon)d\varepsilon < g^2(\varepsilon_F)$, with no need to introduce the Hubbard term [2]. Both criteria allow triggering of the ferromagnetism by varying the atomic charge near surface (hence by varying the DOS position with respect to ε_F , by modulating either the amplitude $g(\varepsilon_F)$ or the sign of its derivative $g'(\varepsilon_F)$).

Several examples will be discussed, yielding surface magnetism of materials which are not ferromagnetic in the bulk. The cleanness and well ordering of these surfaces were carefully characterized by low energy electron diffraction (LEED), atomic resolution scanning tunneling microscopy (STM) and X-ray photoelectron spectroscopy (XPS). The spin asymmetry was detected by using spin-resolved valence band photoemission spectroscopy (SRPES).

The first example is the Pt(001)–*hex.* surface where, according to Friedel oscillations or to density functional consideration, the surface is enriched in electrons, hence the surface DOS is shifted towards lower energies with respect to the Fermi level and this induces $g'(\varepsilon_F) < 0$ for surface atoms [3]. Another example is the partially reduced SrTiO₃(001) surface, where a spin asymmetry of O 2p orbitals was detected [4]. In the case of the SrTiO₃(011) surface, the fact that this crystal orientation supposes the alternance of charged planes such as SrTiO⁴⁺ and O₂⁴⁻, the O₂ –terminated surface can be stabilized by supposing a reduction of the charge of the last layer, e. g. O₂²⁻. In this case, surface oxygens will feature a 2p⁵ electronic configuration, with a net spin of 1/2 each, which induce a robust surface spin asymmetry [5].

The last case which will be analyzed is that of ferroelectric BaTiO₃(001), where the ferroelectricity is accompanied by charge accumulated at surface [6]. BaO terminated surfaces are positively charged, and the associated electron depletion is distributed on both lowest binding energy occupied O 2p and on the deeper Ba 5p orbitals, yielding a “ferroelectric-induced permanent inversion of population” with a consistent associated spin asymmetry [7].

Keywords: surface magnetism, surface charge accumulation, criteria for ferromagnetism, spin-resolved photoelectron spectroscopy, XPS, LEED, STM.

References:

- [1] E. C. Stoner, *Proc. Roy. Soc. London* **165**, 372–414 (1938).
- [2] C. M. Teodorescu, *Res. Phys.* **25**, 104241 (1–10) (2021).
- [3] L. E. Borcan, C. M. Teodorescu, A.-C. Iancu, N. G. Apostol, A. Nicolaev, R. M. Costescu, M. A. Huşanu, D. G. Popescu, G. A. Lungu, M. Bianchi, *J. Phys.: Mater.*, resubmitted, in peer review (2025).
- [4] D. G. Popescu, A. Nicolaev, R. M. Costescu, L. E. Borcan, G. A. Lungu, C. A. Tache, M. A. Huşanu, C. M. Teodorescu, *Phys. Scr.* **99**, 105925(1–11) (2024).
- [5] L. E. Borcan, A.-C. Iancu, D. G. Popescu, C. M. Teodorescu, *J. Chem. Phys.* **162**, 054707(1–13) (2025).
- [6] C. M. Teodorescu, *Phys. Chem. Chem. Phys.* **23**, 4085–4093 (2021).
- [7] L. E. Borcan, A.-C. Iancu, N. G. Apostol, A. Nicolaev, C. M. Teodorescu, *Mater. Adv.*, submitted (2025).

CMP-P01

EFFECT OF PROCESS PARAMETERS ON THE PROPERTIES OF YTTRIUM OXIDE CERAMICS

Vasilica Țucureanu^{1*}, Oana Brâncoveanu¹, Cosmin Romanițan¹,
Iuliana Mihalache¹, Alina Matei^{1*}

¹National Institute for Research and Development in Microtechnologies (IMT-Bucharest),
Erou Iancu Nicolae Street, 126A, 077190, Bucharest, Romania

*Corresponding author: e-mail: vasilica.tucureanu@imt.ro; alina.matei@imt.ro

The demand for innovative materials with multiple properties, that are economically feasible, has opened the way for materials such as polycrystalline transparent ceramics. These ceramics have the advantage of materials with high mechanical resistance, good thermal and chemical stability, optical transparency, biocompatibility, adaptable properties, transmission range from UV to IR, the possibility of doping with rare earths. In addition, they have found their utility in aerospace and military applications, the manufacturing of high-temperature IR windows or armored windows, electro-optical devices, lasers, scintillators, catalysts, fluorescent markers etc [1,2]. In this paper, we studied the influence of process parameters on the hydrothermal synthesis of yttrium oxide ceramics. Practically, we used yttrium nitrate and urea in the presence of polyethylene glycol, and the colloidal precipitate was transferred to a 40 ml autoclave and maintained at 150°C for 12 hours. The resulting precursor was subjected to a thermal treatment at 600°C for 3 hours. The effects of the process parameters on the structure, morphology and optical properties were investigated in detail. The transition from the precursor to the crystalline phase of yttrium oxide was observed by Fourier Transform Infrared (FTIR) spectrometry and x-ray diffraction (XRD). FTIR spectroscopy confirmed the formation of M-O bonds, while XRD data demonstrated the progression of the crystalline phase. The particles' spherical form and rounded edges were seen at SEM. The optical investigations validated the utility and suitability of the proposed method for the production of yttrium oxide-based ceramics.

Keywords: Y₂O₃, hydrothermal process, ceramics.

Acknowledgements

This work was supported by a grant of the Ministry of Research, Innovation and Digitization, CNCS-UEFISCDI, project number PN-IV-P2-2.1-TE-2023-0417 (BioYDetect, Contract no. 30TE/2025), within PNCDI IV. Also, this work was supported by the Core Program within the National Research Development and Innovation Plan 2022-2027, carried out with the support of MCID, project no. 2307 (μNanoEl).

References:

- [1] O. J. Akinribide, G. N. Mekgwe, S. O. Akinwamide, F. Gamaoun, C. Abeykoon, O. T. Johnson, P. A. Olubambi, *Journal of Materials Research and Technology*, **21**, 712-738 (2022) <https://doi.org/10.1016/j.jmrt.2022.09.027>.
- [2] Q. Q. Zhu, P. F. Yang, Z. Y. Wang, P. C. Hu, *Journal of the European Ceramic Society*, **40** (6), 2426-2431 (2020) <https://doi.org/10.1016/j.jeurceramsoc.2020.02.005>.

CMP-P02

IMPACT OF RAPID THERMAL ANNEALING UNDER VARIOUS TEMPERATURES ON THE YTTRIUM OXIDE NANOPARTICLES

Alina Matei^{1*}, Oana Brîncoveanu¹, Cosmin Romanițan¹, Cristina Pachiu¹,
Vasilica Țucureanu^{1*}

¹National Institute for Research and Development in Microtechnologies IMT-Bucharest (126 A, Erou Iancu Nicolae Street, 077190, Voluntari, Ilfov, ROMANIA)

*Corresponding author: e-mail: Email: alina.matei@imt.ro; vasilica.tucureanu@imt.ro

Oxide materials, particularly Y_2O_3 , have proven useful in advanced biomedical applications, with high impact in the fields of biosensors, biological imaging, photodynamic therapies, fluorescent biomarkers, bioactive ceramics, implants etc. Y_2O_3 NPs contribute to the development of efficient solutions in the targeted field due to their thermal stability, chemical durability, antioxidant and antibacterial activity, optical transparency, magnetic properties, and biocompatibility. To obtain Y_2O_3 with established characteristics, the synthesis method is essential, having an impact on their physicochemical properties and performance.

In the present paper, the research was focused on the synthesis of Y_2O_3 NPs by a chemical method using yttrium nitrate hexahydrate, urea and ammonium hydroxide, deposition of the oxide precursors as thin films on silicon substrate, and drying in a desiccator at room temperature before thermal treatment. Then, the prepared samples were subjected to rapid thermal annealing at a heating rate of $10^\circ C/sec.$ reaching 600 and $900^\circ C$ for 600 sec. in nitrogen atmosphere. The morphological, structural, and wettability characteristics of Y_2O_3 films have been obtained using advanced analytical techniques. Morphological characterization (SEM) reveals nanometric particle sizes with a rough surface, and a slight tendency to agglomeration. The compositional analysis (EDX) revealed Y_2O_3 nanoparticles without impurities, supported by specific Y and O elements. The study of the vibrational characteristics of the synthesized samples was conducted using two complementary spectrometric techniques (FTIR and RAMAN), which revealed the characteristic vibration bands of the Y-O bond. The structural analysis (XRD) shows a cubic crystalline structure, revealing the high purity of the Y_2O_3 samples. The surface wetting capacity of Y_2O_3 films, as investigated by contact angle measurement, indicates a hydrophilic character and good percolation, with a direct impact on the performance of the material in various technological sectors.

Keywords: yttrium oxide, chemical synthesis, rapid thermal annealing.

Acknowledgments:

This work was supported by a grant of the Ministry of Research, Innovation and Digitization, CNCS-UEFISCDI, project number PN-IV-P2-2.1-TE-2023-0417 (Contract no. 30TE/2025), within PNCIDI IV. Also, this work was supported by the Core Program within the National Research Development and Innovation Plan 2022-2027, carried out with the support of MCID, project no. 2307 (μ NanoEl).

References:

- [1] G. Rajakumar, L. Mao, T. Bao, W. Wen, S. Wang, T. Gomathi, N. Gnanasundaram, M. Rebezov, M.A. Shariati, I.-M. Chung, M. Thiruvengadam, Z. Zhang, *Appl. Sci.* **11**, 2172 (2021). <https://doi.org/10.3390/app11052172>
- [2] T.M. Abdalkreem, H.C. Swart, R.E. Kroonr, *Nano-Structures & Nano-Objects.* **35**, 101026 (2023). <https://doi.org/10.1016/j.nanoso.2023.101026>

CMP-P03

INTERACTIONS BETWEEN GLASS MATRICES AND RARE-EARTH IONS: ENERGY TRANSFER PATHWAYS

Petr Kostka^{1,2}, Roman Yatskiv³, Jiri Zavadil¹, Olga Prochazkova¹, Petar Gladkov³,
Stanislav Tiagulskyi³

¹*Institute of Rock Structure and Mechanics, Czech Academy of Sciences, V Holešovičkách 41, 182 09 Praha, Czech Republic*

²*University of Chemistry and Technology Prague, Czech Republic*

³*Institute of Photonics and Electronics, Czech Academy of Sciences, Czech Republic*

We analyze the optical properties of rare-earth doped glasses, focusing on materials with varying phonon energy levels, absorption edge positions, and presence of transition metals. This study investigates the absorption spectra and photoluminescence characteristics of pure silica and tellurite glasses doped with rare-earth ions, as well as tellurite glasses containing chromium. By examining selected glass matrices, we demonstrate that, under certain conditions, the embedded rare-earth ions can be efficiently excited not only through direct photon absorption at the corresponding energy matching the rare-earth ion transition but also via energy transfer from the excited glass matrix near the ion. This mechanism enables the excitation of rare-earth doped ions over a wide range of wavelengths and allows the observation of their radiative transitions, which remain inactive in other glasses (in our case the pure silica glass) under otherwise identical experimental conditions.

Keywords: tellurite glass, quartz glass, rare earths, photoluminescence, energy transfer, excitation.

References:

- [1] P. Kostka, Z.G. Ivanova, M. Nouadji, E. Černošková, J. Zavadil, *Journal of Alloys and Compounds* **780**, 866-872 (2019).
- [2] P. Kostka, J. Zavadil, M. S. Iovu, Z. G. Ivanova, D. Furniss, A. B. Seddon, *Journal of Alloys and Compounds* **648**, 237-243 (2015).

CMP-P04

SPECTROSCOPIC ANALYSIS OF X-RAY INDUCED VALENCE CHANGES IN Tm-DOPED CaF₂ CRYSTALS

Carla Schornig¹ Marius Ștef¹ Philippe Veber¹ Daniel Vizman¹ Maria Poienar² and Gabriel Bușe²

¹ Faculty of Physics, West University of Timisoara 300223, Timisoara, Romania

² ICAM, West University of Timisoara 300223, Timisoara, Romania

The ability to manipulate the charge conversion of rare-earth ions in fluoride crystals is of increasing interest for the development of photonic devices, scintillators, and solid-state dosimetry systems. In this context, the radiation-induced conversion between Tm³⁺ and Tm²⁺ ions has attracted attention due to the distinctive optical properties of the divalent state. Although the emergence of Tm²⁺ absorption features in CaF₂ crystals and similar hosts by irradiation has been previously reported, the effect of dopant concentration on the spectroscopic behavior and temporal evolution of these centers is not yet fully understood.

In this work, we explore the behavior of Tm²⁺ centers generated in CaF₂:TmF₃ single crystals exposed to X-ray radiation, using three different doping levels: 0.1, 1, and 5 mol%. UV-VIS absorption spectroscopy was employed to monitor spectral changes before and after irradiation. Multiple absorption bands associated with Tm²⁺ ions and radiation-induced color centers were identified in the 190–210 nm, 290–330 nm, and 390–420 nm ranges. At 0.1 mol%, Tm²⁺ absorption increased moderately during irradiation and remained stable over time. The 1 mol% crystal showed a more pronounced response, followed by a gradual decay, while the 5 mol% sample reached saturation and maintained its Tm²⁺ features for at least 20 days post-irradiation. Exponential kinetic modeling provided reliable fits for both the formation and relaxation stages, confirming the reproducibility of the observed behavior and emphasizing the role of dopant concentration in charge-state control under X-ray exposure.

References:

- [1] M. Ștef et al., *Radiation Physics and Chemistry*, 176 (2020) 109024.
- [2] M. Grinberg et al., *Optical absorption spectra of X-ray irradiated alkaline earth fluoride crystals doped with divalent rare-earth ions studied by thermal bleaching*, *Radiation Measurements*, 56 (2013) 137–141.
- [3] J. Zhang et al., *Controlled Generation of Tm²⁺ Ions in Nanocrystalline BaFCl:Tm³⁺ by X-ray Irradiation*, *The Journal of Physical Chemistry A*, 121 (2017) 803–809.

Acknowledgements

This work is supported by a grant PNRR/2022/C9/MCID/I8, project title “Enhanced Single Crystal Applications and Research in the Growth of new Optical rare earth-based compounds for sustainable and efficient Technologies (ESCARGOT), contact number 136/15.11.2022.

MACHINE LEARNING MODEL FOR PREDICTING INTERATOMIC DISTANCES IN A₂O₃ OXIDES AND CORRELATIONS WITH STARK SPLITTING OF LANTANIDE DOPANT ENERGY LEVELS

A. V. Racu¹, G. Dima¹, M-G. Ivanovici¹, D. Vizman², M. Buryi³,
T. Yamamoto⁴, M. G. Brik^{1,5,6,7,8}

¹National Institute of Research & Development for Electrochemistry and Condensed Matter, Timisoara, Romania.

²West University of Timisoara, Timisoara, Romania

³Institute of Plasma Physics of the Czech Academy of Sciences, Czech Republic.

⁴Faculty of Science and Engineering, Waseda University, Tokyo, Japan.

⁵Centre of Excellence for Photoconversion, Vinča Institute of Nuclear Sciences, University of Belgrade, Serbia.

⁶School of Optoelectronic Engineering and CQUPT-BUL Innovation Institute, Chongqing, PR China

⁷Institute of Physics, University of Tartu, Estonia.

⁸Academy of Romanian Scientists, Bucharest, Romania

Understanding the correlations between the structure of host materials and optical spectroscopic data can be significantly enhanced through the use of predictive models for crystal structure parameters based on machine learning (ML) approaches [1]. Local symmetry and interatomic distances play a critical role in the splitting of energy levels of lanthanide dopants [2]. These distances are often challenging to determine and may require sensitive techniques such as electron paramagnetic resonance (EPR) [3].

In this work, a machine learning model employing the Random Forest algorithm was developed and utilized to predict local symmetry-related interatomic distances in a series of A₂O₃ oxides. The model was trained on a dataset comprising 22 structural descriptors. The predictive performance of the model yielded a mean absolute error (MAE) of 0.01 Å, indicating high precision in estimating interatomic distances. The low MAE and the consistent accuracy of the predictions underscore the model's robustness and reliability.

Keywords: machine learning, random forest model, optical materials.

Acknowledgments: This study was supported by Romania's National Recovery and Resilience Plan – NRRP (PNRR), Project C9-I8-C28, and Contract 760107/2023.

References:

- [1] N. Srivastava, G. Hinton, A. Krizhevsky, I. Sutskever, R. Salakhutdinov, *J. Mach. Learn. Res.*, **15**, 1929-1958 (2014).
- [2] P. Dorenbos, *Journal of Luminescence*, **135**, 93-104 (2013).
- [3] M. Buryi, V. V. Laguta, E. Mihóková, P. Novák, M. Nikl, *Phys. Rev. B*, **92**, 224105(2015).

**MACHINE LEARNING-BASED PREDICTION OF 5D-LEVEL
ABSORPTION OF Pr³⁺ IN ABO₃ OXIDES**

G. Dima¹, A. V. Racu¹, R. Bucur¹, M. Iorga¹, Z. Antić^{1,2}, M. Buryi³,
M.D. Dramićanin^{1,2}, M. G. Brik^{1,2,4,5,6}

¹National Institute of Research & Development for Electrochemistry and Condensed Matter, Timisoara, Romania. ²Centre of Excellence for Photoconversion, Vinča Institute of Nuclear Sciences, University of Belgrade, Serbia.

³Institute of Plasma Physics of the Czech Academy of Sciences, Czech Republic.

⁴Faculty of Science and Technology, Jan Długosz University, Częstochowa, Poland.

⁵Institute of Physics, University of Tartu, Estonia.

⁶Academy of Romanian Scientists, Bucharest, Romania

Accurate prediction of 5d-level positions in ABO₃ compounds is essential for the design of UV-C emitting phosphors based on lanthanide-doped materials [1]. These energy levels, particularly from the 4fⁿ5d¹ configuration, are highly sensitive to the local crystal field environment, necessitating a deep understanding of host–dopant interactions [2]. In this study, we present a machine learning model based on the Random Forest algorithm to predict the lowest 5d-level energies of Pr³⁺ and Ce³⁺ ions across various ABO₃ host materials. The model was trained on a dataset comprising 22 descriptors, including structural features, band gaps, ionic radii, and coordination environments.

The model demonstrates high predictive accuracy, with mean absolute errors below 6 nm, and shows strong consistency with experimental data, underscoring its potential for guiding materials discovery in lanthanide-doped oxides.

Keywords: machine learning, random forest model, optical materials.

Acknowledgments: This study was supported by Romania’s National Recovery and Resilience Plan – NRRP (PNRR), Project C9-I8-C28, and Contract 760107/2023.

References:

- [1] S.L. Cates, E.L. Cates, M. Cho, J.-H. Kim, *Environ Sci Technol*, **48**, 2290 (2014).
- [2] Z. Wang, A. Chen, K. Tao, J. Cai, Y. Han, J. Gao, S. Ye, S. Wang, I. Ali, J. Li, *Nature –Npj Comput Mater*, **9**, 1–9 (2023).
- [2] P. Dorenbos, *Journal of Luminescence*, **135**, 93-104 (2013).

**APPLIED PHYSICS AND
INTERDISCIPLINARY (API)**

ATMOSPHERIC PRESSURE PLASMA AND LIFE SCIENCES: RECENT ADVANCES IN MEDICINE, AGRICULTURE AND BIOENGINEERING

Ionut Topala¹, Ioana Cristina Gerber², Ilarion Mihaila², Valentin Pohoata¹

¹*Faculty of Physics, Iasi Plasma Advanced Research Center (IPARC), Alexandru Ioan Cuza University of Iasi, Blvd. Carol I, No. 11, 700506 - Iasi, Romania*

²*Integrated Center of Environmental Science Studies in the North-Eastern Development Region, Blvd. Carol I, No. 11, 700506 - Iasi, Alexandru Ioan Cuza University of Iași, Romania*

Atmospheric pressure plasma (APP) sources have emerged as a transformative technology in the life sciences, offering innovative applications due to the unique physicochemical environment that is generated and applied to biologicals targets. These non-thermal plasma sources operates at ambient conditions, enabling its use in various biological and medical contexts without causing thermal damage to tissues or materials.

In the medical field, APP has shown significant promise in oncology and dermatology. Studies have demonstrated that low-temperature plasmas can induce apoptosis in cancer cells, providing a potential therapeutic avenue for cancer treatment [1,2]. Cold atmospheric plasma has been effectively used to treat chronic wounds, demonstrating enhanced healing rates and reduced infection risks [3].

The agricultural sector has explored APP for its potential to enhance crop production and safety. Non-thermal plasma treatments have been investigated as environmentally friendly technologies to improve seed germination rates, promote plant growth, and protect against pathogens. By modulating the surface properties of seeds and inactivating surface-borne pathogens, APP contributes to healthier crop yields [4,5].

In the bioengineering field, APP plays a crucial role in material science, particularly in surface modification. This method ensures uniform coatings at ambient conditions, making it both cost-effective and versatile [6,7].

Atmospheric pressure plasma stands at the intersection of physics, chemistry, and biology, offering a versatile platform for advancements across the life sciences. Its ability to operate under ambient conditions without thermal damage, coupled with its efficacy in microbial inactivation, tissue regeneration, and material modification, underscores its potential to revolutionize practices in medicine, agriculture, and food safety. Ongoing research continues to unravel the full spectrum of APP's capabilities, paving the way for innovative solutions to longstanding challenges in the life sciences.

Keywords: atmospheric pressure plasma, life science applications.

References:

- [1] Mihai, C. T., Mihaila, I., Pasare, M. A., Pintilie, R. M., Ciorpac, M., & Topala, I. *Current Issues in Molecular Biology*, **44**, 1995 (2022).
- [2] Stache, A. B., Mihăilă, I., Gerber, I. C., Dragoș, L. M., Mihai, C. T., Ivanov, I. C., ... & Gorgan, D. L. *Applied Sciences*, **13**, 7803 (2023).
- [3] Nastuta, A. V., Topala, I., Grigoras, C., Pohoata, V., & Popa, G., *Journal of Physics D: Applied Physics*, **44**, 105204 (2011).
- [4] Leti, L. I., Gerber, I. C., Mihaila, I., Galan, P. M., Strajeru, S., Petrescu, D. E., ... & Gorgan, D. L. *Plants*, **11**, 2181 (2022).

- [5] Bilea, F., Garcia-Vaquero, M., Magureanu, M., Mihaila, I., Mildažienė, V., Mozetič, M., ... & Žūkienė, R. *Critical Reviews in Plant Sciences*, **43**, 428 (2024).
- [6] Nastuta, A. V., Asandulesa, M., Doroftei, F., Dascalu, I. A., Varganici, C. D., Tiron, V., & Topala, I. *Polymers*, **16**, 240 (2024).
- [7] Nastuta, A. V., Butnaru, M., Cheatham, B., Huzum, R., Tiron, V., & Topala, I. *Chinese Journal of Polymer Science*, **42**, 1156 (2024).

API-I02

SMART Growth: Artificial intelligence enhanced, sustainable growth of rare-earth materials based laser

Philippe Veber^{*1,2}, Dragos Tatomirescu¹, Alexandra Popescu¹, Gabriel Buse², Daniel Vizman¹, Natasha Dropka³

¹Faculty of Physics, Crystal growth laboratory, West University of Timisoara (Romania)

²Institute for Advanced Environmental Research (ICAM), West University of Timisoara (Romania)

³Leibniz Institute for Crystal Growth, IKZ, Berlin (Germany)

Crystal growth, by Czochralski method [1] (Fig. 1) for instance, for industrial photonics applications, is one of the crucial technologies for a modern society. Their manufacturing technology involves rare materials, high amount of energy, and a lot of dedicated process knowledge. The crystal, as a product itself, is a core component of many photonics systems such as the broad field of lasers for various applications. Nevertheless, the value chain for crystal growing is rarely based on Zero-Defect Manufacturing approaches that could enable a sustainable implementation of this crucial process.

SMART Growth project aims at developing single crystals for lasers and photonics applications under the supervision of Artificial Intelligence. Detecting, predicting and preventing failures in a typical crystal growth process are the key points for improving the yield of crystal production, reducing the amount of energy required and improving the quality of the as-grown crystal.

We present a study that integrates machine learning with numerical modeling. The objective is to unravel the nonlinear relationship between crystal growth process parameters and furnace geometry on one side, and solid/liquid interface shape and v/G (growth rate over temperature gradients) on the other side. We exemplify this approach by focusing on defect-free YAG and Ge crystals [2].

The authors acknowledge the European Innovation and SME Council Executive Agency (EISMEA) for funding "Smart Growth" project (n°: 101115130) under the Interregional Innovation Investment (I3) Instrument.

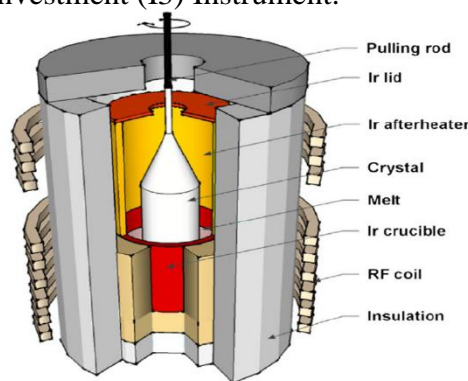


Figure 1: Example of Czochralski furnace for the growth of oxides

Keywords: crystal growth, artificial intelligence, optical crystals.

References:

- [1] Z. Galazka, "Czochralski method" in "Gallium Oxide, Materials Properties, Crystal Growth, and Devices", Springer Nature, Ch.2 (2020) 15-36
- [2] N. Dropka et al., « Smart design of Cz-Ge crystal growth furnace and process», Crystals, 12 (2022) 1764

CT SIMULATION RECONSTRUCTIONS AND THEIR IMPLICATION IN RADIOTHERAPY

Mihai – Stefan Barhala^{1,2}, Tia Popescu^{1,2}

¹*Faculty of Physics, University of Bucharest, Magurele, Jud. Ilfov, Romania*

²*Neolife, Bucharest, Romania*

In radiotherapy patient simulation using CT is a key element for the delivery of a complex and accurate radiotherapeutic treatment. Since these data are used in the calculation of the dose distribution inside the patient, it is necessary to realize a correlation between the physical properties of the tissues present inside the body and the specific attenuation coefficient of each voxel [1].

Given the availability of variation of the parameters of a CT acquisition for the simulation of radiotherapy patients, except for the accelerating voltage of electrons, these acquisitions can be optimized according to the area of interest. These optimizations can be done both during the scan and afterwards, in the form of reconstructions, with the possibility of applying different data processing filters [2].

The aim of this work is to evaluate the advantages of the additional use of reconstructions in radiotherapy, both from the point of view of performing contouring of target volumes and organs at risk, and from the point of view of the correctness and accuracy of dose calculation in these images.

Keywords: CT Reconstructions, CT Calibration Curve, CT Reconstruction Algorithms, CT Scanning Parameters

References:

- [1]. Thomas S. J. (1999). Relative electron density calibration of CT scanners for radiotherapy treatment planning. *The British journal of radiology*, 72(860), 781–786. <https://doi.org/10.1259/bjr.72.860.10624344>
- [2]. Li, H., Dolly, S., Chen, H. C., Anastasio, M. A., Low, D. A., Li, H. H., ... & Mutic, S. (2016). A comparative study based on image quality and clinical task performance for CT reconstruction algorithms in radiotherapy. *Journal of applied clinical medical physics*, 17(4), 377-390.

**STABILITY OR INSTABILITY OF A STATIC MENISCUS
APPEARING IN RIBBON SINGLE CRYSTAL GROWTH FROM
MELT USING E.F.G. METHOD**

¹Andreea V. Cojocaru, ²Adriana Tanasie, ³Stefan Balint , ⁴Sorina M.D.Laitin,

¹ West University of Timisoara, Department of Computer Science. ² West University of Timisoara, Department of Computer Science.

³West University of Timisoara, Department of Computer Science, ⁴Victor Babes University of Timisoara, Department 13.

This study presents necessary conditions for existence and sufficient conditions for stability or instability of a static meniscus (liquid bridge) appearing in the ribbon single crystal growth from the melt, of predetermined sizes, by using the edge-defined-film- fed (EFG) growth method. The cases when the contact angle α_c and the growth angle α_g verify the inequality $0 < \alpha_c < \frac{\pi}{2} - \alpha_g$ or $\frac{\pi}{2} > \alpha_c > \frac{\pi}{2} - \alpha_g$ are treated separately. Experimentally, only static meniscus (liquid bridges) which verifies the necessary condition of existence and the sufficient conditions of stability can be created; static meniscus (liquid bridges) which does not verify both of these conditions, exist only in theory because in reality they collapse. The results of this study is significant for thin ribbon single crystal growth from melt, with prior given macroscopic dimensions, using prior given specific equipment. That is because the obtained inequalities represent limits for what can and cannot be achieved experimentally.

Keywords: static stability, meniscus, ribbon growth, edge-defined-film-fed-growth.

References:

[1] A.V.Cojocaru, St.Balint, *Fluids*, 9, 176. (2024)

QUALITY INDEXES MODELING AND EVALUATION FOR ASSESSING THE QUALITY OF SRS/ SRT PLANS

Tia Popescu^{1,2}, Mihai Barhala^{1,2}, Ionut Dumitru²

¹Faculty of Physics, University of Bucharest, Magurele, Jud. Ilfov, Romania

²Neolife, Bucharest, Romania

Brain tumor control plays an important role in the patient's neurological integrity and quality of life. The principle underlying radiosurgery treatments is the delivery of large doses, up to 24 Gy/fraction [1], to the tumor, sparing the healthy normal tissues. In order to obtain the best results a very precise delivery is necessary, which depends on several factors, such as immobilization devices, daily imaging, surface guidance, and a rigorous quality assurance program to maintain a sub-millimeter accuracy. The closer the prescription dose is matched to the treated target and the steeper the dose gradient around the target, the less normal tissue is irradiated. For most rigorous evaluation of stereotactic treatment plans, parameters such as gradient index, conformity index or the gradient in millimeters must be evaluated [2]. All these parameters depend on volume position, dimension, their position in relation to other critical structures or beam energy.

This work aims to compare the indices used in the evaluation of stereotactic treatments by making several treatment plans to see the variability from planner to planner and how far can go in conforming doses for such treatments, thus in order to standardize the quality of plans. The selected patients have single brain metastases, with volumes ranging from 0,3 cm³ to 100 cm³, some of them being close to critical structures. This analysis is based on comparing the values obtained in clinical practice with an experimental model which is based on a phantom, treated with a hypothetical treatment, which cannot be achieved in practice.

Moreover, the quality indexes obtained from multiple lesion plans were analyzed and compared with the experimental model.

Keywords: Brain, Stereotactic, Radiosurgery, Dose Gradient, Conformity

References:

- [1] Palmans, H., Andreo, P., Huq, M. S., Seuntjens, J., Christaki, K. E., & Meghizifene, A. (2018). Dosimetry of small static fields used in external photon beam radiotherapy: Summary of TRS-483, the IAEA-AAPM international Code of Practice for reference and relative dose determination. *Medical Physics*.
- [2] Stanley, J., Breitman, K., Dunscombe, P., Spencer, D. P., & Lau, H. (2011). Evaluation of stereotactic radiosurgery conformity indices for 170 target volumes in patients with brain metastases. *Journal of Applied Clinical Medical Physics*, 12(2), 245–253.

IMPACT OF MAGNETIC FIELD-ASSISTED POLYMERIZATION ON THE ELECTRICAL PROPERTIES OF ELASTOMER-FERROFLUID COMPOSITES

C. N. Marin ¹, I. Malaescu ², O. M. Bunoiu ¹, C. Casut ³, D. D. Darie ¹

¹ Faculty of Physics, West University of Timisoara, Bd. V. Parvan No. 4, 300223 Timisoara, Romania

² Institute for Advanced Environmental Research, West University of Timisoara (ICAM-WUT), Oituz Str., No. 4, 300086 Timisoara, Romania

³ National Institute for Research and Development in Electrochemistry and Condensed Matter (INCEMC), Dr. A.P. Podeanu Str. No. 144, 300569, Timisoara, Romania

Obtaining and electrical properties of elastomer-ferrofluid composites are reported. The samples were prepared by combining silicone rubber (RTV-530) with a kerosene-based ferrofluid containing magnetite particles at three varying volume fractions of ferrofluid, ϕ : 1.48 %, 2.91 %, and 4.32 %. For each volume fraction, ϕ , two samples were prepared, one polymerized under the influence of a magnetic field, $H = 43$ kA/mH and another one polymerized in the absence of magnetic field.

The frequency dependence of electrical conductivity of samples, $\sigma(f)$ was determined from measurements of the complex dielectric permittivity [1], adhering to Jonscher's universal law [2]. From $\sigma(f)$, the static conductivity σ_{DC} of the composite samples was extracted. With an increase in ϕ from 1.48 % to 4.32%, σ_{DC} increased from 4.26×10^{-9} S/m to 1.03×10^{-8} S/m for the samples polymerized in the absence of the magnetic field, and from 4.93×10^{-9} S/m to 1.86×10^{-8} S/m for the samples polymerized in the presence of the magnetic field. Additionally, the results facilitated the estimation of the barrier energy for the electrical conduction process, W_m . For the same ϕ , W_m was found to be lower, and σ_{DC} higher, in samples polymerized under the influence of a magnetic field compared to those polymerized in the absence of a magnetic field.

This study provides valuable insights for the fabrication of composite materials with tailored properties. Specifically, it highlights the feasibility of developing devices for flexible electronics, where properties can be precisely controlled through the adjustment of particle volume fraction or the application of an external magnetic field.

Keywords: ferrofluid, elastomer, dielectric permittivity, electrical conductivity.

References:

- [1] ASTM D150-98 - Standard test methods for AC loss characteristics and permittivity (dielectric constant) of solid electrical insulation.
- [2] A. K. Jonscher, Universal Relaxation Law, 1st edn.: Chelsea Dielectrics Press: London, (1996).

DISTINGUISHING ANTHROPOGENIC SIGNALS IN SEISMIC MONITORING OF THE BANAT - DANUBIAN REGION

Adina Rău^{1,2}, Raluca Dinescu¹, Mircea Radulian^{1,3,4}, Mihaela Popa³, Antoanetta Lungu⁵
Mihail Lungu²

¹ National Institute for Earth Physics, Magurele, Romania

² West University of Timisoara, Faculty of Physics, Timisoara, Romania

³ Academy of Romanian Scientists, Bucharest, Romania

⁴ Romanian Academy, Bucharest, Romania

⁵ Technical College "E. Ungureanu" Timisoara, Romania

The Banat-Danubian region, located in western part of Romania, is a seismicity-prone area at shallow depths in the crust [1]. Recent network improvements boosted event detection in the low magnitude range which led to a sharp contamination in the Romanian (ROMPLUS) catalogue with anthropic events.

Differentiating between tectonic and anthropic events has become essential in characterizing regional seismicity [2]. In this study we focus our analysis on Hauzesti and Paulis quarries, as we relocated events within a 30 km radius around the exploitation sites using a refined 1D velocity model [3]. We propose a detailed analysis on the recalculated hypocenters, waveform analysis and applying discrimination criteria in order to identify tectonic activities from anthropic events.

We will present the implication of the improved microseismic source determination on the seismic hazard assessment in the study region.

Keywords: Banat-Danubian seismicity, microseismicity, discrimination of anthropic events.

References:

- [1] Radulian M, Dinescu, Popa M, *Earthquake-prone areas in Romania*. Annals of the Academy of Romanian Scientists, Series on Physical Sciences Vol 4, number 1/2019, ISSN 2559-1061, (2019)
- [2] Vanciu Rau A., Dinescu R., Popa M., Radulian M., Lungu M., *Identification of anthropogenic activities interference in the seismic catalogue for Banat and Danubian region, Romania*, Acta Geophysica, DOI:<https://doi.org/10.1007/s11600-025-01531-7>, (2025)
- [3] Rău A., Dinescu R., Popa M., Radulian M., Lungu M., *A proposed velocity model applied for Banat and Danubian seismic zones*, Romanian Journal of Physics, Vol 70, nr. 1-2, DOI:<https://doi.org/10.59277/RomJPhys.2025.70.802>, (2025)

Ga, In AND La DOPING OF NICKEL OXIDE: TECHNOLOGY VS PHYSICAL PROPERTIES

Gheorghe Ghilețchi¹, Igor Narolschi¹, Petronela Garoi², Oleg Shapoval¹, Alexandru Belenchuk¹, Oleg Palamarciuc¹, Valentin Ion², Valentin Craciun², Elmira Vatavu¹, Antoniu Moldovan², Ștefan-Andrei Irimiciuc², Sergiu Vatavu¹

¹*Faculty of Physics and Engineering, Moldova State University, 60 A. Mateevici str, Chisinau, Moldova*

²*National Institute for Laser, Plasma and Radiation Physics, 409 Atomistilor Street, Bucharest, Romania*

Among various strategies used to improve electrochromic coatings based on nickel oxide (NiO), doping stands out as a key method for enhancing electrochromic performance. NiO is typically doped with trivalent elements to achieve the desired electrical properties [1] and shows promising potential for applications in optoelectronics [2]. This work aims to prepare NiO films doped with trivalent elements Ga, In, La, revealing a highly crystalline structure.

The Metalorganic Aerosol Deposition [3] technology's strengths lie in the precise control of impurity concentration and the flexibility to alter the doping element, making it a valuable tool for optimizing electrochromic functionality and optoelectronic properties. The deposition solution was prepared by dissolving 0.1 mol nickel acetylacetonate [Ni(acac)₂] along with 0.5-6 mmol of one of the dopant precursors – [Ga(acac)₃], [In(acac)₃] or [La(acac)₃]. To improve the accuracy of the impurity content, a dilution technique was used. Doped nickel oxide films were successfully synthesized by tuning the substrate temperature (ranging from 400 to 550 °C). Atomic Force Microscopy and scanning electron microscopy analysis revealed that the surfaces are composed of densely packed grains of homogeneous nanocrystals, their average sizes being influenced by growth temperature and doping conditions. Grazing Incidence X-ray Diffraction along with Rietveld refinement and Williamson–Hall plot analysis, revealed competition between the cubic NiO phase and, presumably, the hexagonal Ni₂O₃ phase, depending on the substrate temperature, the dopant impurity, and its concentration. The impurity content in doped nickel oxide films was quantitatively analysed using spectra acquired through the energy dispersion x-ray spectroscopy and x-ray photoelectron spectroscopy, involving the processing by the National Institute of Standards and Technology's Desktop Spectrum Analyzer software for enhanced precision. The optical characterization techniques imply the use of ellipsometry at room temperature.

The synthesis of high-quality nickel oxide films doped across a broad concentration range and with various trivalent doping impurities has been achieved.

Keywords: nickel oxide, Metalorganic Aerosol Deposition, x-ray diffraction.

Acknowledgements: CNCS-UEFISCDI, project number 18ROMD/20.05.2024, project PN-IV-P8-8.3-ROMD-2023-0186, within PNCDI IV and MEC subprogram 011207

References:

- [1] R. Cao, H.-X. Deng, and J.-W. Luo, *ACS Applied Materials & Interfaces* **11**, 24837–24849 (2019).
- [2] M. Napari, T. N. Huq, R. L. Z. Hoye, J. L. MacManus-Driscoll, *InfoMat*. **3**, 536–576 (2021)

- [3] S. Hoffmann-Urlaub, U. Ross, J. Hoffmann, A. Belenchuk, O. Shapoval, V. et al, *Advanced Materials Interfaces* **8(7)**, 2002049 (2021).
- [6] M. Rada, S. Rada, E. Culea, Structural properties of the tungsten-lead-borate glasses before and after laser irradiation, *J. Non-Cryst. Solids* 357 (2011) 2024 –2028.
- [7] S. Rada, M. Zagrai, M. Rada, E. Culea, L. Bolundut, M.L. Unguresan, M. Pica, Spectroscopic and electrochemical investigations of lead –lead dioxide glasses and vitroceramics with applications for rechargeable lead–acid batteries, *Ceram. Int.* 42 (3) (2016) 3921–3925.
- [8] S. Rada, R. Chelcea, M. Rada, A. Bot, N. Aldea, V. Rednic, E. Culea, Electrochemical characterization and structure of tungsten-lead-germanate glasses and glass ceramics, *Electrochim. Acta* 109 (2013) 82 –88.
- [9] U. Hoppe, R. Kranold, A. Ghosh, C. Landron, J. Neuefeind, P. Jónvári, Environments of lead cations in oxide glasses probed by X-ray diffraction, *J. Non-Cryst. Solids* 328 (1 –3) (2003) 146 –156.
- [10] H. Wen, P.A. Tanner, B.M. Cheng, Optical properties of 3dN transition metal ion-doped lead borate glasses, *Mater. Res. Bull.* 83 (2016) 400–407
- [11] B. Sreedhar, C.H. Sumalatha, K. Kojima, ESR and optical absorption spectra of Ni(II) ions in lithium fluoroborate glasses, *J. Mat. Sci.* 31 (6) (1996) 1445 –1448
- [12] B. Johnson, N.R.K. Chand, B.K. Sundhakar, G.S. Rao, Chemical durability, thermal stability and spectroscopic studies of the influence of Ni²⁺ ions in oxy fluorophosphate glasses, *J. Mater. Sci. Mater. Electron.* 27 (2016) 8833–8847.

LOAD MODELING FOR MULTI-GENERATOR DISPATCH AND PROTECTION IN URBAN NETWORKS USING A FRACTAL DISPATCH MODEL

Ovidiu Postelnicu*, Dragos Bordescu, Emil Cazacu

Politehnical University Bucharest
 * ovidiu.postelnicu @osim.gov.ro

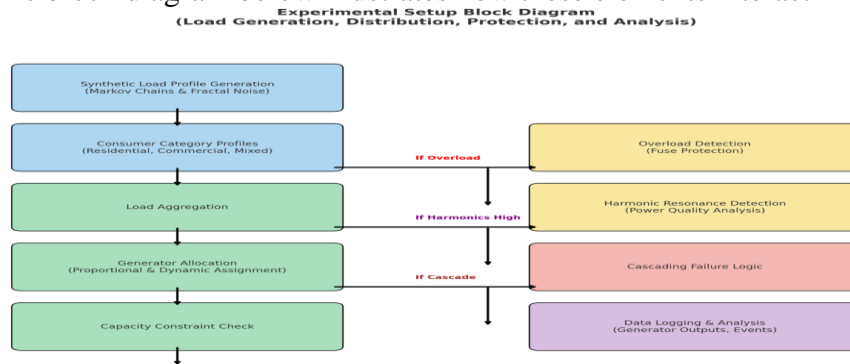
Through this work we introduce a **multi-generator load simulation** framework that unifies **Markov chain load transitions**, **fractal noise**, **generator dispatch**, and **protection logic** into a single update operator Φ . Specifically, at each time step t , the system's state $S(t)$ (including consumer loads, total demand, generator outputs, fuse statuses, and harmonic indicators) is mapped to $S(t+1)$ via:

$$S(t+1) = \Phi(S(t); P_{\text{Markov}}, \text{Noise}_{\text{fractal}}, \{C_i\}, I_{\text{fuse}}, \text{THD}_{\text{max}}). \quad (1)$$

where:

- $\mathcal{S}(t) = \{\ell_u(t), L(t), G_i(t), \text{FuseStates}(t), \text{Harmonics}(t)\}$
- P_{Markov} is the **Markov transition matrix** describing load-state evolution for each consumer.
- $\text{Noise}_{\text{fractal}}$ (e.g. $1/f$) introduces **long-range correlations** in load demand.
- $\{C_i\}$ denotes the **capacities** of multiple generators, used in **proportional dispatch**.
- I_{fuse} is the **current threshold** for fuse overload protection.
- THD_{max} is the **harmonic distortion limit** for resonance detection.

The block diagram below illustrates how these elements interact in the code:



Through iterative execution of this pipeline, the simulation captures **stochastic demand** (Markov + fractal), **adaptive generator control**, and **network protection** in a unified manner. Results highlight how correlated consumer fluctuations interact with capacity-limited dispatch, fuse overloads, and harmonic distortions, thereby informing more robust designs for **urban distribution networks**.

Keywords: Markov chain, fractal noise, multi-generator dispatch, fuse protection, harmonic resonance

References

[1] J. Kracík, H. Lavička, *Fluctuation analysis of high frequency electric power load in the Czech Republic*, arXiv:1602.05498(2016).
 [2] K. Mamun et al., *Markovian Models for Home Electricity Consumption*, SIGCOMM (2011).
 [3] H.C. Jeong et al., *Clustering of Load Profiles of Residential Customers*, Electronics 10(3), 290 (2021).
 [4] Y. Chen et al., *Control and Operation of Multiple Distributed Generators in a Microgrid*, Missouri S&T Thesis (2015)

TELLURITE GLASSES FOR TEMPERATURE SENSING

R. Yatskiv¹, P. Kostka², J. Grym¹, J. Zavadil²

¹*Institute of Photonics and Electronics, Czech Academy of Sciences, Chaberská 57, 182 51 Prague, Czech Republic*

²*Laboratory of Inorganic Materials, Joint Workplace of the University of Chemistry and Technology Prague and the Institute of Rock Structure and Mechanics of the Czech Academy of Sciences, V Holešovičkách 41, 182 09 Prague, Czech Republic*

Precise temperature determination is essential in many domains including medicine, military applications, and various technological and industrial processes. This is especially important in applications where the use of conventional contact sensors is limited due to, for example, exposure to strong electromagnetic fields, spatial limitations, extreme pressure conditions etc.

In this study, we explore the potential applications of erbium-doped tellurite glasses for temperature sensing. We demonstrate that the thermally uncoupled levels and Stark sublevels of Er³⁺ ions can be used in addition to the thermally coupled levels. We also demonstrate that these uncoupled levels offer the possibility to measure the temperature down to cryogenic temperatures (4 K and possibly below). Naturally, the optical properties of the investigated glasses depend on the glass composition and the concentration of embedded erbium ions, which opens the possibility to optimize the glass for its use in temperature sensing.

Keywords: tellurite glasses, optical temperature sensor, rare earths

References:

- [1] R. Yatskiv, P. Kostka, J. Grym, and J. Zavadil, *J Non-Cryst Solids* **575**, 121183 (2022), <https://doi.org/10.1016/j.jnoncrysol.2021.121183>
- [2] P. Kostka, R. Yatskiv, J. Grym, and J. Zavadil, *J Non-Cryst Solids* **553**, 120287 (2021), <https://doi.org/10.1016/j.jnoncrysol.2020.120287>

COMPARATIVE STUDY BETWEEN SEPIOLITE AND Mg₃Al-LAYERED DOUBLE HYDROXIDE AS CLAY-BASED MATERIALS USED IN WATER TREATMENT - A STATISTICAL APPROACH

Marina Alexandra Tudoran¹, Adina Căta¹, Nick S. Țolea¹, Antonina Lazăr¹, Ioana M.C. Ienașcu^{1,2} and Bogdan-Ovidiu Taranu¹

¹ National Institute of Research and Development for Electrochemistry and Condensed Matter, Dr. A.P. Podeanu Street, No. 144, 300569, Timisoara, Romania, e-mail:;

² "Vasile Goldiș" Western University of Arad, Faculty of Pharmacy, Liviu Rebreanu 86, 310045, Arad, Romania.

Water contamination is a pressing issue that can have far-reaching consequences for the environment, consumption patterns, agriculture, and industrial activities alike. A growing body of research has demonstrated that the presence of pharmacological contaminants in aquatic ecosystems is detrimental to ecosystem integrity, leading to a decline in biodiversity, particularly among microinvertebrates, and exerting toxicological effects on aquatic biota. However, conventional wastewater treatment techniques have proven ineffective in eliminating pharmaceutical compounds from water systems due to their low biodegradability and high hydrophilicity. In this context, adsorption technology has garnered significant interest due to its simplicity, cost-effectiveness, environmental sustainability, and high treatment efficiency [1-3]. Among the array of available adsorbents, clays have been identified as a particularly versatile option for water remediation applications, due to their non-toxic nature and cost-effectiveness [1,4]. Starting from these considerations, in the present study, a 2x3 factorial ANOVA was conducted to compare the adsorption density of sepiolite and Mg₃Al-LDH in solutions containing either 2-acetyloxybenzoic acid (aspirin) or 4-hydroxyacetanilide (paracetamol), at three distinct contact time intervals (5–10 minutes, 15–20 minutes, and 25–30 minutes). When a significant difference was identified, the Tukey procedure was employed to conduct multiple comparisons, with a significance level of $\alpha = 0.05$ [5]. In the case of *sepiolite*, the ANOVA results indicated a significant main effect for type of pharmaceutical compound, $F(1, 18) = 12659.3$, $p < 0.001$, a significant main effect for contact time, $F(1, 18) = 18.8$, $p < 0.001$, and a significant interaction between the type of pharmaceutical compound and contact time, $F(2, 18) = 31.6$, $p < 0.001$. This interaction was further investigated by conducting post-hoc tests. The results revealed no significant differences in contact time when 4-hydroxyacetanilide was used; however, a statistically significant difference was identified for 2-acetyloxybenzoic acid. The results of ANOVA for *Mg₃Al-LDH* demonstrated a significant main effect for both pharmaceutical compounds, with a value of $F(1, 18) = 683.3$, $p < 0.001$, as well as for contact time, with a value of $F(1, 18) = 44.1$, $p < 0.001$; the interaction between them was also significant $F(2, 18) = 87.5$, $p < 0.001$. According to the results of the post-hoc tests (employing the Tukey correction), no statistically significant differences were observed in contact time for 4-hydroxyacetanilide; however, for 2-acetyloxybenzoic acid, significant variations were detected.

Keywords: two-way ANOVA, adsorption density, clay.

References:

- [1] D. Ewis, M. M. Ba-Abbad, A. Benamor, M. H. El-Naas, *Appl. Clay Sci.* **229**, 106686 (2022).
- [2] D. B., França, L. S. Oliveira, F. G. Nunes Filho, E. C. Silva Filho, J. A. Osajima, M. Jaber, M. G. Fonseca, *J. Environ. Chem. Eng.* **10**, 107341 (2022).
- [3] F. Mansouri, K. Chouchene, N. Roche, M. Ksibi, *Appl. Sci.* **11**, 6659 (2021).
- [4] S. Khan, S. Ajmal, T. Hussain, M. U. Rahman, *Journal of Umm Al-Qura University for Applied Sciences*, 1-16 (2023).
- [5] R. S. de Souza, C. A. Sequeira, E. M. Borges, *J. Chem. Educ.* **101**, 5027-5039 (2024).

GUIDING CURVES FOR H-LIKE ATOMIC ORBITALS

Diana R. Radnef-Constantin¹, Sorin S. Radnef² and Valentin I. Niculescu³

¹*Astronomical Institute of the Romanian Academy
Strada Cuțitul de Argint 5, Bucharest 052034, Romania
ghe12constantin@yahoo.com*

²*INCAS – National Institute for Aerospace Research “Elie Carafoli”
B-dul Iuliu Maniu 220, Bucharest 061126, Romania*

³*National Institute for Lasers, Plasma and Radiation Physics, Atomistilor 409, Magurele, Ilfov, Romania*

Starting from the quantum model for the hydrogen-like atom and taking into account some concepts of differential geometry, we calculate the curvature of some types of atomic orbitals. Using this concept of intrinsic curvature [1], a geometric classification of atomic orbitals is given. We discuss the implications of characterizing atomic quantum states [2] by the geometric curvatures of the guiding curves for these orbitals.

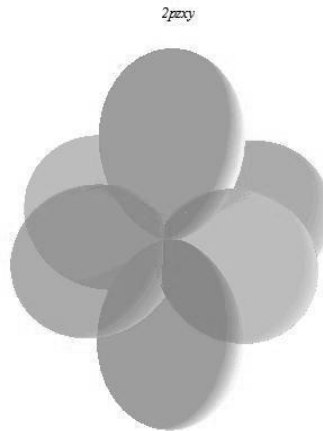


Figure 1: Superposition of the hydrogen-like orbitals $2p_x$, $2p_y$, $2p_z$

Keywords: atomic quantum physics; differential geometry; guiding curve; atomic orbitals.

References:

- [1] Sorin Stefan Radnef, *Incas Bulletin* **15**, 4, pp 211 – 219 (2023).
- [2] Diana Rodica Constantin et al., *Rom. Astron. J.* **30**, 1, pp 35-41 (2020).

PHASE TRANSITION OF PLASMA CRYSTALS INDUCES BY AN ELECTRON BEAM

Beatrice Paraschiv^{1,2}, Dorina Ticoș¹, Nicoleta Udrea¹, Maria Luiza Mitu¹, Adrian Scurtu¹, Mihai Oane¹, Catalin M. Ticoș^{1,3}

¹National Institute for Laser, Plasma and Radiation Physics, 077125 Magurele, Romania

²Faculty of Physics, University of Bucharest, 077125 Magurele, Romania

³Extreme Light Infrastructure-Nuclear Physics (ELI-NP), Horia Hulubei National Institute for R&D in Physics and Nuclear Engineering, 077125 Magurele, Romania

Plasma crystals are ordered structures of charged microparticles in complex plasmas that undergo phase transitions under external influences. While temperature and pressure effects are well-understood [1], the role of electron beam energy is less clear [2]. This study investigates a 2D plasma crystal of 11.8 μm melamine-formaldehyde particles in an argon RF plasma, melted by electron beams (10–14 keV). High-speed imaging enabled analysis through Voronoi diagrams, pair correlation functions, and particle tracking velocimetry. Results show that electron beam energy governs melting: at 9–10 keV, a second-order phase transition occurs, while at 11–14 keV, a first-order transition is observed, with melting times reducing from 8.33 to 0.208 seconds. Kinetic energy analysis confirms these transitions, highlighting the electron beam's role in plasma crystal dynamics with potential applications in astrophysics [3].

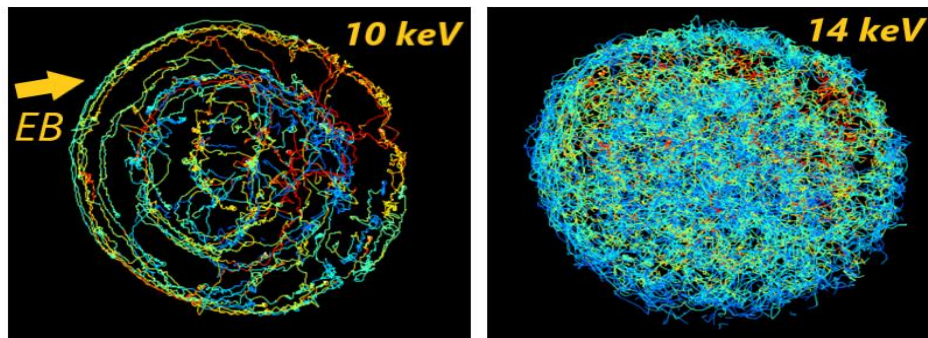


Figure 2: Particle trajectories tracked during the melting of a crystal in plasma, induced by an electron beam with energies of 10 keV and 14 keV.

Keywords: electron beam, plasma crystal, dusty plasma

References:

- [1] A. Melzer, A. Homann, A. Piel, *Phys. Rev. Lett.* **vol. 80**, 5345–5348 (1998).
- [2] C. M. Ticoș, D. Ticoș, M. L. Munteanu, N. Udrea Banu, A. Scurtu, *J. Plasma Phys.* **vol. 79**, 273–285 (2013).
- [3] G. E. Morfill, A. V. Ivlev, *Rev. Mod. Phys.* **vol. 81**, 1353–1367 (2009).

MEASURED SPECTRAL CHARACTERISTICS OF DIRECT NORMAL IRRADIANCE IN TIMISOARA, ROMANIA

Sergiu-Mihai Hategan^{1,2}, Marius Paulescu¹

¹Faculty of Physics, West University of Timisoara, Timisoara, Romania

²Institute for Advanced Environmental Research, West University of Timisoara, Timisoara, Romania

The efficiency of photovoltaic (PV) modules is evaluated under standard test conditions (STC). These conditions assume 1000 W/m^2 incident solar irradiance with a given spectral distribution AM1.5G, or AM1.5D in the case of direct normal irradiance [1]. Studying the influence of solar spectrum on PV module performance requires solar spectral irradiance measurements on a routine basis [2]. Most studies are concerned with simulated clear-sky spectral irradiance, due to the scarcity of spectral measurements. In the present study we investigate direct normal spectral irradiance, as measured in Timisoara, Romania, under various sky conditions.

At the Institute for Advanced Environmental Research, a newly installed EKO MS-711N spectroradiometer is available. The spectroradiometer has been in continuous operation since April 2024. The instrument operates in the 300-1100 nm range, taking measurements of direct normal irradiance (DNI) at 10-minute interval. In this study we analyze the spectral signature of the measured DNI spectra during the month of August 2024. The characteristics of direct solar irradiance are captured by the average photon energy (APE) index, which is usually calculated in the 350-1050 nm range [3]. Preliminary results show a difference between the measured APE values and the AM1.5D spectrum APE value.

Keywords: solar spectral irradiance, spectroradiometer, average photon energy.

References:

- [1] <https://www2.nrel.gov/grid/solar-resource/spectra-am1.5> (Accessed April 2025).
- [2] C. Cornaro, A. Andreotti, *Progress in Photovoltaics*, **21**, 996-1003 (2013).
- [3] B. R. Paudyal, S. G. Samasundaram, A. Louwen, A. H. M. E. Reinders, W. G. J. H. M. van Sark, D. Stellbogen, C. Ulbrich, A. G. Imenes, *Renewable Energy*, **224**, 120057 (2024).

SYMMETRICAL VORTICES AND LAMINAR DUST FLOW INDUCED BY AN ELECTRON BEAM IN STRONGLY COUPLED DUSTY PLASMA

D. Ticos¹, A. Scurtu¹, M.L. Mitu¹, N. Udrea¹, M. Oane¹, J. Williams², C.M. Ticos^{1,3}

¹ National Institute for Lasers, Plasma and Radiation Physics, Magurele, Ilfov 077125, Romania

² Physics Department, Wittenberg University, Springfield, Ohio 45501, USA

³ ELI-NP, Horia Hulubei National Institute for R&D in Physics and Nuclear Engineering, Magurele, Ilfov 077125, Romania

A quasi-two-dimensional dusty plasma, electrostatically confined in the sheath of a radio frequency plasma, is exposed to a 13 keV pulsed electron beam (e-beam) with a peak current of 30 mA per pulse. The e-beam's drag force induces a fast-moving stream of charged dust particles within the dust crystal, splitting into two symmetrical branches at the circular crystal boundary. These branches form a double vortex flow, with particles moving along the irradiation path, diverging laterally, and returning to the e-beam entry point. The flow remains laminar, with central region speeds peaking at 12 mm/s within 200 ms, then stabilizing at 5–6 mm/s over a 360 ms relaxation period. Vorticity peaks at $\pm 3.8 \text{ s}^{-1}$, settling to $\pm 2.5 \text{ s}^{-1}$ in the steady state. Time-resolved particle-image-velocimetry and particle-tracking-velocimetry characterize the flow, while molecular dynamics simulations qualitatively reproduce the observed dust stream and vortex patterns.

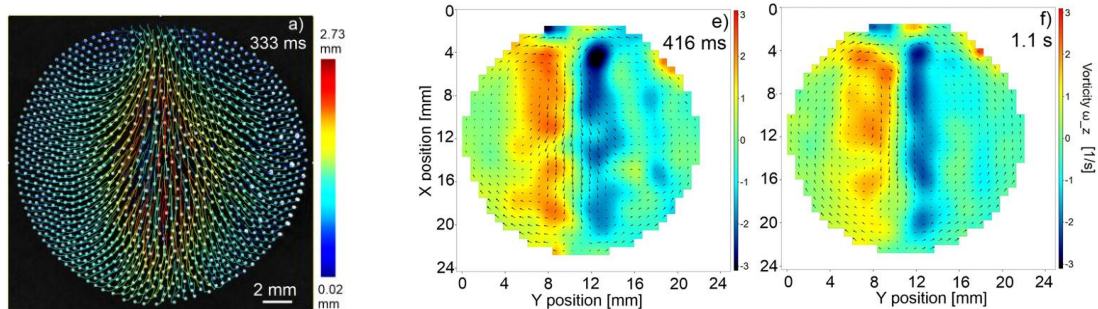


Figure 1: Trajectories of all dust particles obtained with PTV and time resolved vorticity maps in 2D.

Keywords: electron beams, dusty plasma, symmetrical vortices.

References:

- [1] D. Ticos, et all, *Sci. Rep.* **1**, 940 (2023).
- [2] C. M. Ticoș, et all, *Plasma Phys. Controlled Fusion* **62**, 25003 (2020).
- [3] D. Ticoș, et all, *Phys. Rev. E* **103**, 023210 (2021)

MACHINE LEARNING FOR A DUST CLUSTER ROTATION UNDER THE INFLUENCE OF AN ELECTRON BEAM

M.L. Mitu¹, D. Ticoș¹, N. Udrea¹, A. Scurtu¹, B. Paraschiv¹, C.M. Ticoș^{1,2}

¹ National Institute for Laser, Plasma and Radiation Physics, Atomistilor Street 409, Magurele, Ilfov 077125, Romania

² Horia Hulubei National Institute for R&D in Physics and Nuclear Engineering, 077125 Magurele, Romania

In this paper, we present a few significant results from the implementation of artificial intelligence (AI) techniques in the study of cold plasmas, with a particular focus on the dynamics of dust clusters levitated within such environments. We used a combination of clustering methods and statistical techniques to analyze and group the trajectories of microparticles in dust clusters levitated within cold plasmas, with the ultimate goal of identifying patterns and enabling predictions based on initial positions and other parameters. The methods chosen for trajectory clustering include K-means, DBSCAN, Hierarchical clustering. Each method was selected for its unique strengths in handling the complex, high-dimensional, and often noisy data generated from experimental observations of dust particle dynamics. Our study demonstrates the power of combining data science with experimental plasma physics to address challenges in manipulating levitated dust clusters. The predictive model not only enhances our ability to control dust dynamics in cold plasmas but also serves as a versatile tool for future research in dusty plasma systems.

Keywords: Artificial intelligence, machine learning, cold plasma.

References:

- [1] L., Wang, Q., Zhang, W., Liu, X., Chen, J., Li, Y., Xu, *Sci. Rep.* **9**, 5432 (2019).
- [2] C., Schirripa Spagnolo, S., Luin, *Int. J. Mol. Sci.* **25**, 8660 (2024).
- [3] J., Trieschmann, L., Vialetto, T., Gergs, *J. Micro/Nanopatterning Mater. Metrol.* **22**, 041504 (2023).

CYLINDRICAL PARTICLES LEVITATED IN LOW MAGNETIC FIELD PLASMA

N. Udrea¹, M.L. Mitu¹, P. Beatrice¹, D. Ticoș¹, A. Scurtu¹, C.M. Ticoș^{1,2}

¹ National Institute for Laser, Plasma and Radiation Physics, Bucharest 077125, Romania

² Horia Hulubei National Institute for R&D in Physics and Nuclear Engineering (IFIN-HH)

The dynamics of cylindrical nylon particles (300 μm in length and 5 μm in diameter) in a radiofrequency argon plasma (400 mTorr, 7 W) under a vertical magnetic field ($B_z \approx 14\text{--}19.5$ mT) were studied. The magnetic field was applied using a coil with the RF electrode as a ferromagnetic core. In the absence of the field, a stable ring was formed by charged particles ($2.34 \times 10^4 e$). However, the introduction of a magnetic field resulted in the induction of ring rotation, with a velocity ranging from 2 to 13 mm/s. The ring's maintenance was attributed to strongly coupled particles, while edge particles (distance > 0.8 mm) decoupled due to a reduced Coulomb force (1.8×10^{-15} N) in comparison to the ion drag force ($1.13\text{--}1.49 \times 10^{-10}$ N). These edge particles followed cycloidal trajectories. The dumbbell-like shape of the particles induced individual spin via torque, thereby highlighting the role of particle shape in dusty plasma dynamics.



Figure 1: Representative experimentally investigated particle trajectories.

Keywords: cylindrical particles, low magnetic field, cycloid.

References:

- [1] N. Banu, C. M. Ticoș, *Physics of Plasmas* **22**, 103704 (2015);
- [2] P.K. Kaw, K. Nishikawa, N. Sato, *Physics of Plasmas* **9**, 387–390 (2002)
- [3] A. V. Ivlev, et al. *Physical Review E*, **68**(2), 026405, (2003)
- [4] P. K., Shukla, & A. A. Mamun, *Institute of Physics Publishing* (2002).

API-P07

IMPACT OF INFERRING ATMOSPHERIC PARAMETERS ON SOLAR IRRADIANCE ESTIMATION

Jordan Ciucea, Andreea Sabadus and Marius Paulescu

Faculty of Physics, West University of Timisoara, Timisoara, Romania

This study focuses on the computation of solar irradiance available in a specific location using mean and interpolated atmospheric parameters values. A parametric solar irradiance model [1] derived from a spectral code is employed. The model uses only surface meteorological data as input parameters. The influence of averaging and interpolation of the atmospheric parameters on the model accuracy is evaluated. The analysis is performed on a dataset comprising ground-based measurements from the Solar Platform of the West University of Timisoara [2], complemented by atmospheric parameters obtained from the Aerosol Robotic Network (AERONET) [3]. Particular attention is given to the influence of Ångström turbidity coefficient, which is known to play a critical role in the attenuation of solar radiation when passing through the atmosphere. The results indicate that the use of mean values does not significantly compromise the overall accuracy of the solar irradiance estimates. However, due to the sensitivity of the model to aerosol-related parameters, it is advisable to employ interpolated values for the Ångström turbidity coefficient to enhance the accuracy of irradiance estimations under varying atmospheric conditions.

Keywords: solar irradiance, atmospheric parameters, Ångström turbidity coefficient.

References:

- [1] M. Paulescu, Z. Schlett, *Theor. Appl. Climatol.* **75**, 203-212 (2003).
- [2] Solar Platform of the West University of Timisoara, Romania <http://solar.physics.uvt.ro/srms>
- [3] Aerosol Robotic Network (AERONET) <https://aeronet.gsfc.nasa.gov>

EFFECTS OF HEADSPACE PRESSURE ON THE LEACHED BED REACTOR METABOLITE, HYDROGEN AND METHANE YIELD DURING TWO STAGE ANAEROBIC DIGESTION OF KITCHEN WASTE

Debkumar Chakraborty^{1,2}, Gorakhanath Jadhav^{1,5}, Anil Dhanda^{1,3}, Makarand Ghangrekar^{1,3*}, Abhishek Pitta², Ionel Balcu¹, Corina Macarie¹, Paula Sfirloaga¹, Narcis Duteanu^{1,4}

¹ Natl Inst Res & Dev Electrochem & Condensed Matter, 144 Dr A P Podeanu, Timisoara 300569, Romania

² Departments of Life Sciences, GITAM University, Visakhapatnam, AP, India, Pin 530045

³Department of Civil Engineering, Indian Institute of Technology Kharagpur, Kharagpur, West Bengal, India

⁴Polytech Univ Timisoara, Fac Chem Engn Biotechnol & Environm Protect, Victoriei Sq, 2, Timisoara 300006, Romania

⁵ School of Environmental Science and Engineering, Indian Institute of Technology Kharagpur, Kharagpur, West Bengal, India

The batch investigation into the redirection of acidogenic off-gas from the leach bed reactor (LBR) to the up flow anaerobic sludge blanket (UASB) reactor present a higher influence over the acidogenic leachate composition, leading simultaneously at an enhanced energy recovery in the form of gas production. LBR-off gas redirection affects the in-situ head space pressure into the acidogenic reactors, changing the quality of the leachate that is produced. Continuously maintaining head space pressure at 3 and 12 psi by injecting a premix bio-gas, is alter the metabolic pathway concomitant with the quality of the produced leachate inside of the used acidogenic reactor during anaerobic digestion of food waste.

Compared with 3 psi, hydrolysis, total soluble protein production (TSP) and acetogenesis performed better at 12 psi. Similar was observed that the cumulative COD yield varied in daily production rate being higher when the treatment was performed at 12 psi (559.2 g / Kg VS compared with 425.1 g / Kg VS). With variation in pH and VFA distribution, the cumulative TSP output was 294 and 362 g TSp / Kg VS for 3 and 12 psi, respectively. Lactate, acetate and ethanol provided over 95 % of volatile fatty acids (VFA) in studied cases during the first week. After this initial period, butyrate remains the only significant product that contributed over 80 % of VFA, indicating a real change into the metabolic pathway.

Keywords: food waste, dark fermentation, energy recovery.

Acknowledgements

This work was supported by the CF 39/28.07.2023, PNRR-III-C9-2023 I8: „Selective resource recovery from kitchen waste by integrated Dark Fermentation-Microbial electrolysis cell and ion substitution electro dialysis” project.

ALTITUDE ADJUSTMENT OF EMPIRICAL MODELS FOR ESTIMATING CLEAR-SKY SOLAR IRRADIANCE

Anamaria-Giulia Goilean, Eugenia Paulescu, Marius Paulescu

Faculty of Physics, West University of Timisoara, Romania

The estimation of clear-sky solar irradiance is a focal prerequisite in the evaluation of solar resources. This study reports on expanding geographical area of applicability of our empirical model G-EM for estimating clear sky global solar irradiance [1]. Although the model is of an empirical nature, the mathematical equations are inspired by the physics behind radiative transfer in the atmosphere [2]. G-EM requires as input only the geographical coordinates and the temporal reference. The pathlength of solar radiation through the atmosphere depends on the local altitude. Thus, the frozen coefficients in the G-EM model were replaced with dynamic coefficients, which capture the dependence of global solar irradiance on altitude. The study was conducted with synthetic data generated with PEM, a high performant clear sky solar irradiance model [3]. The results of testing the new model show a significant increase in accuracy in high altitude locations. Requiring only deterministic quantities as input, the new model effectively blends two key requirements in practice: high accessibility and reasonable accuracy.

Keywords: solar irradiance, empirical modeling, clear-sky, altitude.

References:

- [1] A. G. Goilean, E. Paulescu, M. Paulescu. Annals of West University of Timisoara – Physics 66(1) 241-250 (2024) , pp. 241-250.
- [2] Gueymard CA. SMARTS2 FSEC-PF-270-95 (1995)
<https://www.nrel.gov/grid/solar-resource/smarts.html>
- [3] E. Paulescu, M. Paulescu. Renewable Energy 179, 2094-2103 (2021).

INFLUENCE OF ATMOSPHERIC PARAMETERS ON BIOLOGICALLY EFFECTIVE SOLAR UV IRRADIANCE

Andrea-Florina Codrean, Marius Paulescu

Faculty of Physics, West University of Timisoara, Romania

Solar ultraviolet (UV) radiation has multiple effects, both positive and negative, on human beings. Modeling of solar UV spectral irradiance is carried out from various perspectives [1], being a current topic in research. In this study, the influence of the main atmospheric parameters, ozone and aerosol, on the level of biologically effective solar irradiance is analyzed. The study compares the action of UV radiation on the skin with the action on the retina. The analysis is performed using synthetic solar UV spectra generated with SMARTS2 [2], a high-quality spectral solar irradiance model. The novelties reported by this study: (1) a continuous equation for the biological action function associated with cataract, (2) increasing the wavelength density at which the synthetic UV spectra are defined and (3) a comparative analysis of the effective irradiances, depending on the class of atmospheric aerosol [3].

Keywords: UV solar irradiance; erythemal spectrum; cataract spectrum; aerosol; ozone

References:

- [1] Codrean A-F, Bunoiu OM, Paulescu M. Atmosphere 2025, 16, 427.
- [2] Gueymard CA. SMARTS2 FSEC-PF-270-95 (1995)
<https://www.nrel.gov/grid/solar-resource/smarts.html>
- [3] Blaga R, Calinoiu D, Paulescu M. J Renew Sustain Energy 13, 023701 (2021)

API-P11

HARNESSING HIGH-DENSITY PULSED PLASMA FOR SUSTAINED OXYGEN SUPPLY ON MARS

Adrian Scurtu¹, Dorina Ticoș¹, Constantin Diplășu¹, Nicoleta Udrea¹, Maria
Luiza Mitu¹, Beatrice Paraschiv¹, Cătălin M. Ticoș¹

¹ National Institute for Laser, Plasma and Radiation Physics, Bucharest 077125, Romania

For producing oxygen on Mars to support human exploration, high-intensity pulsed plasma jets, characterized by electron densities [1-2] around 10^{21} m^{-3} and electron temperatures up to 13 eV, were employed to dissociate CO₂ at Martian pressures (1–5 Torr). Operating a plasma gun at discharge voltages of 1–2 kV, peak oxygen yield was observed at 2 kV (~0.03 g per 10 pulses), with maximum energy efficiency of 49.94 Wh/g at 1 kV. The dissociation mechanism involved two electron groups: one driving direct CO₂ breakdown and another facilitating vibrational excitation, potentially enhanced by ions accelerated to km/s speeds. In a high-repetition, high-voltage setup with rapid capacitor charging, an oxygen production rate of approximately 137 g/hour is projected.

Keywords: intense plasma jets, CO₂ dissociation, Mars.

References:

- [1] A. Scurtu et al., Splitting CO₂ in Intense Pulsed Plasma Jets. *Int. J. Mol. Sci.* 24, (2023). <https://doi.org/10.3390/ijms24086899>
- [2] A. Scurtu et al., Thrust of a pulsed plasma jet measured from deviations of a ballistic pendulum. *Phys. Scr.* 99, 095607 (2024). <https://doi.org/10.1088/1402-4896/ad6b4d>

ENHANCED DIELECTRICS IN FLEXIBLE PEROVSKITE COMPOSITES

Cătălin Nicolae Marin¹, Daniel Ursu², Marinela Miclău², Iosif Mălăescu^{1,3}, Cristian Casut^{1,2}

¹West University of Timisoara, Bulevardul Vasile Pârvan 4, Timișoara 300223 Timisoara, Romania

²National Institute for Research and Development in Electrochemistry and Condensed Matter—INCEMC, A. Paunescu Podeanu Street, no. 144, 300569 Timisoara, Romania

³Institute for Advanced Environmental Research, West University of Timisoara (ICAM-WUT), Oituz Str., No. 4, 300086 Timisoara, Romania

In this work, we investigate the electrical and dielectric properties of silicone rubber composites doped with a perovskite-phase material, BiFeO₃ (BFO). A series of samples with varying BFO content were prepared and characterized to evaluate the influence of the dopant on conduction mechanisms.

Conductivity measurements were analyzed using both the Arrhenius and Correlated Barrier Hopping (CBH) models. Activation energies (E_a) extracted from Arrhenius fitting ranged between 0.2–0.4 eV, indicating thermally activated hopping.

Additionally, barrier heights (W_m) derived from CBH analysis revealed an inverse correlation with conductivity, confirming the role of shallow localized states introduced by the BFO phase. Dielectric measurements further supported these findings, showing enhanced dielectric constants and reduced loss in the most conductive samples. The sample with the lowest E_a also exhibited the best conductivity performance, suggesting optimized charge transport pathways due to the perovskite filler.

In conclusion, we found that by tuning the dopant concentration, it is possible to control the electrical and dielectric properties of the composite. This tunability points to the potential use of BFO-doped silicone rubber in flexible electronic devices, where tailored conductivity and dielectric response are essential.

Keywords: perovskite, electrical properties, flexible composites

Acknowledgements: The authors acknowledge support given by the West University of Timisoara.

References:

1 - Teusdea, A.; Malaescu, I.; Sfirloaga, P.; Marin, C.N., *Materials* 2022, 15(6), 2309 <https://doi.org/10.3390/ma15062309>

2 - Marin, C.N.; Malaescu, I.; Sfirloaga P.; Teusdea, A.; *JIEC*; 2021, 101, 405-413 <https://doi.org/10.1016/j.jiec.2021.05.042>

IMPROVING DYE-SOLAR CELL EFFICIENCY VIA TiO₂ PASTE BALL-MILLING

Daniel Ursu¹, Melinda Vajda¹, Cristina Mosoarca¹, Marinela Miclau¹, *Cristian Casut*^{1,2}

¹National Institute for Research and Development in Electrochemistry and Condensed Matter, Dr. A. Păunescu-Podeanu Street, no. 144, 300569 Timișoara, Romania;

²Physics Faculty, West University of Timisoara, V. Pârvan Ave., no. 4, 300223 Timișoara, Romania

This study presents a method to boost dye-sensitized solar cell (DSSC) efficiency without altering the TiO₂ photoanode structure or dye composition. By optimizing the ball-milling process of TiO₂ paste using 12 mm balls, we achieved smaller crystallite sizes and increased surface OH groups, enhancing energy conversion.

The TiO₂ paste ball-milling process was optimized for indoor lighting for the first time, enhancing both efficiency and cost-effectiveness through a fast, industrially scalable preparation method for DSSC production.

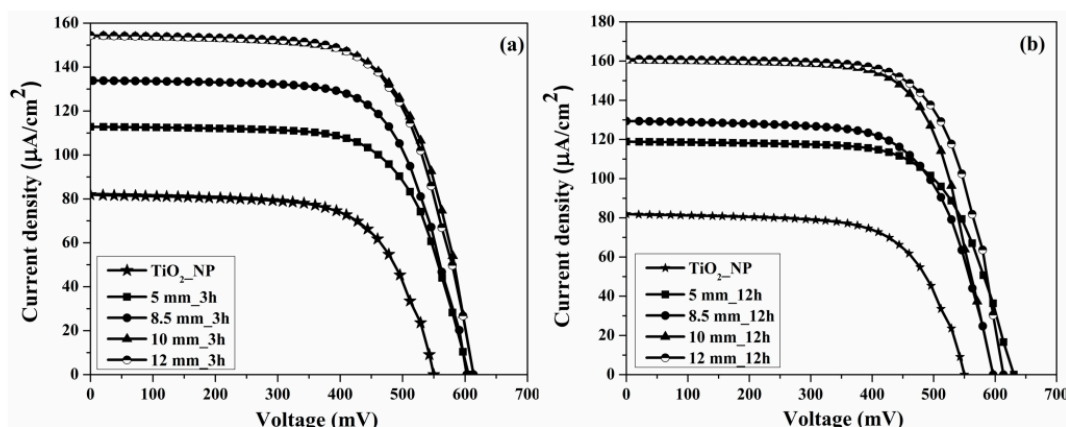


Figure 1: J-V measurements of DSSCs for TiO₂ paste untreated (TiO₂_NP) and obtained from paste milled with 5 mm, 8.5 mm, 10 mm, and 12 mm balls at different rotation time (a) 3 h and (b) 12 h, under 1000 lux illumination.

Our study presents a simple, cost-effective approach that enhances DSSC efficiency under indoor lighting by ~112.3%, without the need for complex TiO₂ architectures or new dye designs.

Keywords: photovoltaics; dye-sensitized solar cell; ball-milling process; TiO₂ surface

Funding: This work was supported by a grant from the Ministry of Research, Innovation and Digitization, CCCDI-UEFISCDI, Project No. PN-III-P2-2.1-PED-2021-0624, within PNCIDI III and project PN 23 27 01 03.

SMARTPHONE DETECTABLE COLOR DEPENDENT TIME RESPONSES OF STRONTIUM ALUMINATES PHOSPHORS

T.Eftimov^{1,2}, V.Vitola³, K.Krizmane³, G K.Nikolov² and S.Fouzar^{1,4}

¹ Université du Québec en Outaouais, 101 rue St-Jean Bosco, Gatineau, J8Y 3G5 Québec, Canada Central

² Laboratory for Applied Physics, BAS, 61 Blvd Sanct Peterburg, 4000, Plovdiv, Bulgaria

³ Institute of Solid State physics, University of Latvia, Ķengaraga iela 8, Latgales priekšpilsēta, Rīga, LV-1063, Latvia

⁴ Centre de Développement des Technologies Avancées CDTA, Baba Hassen, Algiers 16303, Algeria

We report on the ON/OFF time responses of seven Eu/Dy doped strontium aluminates synthesized with different alkaline hydroxide and carbonate precursors: #1 (HMTA), #2 (LiOH), #3 (KOH), #4 (NaOH), #5 (K₂CO₃), #6 (Na₂CO₃) and #7 ((NH₄)₂CO₃). The responses (Fig. 1a,b,c) were measured with a smartphone (Xiaomi, 11T Pro) and a 1000 line/mm transmission diffraction grating which allow measurements of the time responses in the blue, green and red part of the spectrum.

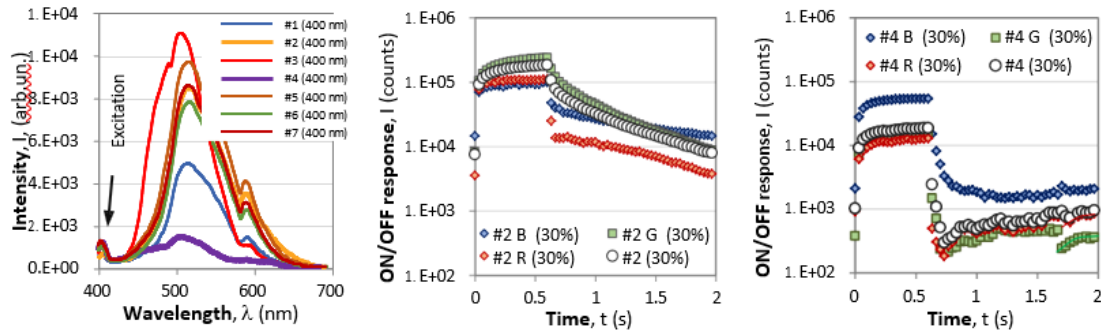


Figure 1: a) Spectral distributions of all the samples and RGB responses of sample #2 - b) and #4- c.)

The spectra of the samples are shown in Fig 1a) and the time responses from the R (red, 460nm), G (green, 510nm) and B (blue, 600 nm) pixels and the overall grey response for samples #2 and #4 - in Fig. 1 b) and c). They reveal that the different spectral components of the luminescence significantly differ from one another [1]. For sample #2 the overall time response is close to that of the dominant green component, follows a power law and is weakly affected by the red component which exhibits an exponential decay. In contrast, sample #4 exhibits a rise behavior following a power law, but the decay responses behave differently. A closer look reveals that the weaker red and green spectral components first exhibit a fast drop of the intensity caused by the disappearance of fluorescence and then the intensity rises periodically to some saturation level, followed by a fast drop and a subsequent re-charging and decays. The main blue component behaves similarly, but over a larger time scale. The results are indicative of the excitation/relaxation dynamics inside the phosphor and can be used for color time-dependent multi-level and multimodal encoding and sensing [2].

Keywords: color dependent time responses, smartphone interrogation.

Acknowledgments are due NSERC DDG grant, Canada and the EU's Horizon 2020 Framework Program, project LZP-2023/1-0521.

References:

- [1] S. Fouzar, I. Kostova, T. Eftimov, A. Benmounah, M. Ouchabane, A. Lakhssassi, *J Mater Sci: Mater Electron*, **33**, 20962–20980, (2022).
- [2] Y. Lu et al., *Nature Photonics*, **8**, 32-36, (2014).

MICROBIOLOGICAL EVALUATION OF THE BACTERICIDAL POTENTIAL OF $\text{Y}_2\text{SiO}_5:\text{Pr}^{3+}$ AND DERIVED POLYMER COMPOSITES

Cristina Moșoarcă¹, Radu Bănică¹, Miroslav D. Dramićanin^{1,2}, Željka Antić^{1,2},
Mirela I. Iorga¹

¹National Institute of Research and Development for Electrochemistry and Condensed Matter, INCEMC, Str. Dr. A.Păunescu Podeanu nr.144, 300569 Timisoara, Romania

²Centre of Excellence for Photoconversion, Vinča Institute of Nuclear Sciences—National Institute of the Republic of Serbia, University of Belgrade, Mike Petrović 12-14, 11000 Belgrade, Serbia

Ultraviolet C (UVC) radiation is extensively applied in antimicrobial treatments due to its ability to induce DNA damage in microorganisms and plays a critical role in the decontamination of water, food, and environmental systems [1]. Blue-to-UVC upconversion (UC) offers the potential to harness readily available and cost-effective blue light sources [1] for antimicrobial and related applications [2, 3]. This study presents a microbiological assessment of the bactericidal potential of $\text{Y}_2\text{SiO}_5:\text{Pr}^{3+}$ and its corresponding polymer-based composites, evaluating their effectiveness against *E. coli* ATCC 8739 through various microbiological assays. FTIR spectroscopy, X-ray diffraction (XRD), and photoluminescence (PL) spectroscopy were employed to characterize the $\text{Y}_2\text{SiO}_5:\text{Pr}^{3+}$ compound and investigate its optical properties, demonstrating its capability for upconversion. For the microbiological assay, the culture medium was prepared, and bacterial pellets were hydrated prior to irradiation. The experiment was carried out in two ways. In the first variant, Y_2SiO_5 was mixed directly with the bacterial suspension, which was not exposed to light. In the second variant, a composite material was created by dispersing $\text{Y}_2\text{SiO}_5:\text{Pr}^{3+}$ in polydimethylsiloxane, which was deposited as a thin film on the inner surface of the reactor before illumination. In the second experiment, two controls were used for comparison: a glass surface without the added material and a negative control made up of a bacterial suspension that wasn't exposed to radiation.

The viable colonies were observed macroscopically, and their growth rate was analyzed in relation to the irradiation through the PDMS/ $\text{Y}_2\text{SiO}_5:\text{Pr}^{3+}$ membrane deposited on glass. The results of the first experiment confirm the moderate toxicity of $\text{Y}_2\text{SiO}_5:\text{Pr}^{3+}$ on *E. coli*. The second experiment confirms that the composite material is non-toxic and that illumination through it leads to a reduction of approximately 25% in the concentration of viable bacteria.

Acknowledgments: This study was supported by Romania's National Recovery and Resilience Plan, NRRP, project grant number C9-I8-28/FC 760107/2023.

References:

- [1] M.D. Dramićanin, M.G. Brik, Ž. Antić, R. Bănică, C. Moșoarca, T. Dramićanin, Z. Ristić, G.D. Dima, T. Förster, M. Suta, *Nanomaterials* **15**, 562 (2025)
- [2] E.L. Cates, A.P. Wilkinson, J.H. Kim, *J. Lumin.* **160**, 202–209 (2015)
- [3] C. Wang, Y. Tang, G. Pu, W. Chen, M. Deng, J. Wang, *Ceram. Int.* **50**, 30579–30586 (2024)

COMPARATIVE STUDY OF YBO₃ PREPARED BY COMBUSTION AND SOLID-STATE METHODS

Radu Banică¹, Cristina Moșoarcă¹, Miroslav D. Dramićanin^{1,2}, Željka Antić^{1,2},
Mirela I. Iorga¹, Mihai-Petru Marghitas^{1,3}

¹National Institute of Research and Development for Electrochemistry and Condensed Matter, INCEMC, Str. Dr. A. Păunescu Podeanu nr.144, 300569, Timisoara, Romania

²Centre of Excellence for Photoconversion, Vinča Institute of Nuclear Sciences—National Institute of the Republic of Serbia, University of Belgrade, Mike Petrović 12-14, 11000, Belgrade, Serbia

³Politehnica University Timisoara, Department of Mechanics and Strength of Materials, Blvd. M. Viteazu No. 1, 300222, Timisoara, Romania

Ultraviolet C (UVC) radiation, due to its special properties, has gained significant and modern applications, including the decontamination of the environment, water and food, cancer therapy, photocatalysis, and the development of invisible identification tags [1]. Materials that exhibit emission in the UVC range through up-conversion under visible light excitation have the potential to significantly reduce the cost of biological water purification. YBO₃ and YAl₃(BO₃)₄ are promising host materials for rare-earth-doped phosphors. A key advantage of these hosts is their transparency in the UVC domain, along with high chemical durability. In the case of YAl₃(BO₃)₄, nonlinear optical properties are also present [2]. The UVC transparency of YBO₃ was previously exploited by X. Zhao et al. [3] in the synthesis of YBO₃:Pr, which showed UVC emission at 263 nm and 274 nm when excited with a 447 nm laser. The combustion method offers advantages such as rapid reaction rates due to high reaction temperatures. Specifically, solution combustion synthesis ensures good precursor homogenization and yields compounds with high specific surface area due to a larger volume of gas release compared to conventional combustion methods. This reduces the need for post-synthesis grinding of the phosphors.

In the present work, a comparative study was performed between the synthesis of YBO₃ by solution combustion using ammonium nitrate as an oxidizer and the solid-state method. It was observed that a temperature of 450 °C is sufficient to ignite the precursor mixture; however, the heat released during the reaction is not enough to form pure-phase YBO₃ in a single step. A phase separation occurs before reaching the ignition point, such that a subsequent thermal treatment at 1000 °C leads to the formation of YBO₃ as the main phase. The final phase composition depends on the maximum temperature reached during combustion. In contrast, the solid-state method yields pure-phase YBO₃ directly. These findings point to the necessity of modifying the solution combustion synthesis route in order to prevent the formation of non-stoichiometric intermediate phases prior to ignition.

Acknowledgments:

This study was supported by Romania's National Recovery and Resilience Plan, NRRP, project grant number C9-I8-28/FC 760107/2023.

References

- [1] M.D.Dramićanin, M.G.Brik, Ž.Antić, R.Bănică, C.Mosoarca, T.Dramićanin, Z.Ristić, G.D.Dima, T.Förster, M.Suta, *Nanomaterials* **15**, 562 (2025).
- [2] Yadav, P.J., Meshram, N.D., &Maharil, S.V. *Optical Materials: X*, 19, 100252 (2023).
- [3] Zhao, X., Liu, F., Shi, T., Wu, H., Zhang, L., Zhang, J., Wang, X., & Liu, Y.*Advanced Photonics Research*, **3**(10), 2200106 (2022).

CRYSTAL GROWTH OF RARE EARTH SESQUIOXIDES

Maximilian Mangra¹, Kesavan Venkatachalam¹, Tiana Ile¹, Gabriel Buse², Daniel Vizman¹,
Philippe Veber^{1,2}

¹Faculty of Physics, Crystal growth laboratory, West University of Timisoara (Romania)

²Institute for Advanced Environmental Research (ICAM), West University of Timisoara (Romania)

Rare-Earth (RE) sesquioxides are a well-known class of compounds recognized for their improved intrinsic properties, in particular their high optical performance in the VIS-NIR range and their significant physicochemical characteristics, such as their non-hygroscopic and non-hazardous nature. For optical applications, RE-sesquioxides single crystals with a cubic structure offer significant advantages such as optical isotropy, chemical stability, and the ability to be easily doped with other rare-earth cations [1,2]. However, growing these materials as bulk single crystals is challenging due to their high melting points and the presence of several structural phase transitions with temperature [3]. In this work, we present the historical and current approaches for growing RE-sesquioxide crystals, highlighting the most commonly used growth methods (Figure 1) and the main areas of application. In the following, a particular attention is paid to cubic Tb₂O₃, a promising material for magneto-optic applications and for the control of polarization rotation in solid-state lasers [3-4]. The most efficient method for its crystal growth, the flux method, is presented in detail.

The authors acknowledge the financial support from the PNRR-III-C9-2022-I8 grant “Enhanced single crystal Applications and Research in the growth of new optical rare earth-based compounds for sustainable and efficient Technologies (ESCARGOT)” (n°: 760080/23.05.2023), for the development of this research field.



Figure 1. Czochralski furnace for rare-Earth sesquioxide growth at ICAM

Keywords: rare-Earth sesquioxide, crystal growth, Tb₂O₃, flux method

References:

- [1] N. Sarukura *et al.*, Handbook of Crystal Growth (Second Edition) Bulk Crystal Growth, Chapter 4, 131-168 (2015)
- [2] G. Adachi *et al.*, Binary Rare Earth Oxides (2004). Springer Dordrecht
- [3] P. Veber *et al.* CrystEngComm, **17** (3), 492-497 (2015).
- [4] P. Veber *et al.*, Luminescence and Faraday Rotation Properties of Tb₂O₃ and Tb:Y₂O₃ Single Crystals, Opt. Mater. (Amst). **157**, 116264 (2024).

CHARACTERIZATION OF MATRICEAL PROTEINS IN THE SHELL OF MARINE RAPANA SNAILS

M.C. Belc¹, I.M.Stanescu²

¹*Ovidius University of Constanta, Applied Sciences and Engineering Faculty, Physics Department*

²*Ovidius University of Constanta, Mechanical, Industrial and Marine Engineering Faculty, Naval and Energetic Engineering Department*

Mollusks are soft-bodied animals and to protect themselves, during their evolution they elaborate an external calcified rigid structure, the shell. The shell fabrication requires a specialized cellular mechanism, which are strictly under the control of many genes which elaborates enzymes for the mineralization process. The calcium carbonate micro crystals that form the shell structure differ in their shape and size from their inorganically formed counterpart, and their shapes are generally complex. These crystals assemble according to different levels of hierarchy being synthesized under special micro environment conditions.

Our results revealed differences of microstructure in the two organism's shells which encourage us to continue our studies regarding the enzymatic properties of the matrix proteins in *Rapana venosa* shell.

Nowadays there is a big interest regarding shell structure of mollusks. These structures serve as models for developing bio-mimetic materials having applications in various fields such as medical prosthetic materials (dental and bone implants). The mollusk shell is formed in a self-organized manner from relatively fragile components arranged in complex hierarchical structures. Such material is characterized by strength and toughness. The best known and studied microstructure of mollusk shell is nacre, the iridescent, aragonite layer, which covers the inner part of most mollusks species. Nacre is a biogenic polymer, a mineral composite formed during a self-assembling process. It is composed by two phases: a mineral one (95%) and an organic one, disposed in a highly organized structure as a brick wall pattern. This structure lead to a material 3000 times tougher than its components. The mineralization process is controlled by the organic matrix (5% of the material). The understanding of the process and the mechanisms which are involved in the formation of nacre has as final purpose the creation of new materials with similar structure and properties. In our study we focused on the primary characterization of shell matrix structure from the Black Sea gastropod *Rapanavenosa*.

IRON OXIDE MICROFIBERS: MANUFACTURING, CHARACTERIZATION AND APPLICATIONS

Madalin Bunoiu¹, Liviu Chirigiu², Eugen Anitas^{3,4}, Gabriel Pascu¹ and Ioan Bica¹

¹West University Timișoara, V. Parvan 4, Timișoara 300223, Romania

²University of Medicine and Pharmacy of Craiova, Petru Rareș 2, Craiova 200349, Romania

³Horia Hulubei National Institute of Physics and Nuclear Engineering, Bucharest-Măgurele 077125, Romania

⁴Joint Institute for Nuclear Research, Joliot Curie 6, Dubna 141980, Moscow Region, Russian Federation

Iron oxide microfibers (Fig.1a) are typically obtained through the thermal decomposition of a mixture composed of silicone oil, carbonyl iron microparticles, and iron pentacarbonyl. [1] They consist of α -Fe₂O₃ (~12 wt%), γ -Fe₂O₃ (~62 wt%), and Fe₃O₄ (~26 wt%) [2,3]. Morphologically, microfibers appear as chains of microparticles (Fig.1b), with diameters from 0.25 μ m to 2.20 μ m. The specific saturation magnetization of these iron oxide microfibers [2,3] is 22.7 Am²/kg, measured at a magnetic field intensity 477 kA/m.

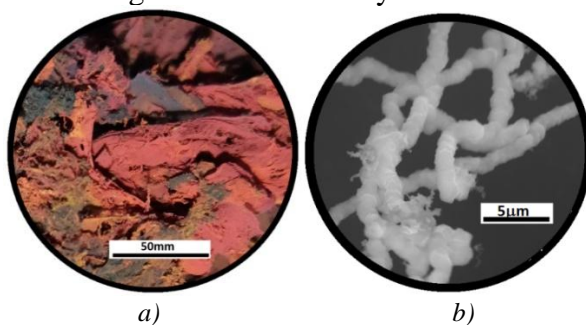


Figure 1: a) Bulk iron oxide microfibers [2]. b) SEM analysis of iron oxide microfibers [2].

Magnetorheological suspensions are obtained by dispersing iron oxide microfibers into silicone oil. These suspensions are used to manufacture electrical circuit components [2] in which the electrical conductance and susceptance can be coarsely adjusted through the volumetric ratio between the microfibers and the silicone oil. In contrast, the fine-tuning is achieved by varying the magnetic flux density, which enables their application in remotely controlled switching circuits. A relation is also shown between viscosity and magnetodielectric effects, a property that proves useful in controlling vibration and oscillation damping in dampers built using such suspensions.

By absorbing these suspensions into cotton-based textiles, hybrid composite materials can be obtained. These materials serve as the basis for the fabrication of passive electrical circuit elements [3], whose equivalent capacitance and resistance vary in a synchronous way with stepwise changes in the applied magnetic field and are sensibly influenced by the field intensity - a behavior that can be exploited in the design of magnetically tunable electrical modules.

Keywords: iron oxide microfibers, magnetorheological suspension, hybrid composite materials.

References:

- [1] I. Bica, E. M. Anitas, H. J. Choi and P. Sfirloaga, *J. Mater. Chem. C* **8**, 6159-6167 (2020).
- [2] Q. Lu, M. Balasoiu, H. J. Choi, E. M. Anitas, I. Bica, and L. M. E. Chirigiu, *J. Ind. Eng. Chem.* **112**, 58-66 (2022).
- [3] I. Bica, E. M. Anitas, H.-J. Choi, and S. Wang, *Micromachines* **14**, 2061 (2023).

API-P20

A PARAMETRIC MODEL FOR ESTIMATING SOLAR ENERGY FLUX UNDER CLEAR-SKY CONDITIONS

Viviana Sîrbu¹ and Eugenia Paulescu¹

¹*West University of Timisoara, V. Pârvan 4, 300223 Timișoara, Romania*

Balancing accuracy and accessibility in solar energy flux estimation models remains a key challenge in radiative transfer research and solar engineering. The proposed model is derived from a clear-sky spectral model that accurately estimates the three components of spectral solar irradiance—direct normal, diffuse, and global—at the ground level under clear-sky conditions. Given that the use of spectral models involves computationally intensive spectral calculations, a widely adopted simplification strategy is to parameterize atmospheric spectral transmittances using various wavelength-averaging formulations. The procedure used to develop our parametric model for estimating solar energy flux under clear-sky conditions involves two main stages. The first stage consists of deriving discrete broadband transmittances through an independent integration scheme applied to the spectral transmittances provided by the source spectral model. The second stage involves fitting these results to obtain continuous broadband atmospheric transmittances, expressed as analytical expressions that depend solely on atmospheric state parameters, independent of wavelength. The new parametric model is validated through testing on a dataset measured across various climatic regions. The results obtained support the characterization of the new model as highly accurate and straightforward to implement.

Keywords: parametric model, spectral model, clear-sky.

DYNAMIC XENON RESPONSE IN A CANDU-600 REACTOR: A SIMULATION STUDY OF POWER VARIATIONS

Andrei Stan¹ and Geoşchun Ferat²

¹*Cernavodă Nuclear Power Plant (stanandrei50@gmail.com)*

²*(feratgeo@gmail.com)*

This paper presents a comparative simulation study of xenon and fission product behavior in a CANDU-600 reactor core operating at nominal full power (100%) and an aging CANDU-600 core limited to 90% power due to end-of-life constraints. The analysis includes not only steady-state operating conditions but also transient phases such as shutdown and start-up, where xenon dynamics significantly impact reactivity management.

Using theoretical reactor physics simulations, the study investigates xenon reactivity worth in both reactor conditions, with particular attention to the influence of fission product buildup and depletion. The simulations are supported by detailed evaluations of the reactivity compensation provided by the Liquid Zonal Controllers (LZCs), Adjuster Banks and Mechanical Control Absorbers (MCAs). The results highlight that while the 90% power core experiences reduced xenon production, it exhibits higher sensitivity to xenon-induced reactivity swings, particularly during power maneuvers and recovery from shutdown.

The total reactivity worth of xenon, in conjunction with the control mechanisms, is quantified throughout the operational cycle. The findings reveal a tighter reactivity balance and reduced control flexibility in the aged core, emphasizing the increasing operational constraints as the reactor approaches end-of-life. These insights are critical for refining control strategies, ensuring safe operation, and optimizing performance across the full power range and operational scenarios of CANDU reactors.

Keywords: CANDU-600, reactor physics, fission products.

References:

- [1] U.S. Department of Energy, *DOE Fundamentals Notebook, Nuclear Physics and reactor theory* (1993)
- [2] Atomic Energy Control Board of Canada, *Fundamentals of Power Reactors, Module two Nuclear Reactor Systems* (1993)
- [3] Editor-in-Chief Wm. J. Garland, *The Essential CANDU, A Textbook on the CANDU Nuclear Power Plant Technology* (2014)
- [4] N. Mihăilescu, *Teoria Reactoarelor Nucleare* (2003).

STRUCTURAL AND PHOTOPHYSICAL PROPERTIES OF THE 1-HYDROXYXANTHONE MOLECULE

Stefania Stepanov¹, Ioana Andreea Scutelnicu¹, Maria Bischin², Elena Bogdan², Monica Focșan¹, João P. Prates Ramalho³, Vasile Chiș¹

¹*Babeș-Bolyai University, Faculty of Physics, Department of Biomolecular Physics, 1 M. Kogălniceanu 1, 400084 Cluj-Napoca, Romania;*

²*Babeș-Bolyai University, Faculty of Chemistry and Chemical Engineering, Department of Chemistry and SOOMCC, Cluj-Napoca, 11 Arany Janos, 400028, Cluj-Napoca, Romania;*

³*Department of Chemistry, School of Science and Technology, University of Évora, Rua Romão Ramalho, 59, 7000-671 Évora, Portugal;*

This study presents a comprehensive investigation of the structural and spectroscopic properties of the 1-hydroxyxanthone (1HX) molecule. This organic compound exhibits interesting characteristics, including the ability to undergo excited-state intramolecular proton transfer (ESIPT) [1] and demonstrates promising potential for biomedical applications [2].

A combination of experimental and computational approaches was employed to explore the conformational landscape of 1HX, as well as its Raman spectrum, and the absorption and fluorescence properties. Computational data have been obtained by using density functional theory (DFT), with various exchange-correlation functionals and basis sets.

Correlation experimental data with computational results enabled a reliable assignment of the Raman spectrum and a detailed characterization of the photophysical properties of both the ground and excited states of 1HX.

By examining the molecular geometry across different states and phases, predicting spectral properties and describing quantitatively the ESIPT process, this work provides new insights into the behavior of the 1HX, supporting its relevance for future biomedical applications.

Keywords: 1-Hydroxyxanthone, Raman spectroscopy, Photophysics, ESIPT.

References:

- [1] Lukeman, M., Burns, M.D. and Wan, P., 2011. Excited state intramolecular proton transfer in 1-hydroxypyrene. *Canadian Journal of Chemistry*, 89(3), pp.433-440.
- [2] Lai CS, Li S, Miyauchi Y, et al. Xanthenes from mangosteen extracts as natural chemopreventive agents: potential anticancer drugs. *Curr Mol Med*. 2011;11(8):666- 677.
- [3] J. A. Preston, E. Parisi, B. Murray, A. I. I. Tyler, E. Simone, *Cryst. Growth Des.* 24, 3256–3268 (2024).

POLARIMETRIC MAGNETIC FIELD SENSOR BASED ON MAGNETO-OPTIC GLASS WITH SMARTPHONE DETECTION

K.Nikolov¹, E. Dinkov¹, T.Eftimov^{2,1}, G.Dyankov^{3,1} and S.Fouzar^{2,4}

¹ Central Laboratory for Applied Physics, BAS, 61 Blvd Sanct Peterburg, 4000, Plovdiv, Bulgaria

² Université du Québec en Outaouais, 101 rue St-Jean Bosco, Gatineau, J8Y 3G5 Québec, Canada

³ Institute of Optical Materials and Technology, BAS, Acad. Georgi Bonchev Str., Bl. 109, 1113 Sofia, Bulgaria

⁴ Centre de Développement des Technologies Avancées CDTA, Baba Hassen, Algiers 16303, Algeria

We report on the development of a three wavelength optical fiber polarimetric magnetic field sensor interrogated by a smartphone spectrometer (Xiaomi 11T Pro, Samsung A51 and a 1000 lines/mm transmission grating). A paramagnetic Faraday rotator glass (∅3.8 x 27mm, MR3-2, Xi'an Aofa Optoelectronics Tech Inc., PR China) was used as a sensing magneto-optic material whose wavelength dependence Verdet constant was measured and shown in Fig.1 a). Quartz-polymer fibers of 600 μm core diameter were used as lead-in from the sources and lead-out to the smartphone.

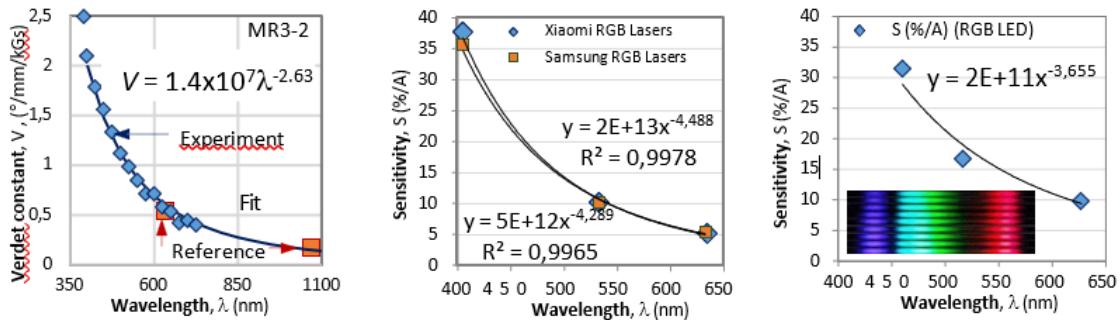


Figure 1: a) Spectral dependence of the Verdet constant; b) sensitivity of the sensor at three laser lines; c) sensitivity of the sensor at three LED lines (observed spectra in the inset)

The analyzer was oriented at 45° with respect to the polarizer to allow detection of the current polarity. Current changes produced variations ΔP around the zero-current intensity $P_0(\lambda)$ and the sensitivities $S = \Delta P/P_0/I$ for laser sources (405 nm LD, 532 nm DPSS and a 632.8nm He-Ne) and for a three wavelength (460 nm, 517 nm, 627 nm) combined LED are shown in Fig. 1b) and c). A photo of the observed spectra of the three color LED for $I = -1.8A$ to $+1.8 A$ is shown in the inset of Fig. 1c). The responses with the lasers exhibited higher sensitivities, compared to the broader-band LEDs because of the spectral dependence of the Verdet constant approximated by a power law function as $V(\lambda) = 1.4 \times 10^7 \lambda^{-2.63}$ (°/mm/kg). In both cases the $\Delta P/P_0$ vs. I dependence was found to be linear within the measurement range. As the sensitivities of the sensor in the visible vary by a factor of 7 to 8, the measurement range can be extended. The smartphone can simultaneously interrogate a large number of sensors and unlike the wavelength shift detection [1], this scheme does not require referencing.

Keywords: polarimetric magnetic field sensors, smartphone interrogation.

Acknowledgements are due to the National Science Fund of Bulgaria for financial support under Project КП-06-Н 48/2.

References:

[1] T. Eftimov, G. Dyankov, K. Nikolov, P. Kolev, D. Brabant, A. Sowa, *Results in Optics*, **18**, 100767 (2024).

ELECTRICAL AND DIELECTRIC PROPERTIES OF BARIUM VANADATE GLASSES WITH ZnO, TiO₂ AND NiO

Ondrej Bošák¹, Marian Kubliha¹, Tina Tasheva², Petr Kostka³, Stanislav Minárik¹

¹ Faculty of Materials Science and Technology, Slovak University of Technology, Böttova 25, 917 24 Trnava, Slovakia.

² University of Chemical Technology and Metallurgy Faculty of Metallurgy and Materials Science, Department of Silicate Technologies, 8 Kliment Ohridski blvd, Sofia 1797, Bulgaria

³ Laboratory of Inorganic Materials, joint workplace of the University of Chemistry and Technology Prague and the Institute of Rock Structure and Mechanics of the CAS, V Holešovičkách 41, 182 09 Prague 8, Czech Republic

Oxide glasses containing transition metal ions, such as vanadium ions show a semiconducting behavior. Small polaron hopping is probably mechanism of electrical conduction in such semiconducting glasses due to the highly polar nature of the structure. In combination with others oxides the significant changes in structure and properties of glasses can be obtained.

Influence of ZnO, TiO₂ and NiO content in glassy system $x\text{ZnO}/\text{TiO}_2/\text{NiO}-(35-x)\text{BaO}-65\text{V}_2\text{O}_5$ on DC and AC conductivity, static permittivity, dielectric relaxation is presented and discussed. DC conductivity values at constant temperature changes by 3 orders of magnitude depending on concentration ($x = 1, 5, 10, 15$). Temperature dependencies of conductivity in temperature range from 20 to 240 °C show difference between the first and second heating cycle. Activation energy changes depend on concentration as well as on temperature ranges used. In high temperature range activation energy is significantly higher. The AC conductivity in frequency ranges (0.1-10⁵ Hz) show low dependency determined values on frequency change.

This work was supported by the Slovak Research and Development Agency under the contract No. APVV-22-0146 and APVV SK-BG-23-0014 and Bulgarian National Science Fund under the contract No KP-06-Slovakia/1.

Keywords: oxide glasses, electrical conductivity, permittivity.

CORRECTION FACTOR FOR FOUR-PROBE ELECTRICAL MEASUREMENT: CASE OF MULTI-LAYER DIELECTRIC STRUCTURES

Marian Kubliha¹, Ondrej Bošák¹, Vladimír Labaš¹, Tina Tasheva², Stanislav Minárik¹

¹ Faculty of Materials Science and Technology, Slovak University of Technology, Böttova 25, 917 24 Trnava, Slovakia.

² University of Chemical Technology and Metallurgy Faculty of Metallurgy and Materials Science, Department of Silicate Technologies, 8 Kliment Ohridski blvd, Sofia 1797, Bulgaria

The study of electrical properties of layered structures lies at the heart of physics of advanced materials. Moreover this study is a prerequisite for development of a wide range of modern technologies. Four-point probe technique is widely used in the semiconductor industry to monitor the production process. Electrical measurements are done on test structures to provide information on the various process steps. As time goes on, structures become more complex and standard procedures for applying this technique needs to be improved.

The application of the four-point probe technique for measuring the electrical properties of two-layer structures is commonly used in various fields of science and technology. In our work we have modified a classic four-point method evaluation procedure to measure multilayered structures. Numerical quantification of multiple effects of the image charges was used for the determination of electrostatic potential within layers regions. Subsequently the conductivity correction factor for four-point experiment to measure complex multilayered structures was evaluated.

This work was supported by the Slovak Research and Development Agency under the contract No. APVV-22-0146 and APVV SK-BG-23-0014 and Bulgarian National Science Fund under the contract No KP-06-Slovakia/1.

Keywords: electrical conductivity, method of images, four-point probe technique, conductivity correction factor

THE COLD ATMOSPHERIC PLASMA: A CROSS-APPROACH TO SOIL HEALTH MANAGEMENT

Adriana-Florica Bogosel¹, Mihail Lungu¹ and Antoanetta Lungu²

¹*Faculty of Physics, West University of Timisoara, Blvd. V. Parvan 4, 300223 Timisoara, Romania*

²*Technical College "E. Ungureanu", P-ta Iancu Huniade 3 Timisoara, Romania*

Cold atmospheric plasma reactors with dielectric barrier discharge offer a farmer-centric solution for sustainable soil health management. By utilizing ionized gases such as nitrogen or air, the cold atmospheric plasma enhances seed germination, strengthens plant resilience, and increases crop productivity while reducing dependence on chemical fertilizers and pesticides. This approach aligns with land and natural resource policies and directives, reinforcing global sustainability goals and supporting regulatory frameworks such as those set by the Environmental Protection Agency. Thus, the non-thermal technology not only improves plant health and yield but also mitigates soil degradation, reduces agricultural pollution, and promotes biodiversity conservation. Additionally, it addresses key challenges such as climate change, resource depletion, and the need for sustainable food production systems. By integrating the cold atmospheric plasma into agricultural practices, farmers can achieve higher efficiency while ensuring long-term ecological balance. As global agriculture faces increasing environmental and food security challenges, the cold atmospheric plasma emerges as a scalable and eco-friendly solution that bridges innovation with sustainability.

Keywords: cold atmospheric plasma, dielectric barrier discharge, fertilizers, soil

References:

- [1] Desai, M., Chandel, A., Chauhan, O. P., & Semwal, A. D. (2024). Uses and future prospects of cold plasma in agriculture. *Food and Humanity*, 2, 100262. <https://doi.org/10.1016/j.foohum.2024.100262>
- [2] Hatzisymeon, M., Tataraki, D., Tsakiroglou, C., Rassias, G., & Aggelopoulos, C. A. (2021). Highly energy-efficient degradation of antibiotics in soil: Extensive cold plasma discharges generation in soil pores driven by high voltage nanopulses. *Science of the Total Environment*, 786, 147420. <https://doi.org/10.1016/j.scitotenv.2021.147420>
- [3] Matra, K., Tanakaran, Y., Sangwang, W., Promping, J., & Theepharaksapan, S. (2023). Plasma activated soil: A novel technique for agricultural soil enhancement. *Engineering Journal*, 27(3), 1-10. <https://doi.org/10.4186/ej.2023.27.3.1>

THE WATER-SPLITTING ELECTROCATALYTIC ACTIVITY OF ELECTRODES MODIFIED WITH A MIXTURE OF Co-DOPED PEROVSKITE AND A SYMMETRICALLY SUBSTITUTED FREE-BASE PORPHYRIN

Bogdan-Ovidiu Taranu, Paula Sfirloaga and Marina Alexandra Tudoran

National Institute of Research and Development for Electrochemistry and Condensed Matter, Dr. A.P. Podeanu Street, No. 144, 300569, Timisoara, Romania, e-mail: b.taranu84@gmail.com

Global warming and the global energy crisis are two of the major problems humanity is currently facing [1,2]. The efforts of the scientific community aimed at addressing these issues have revealed hydrogen as a promising renewable energy carrier of the future, with the potential to replace the environmentally unfriendly reliance on rapidly depleting fossil fuel reserves [3]. Hydrogen has high energy density, low emissions, and the potential to decarbonize various industrial departments [4]. Green hydrogen generated *via* electrochemical water-splitting, also known as water electrolysis, using renewable electricity, is one of the most auspicious ways to achieve net-zero carbon emissions [5]. Given this background, the present work contributes to the ongoing efforts of identifying highly active, durable, and low-cost electrocatalysts for efficient hydrogen production by water electrolysis. It reports the study of the water-splitting electrocatalytic activity of glassy carbon electrodes modified by drop-casting on their surface catalyst inks containing Co-doped YMnO_3 mixed with different amounts of the symmetrically substituted A_4 free-base 5,10,15,20-tetrakis(3-hydroxyphenyl)-porphyrin dissolved in tetrahydrofuran. The experiments were carried out in 0.1 M H_2SO_4 electrolyte solution, and the results show that the highest catalytic activity is exhibited during the hydrogen evolution reaction (HER) investigations by the electrode modified with 10 μL of the catalyst ink containing 5 mg Co-doped YMnO_3 in 450 μL of 5 mM porphyrin solution (Figure 1). The HER overpotential is 0.87 V at the current density of -10 mA/cm^2 . The Tafel slope is 0.135 V/dec, and in terms of electrochemical stability, the recorded chronoamperogram outlines the fair stability of the sample despite the intense hydrogen bubbling.

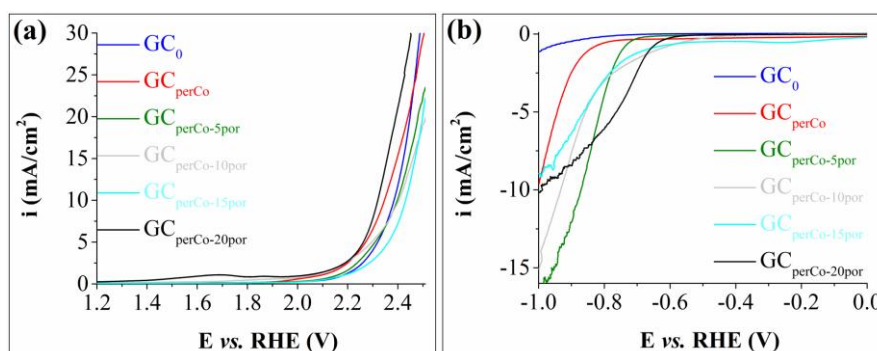


Figure 1: (a) Anodic and (b) cathodic polarization curves recorded on the studied electrodes, in 0.1 M H_2SO_4 solution and at the scan rate of 5 mV/s.

Keywords: water electrolysis, perovskite, porphyrin.

References:

- [1] R. M. Santos, R. Bakhshoodeh, *Heliyon* **7**, 1-15 (2021).
- [2] A. Jilani, H. Ibrahim, *Energies* **18**, 1-29 (2025).
- [3] Q. Hassan, S. Algburi, A. Z. Sameen, H. M. Salman, M. Jaszczur, *Int. J. Hydrogen Energy* **50**, 310-333 (2024).
- [4] L. Zhang, C. Jia, F. Bai, W. Wang, S. An, K. Zhao, Z. Li, J. Li, H. Sun, *Fuel* **335**, 1-24 (2024).
- [5] S. Wang, A. Lu, C.-J. Zhong, *Nano Converg.* **8**, 1-23 (2021).

API-P28

SINGLE CRYSTALS FOR MAGNETO-OPTICAL APPLICATIONS IN UV-VIS-NIR

Kesavan Venkatachalam¹, Maximilian Mangra¹, Gabriel Buse², Daniel Vizman¹, Philippe Veber^{1,2} and Matias Velazquez³

¹Faculty of Physics, Crystal growth laboratory, West University of Timisoara (Romania)

²Institute for Advanced Environmental Research (ICAM), West University of Timisoara (Romania)

³Univ. Grenoble Alpes, CNRS, Grenoble INP, SIMAP, 38000, Grenoble (France)

The Faraday effect in a material describes the interaction between a linearly polarized laser wave and a static magnetic induction oriented parallel to the direction of propagation of the light wave [1]. The polarization of the light undergoes a rotation that is proportional to the applied magnetic induction, the distance travelled within the material and the Verdet constant of the material. This magneto-optical phenomenon is used in particular in optical isolators, especially for frequency-stabilized lasers and high-power sources, to prevent any back-reflected light into the cavity that could destabilize or damage the device. Accordingly, magneto-optical materials are key components in optical isolators using the Faraday rotation and they are of paramount importance for high-power solid-state laser applications [2,3]. In particular, terbium-based single crystals exhibit several advantages such as a wide optical transparency range, low optical absorption, high thermal stability, strong Faraday effect, magnetic field sensing capability, and a high signal-to-noise ratio. Besides, they operate in the ultraviolet (UV), visible (VIS) and near infrared (NIR) optical range.

This work deals with the crystal growth and the magneto-optical properties of particularly efficient crystals, Tb₃Ga₅O₁₂ (TGG), KTb₃F₁₀ (KTF) and Tb₂O₃ (Figure 1) in these spectral regions, as well as their use in experimental setups for designing adaptable optical isolators.

The authors acknowledge the financial support from the PNRR-III-C9-2022-I8 grant “Enhanced single crystal Applications and Research in the growth of new optical rare earth-based compounds for sustainable and efficient Technologies (ESCARGOT)” (n°: 760080/23.05.2023), for the development of this research field.

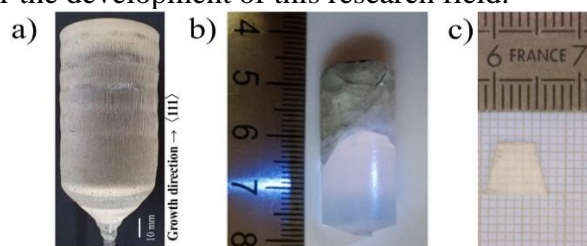


Figure 1. Example of magneto-optical single crystals (a) TGG [4], (b) KTF [5] and (c) Tb₂O₃[6]

Keywords: magneto-optics, crystal growth, Faraday rotator, optical isolator

References:

- [1] V. I. Belotelov *et al.*, *Opt Mater Express*, **12**(5), 2087-2089 (2022)
- [2] P. Veber *et al.*, *Opt Mater (Amst)*, **157**, 116264 (2024)
- [3] I. Snetkov *et al.*, *Magnetochemistry*, **8**(12), 168 (2022)
- [4] M. Watanabe *et al.*, *J Cryst Growth*, **634**, 127687 (2024)
- [5] D. N. Karimov *et al.*, *Crystals (Basel)*, **11**, 285 (2021)
- [6] P. Veber *et al.*, *CrystEngComm*, **17**(3), 492–497 (2015)

EDUCATIONAL PHYSICS (EP)

**INTEGRATING AI-GENERATED ASSESSMENTS IN SCIENCE
COMPETITIONS: A CASE STUDY**

Izabella J. Benczik¹ and Emese Hanolné Toldy²

¹*Eszterházy Károly Catholic University, 3300 Eger, Eszterházy tér 1, Hungary*

²*Deák Ferenc Secondary School, 7030 Paks, Tolnai út 19, Hungary*

Although artificial intelligence (AI) has been widely applied in physics education, its potential in test creation is still relatively underexplored and underrepresented in empirical studies [1,2]. This paper investigates the use of AI-generated multiple-choice questions (MCQs) as formative assessment tools during a national physics and astronomy competition in Hungary (2024/25), organized by the Astronomy Tower of Eszterházy Catholic University Eger. Participants were given 65 mandatory, human-authored MCQs and 168 optional, AI-generated questions, both based on a common written curriculum. The AI-generated questions provided instant feedback and allowed unlimited practice attempts. We compared the outcomes of students who engaged with AI-generated questions (n = 71) to those who used only human-authored content (n = 417), and observed moderate improvements in performance. Our findings suggest that AI tools can effectively support self-paced learning and offer time-efficient assessment solutions, especially benefiting lower-performing students, although human oversight remains essential for content quality.

Keywords: AI-generated tests, formative assessment,

References:

- [1] Q. Xia et al., *Int. J. Educ. Technol. High. Educ.* **21**, 40 (2024).
- [2] T. A. May et al., *Educ. Sci.* **15**, 144 (2025).

EP-O02

THE PLANETARIUM OF THE PHYSICS DEPARTMENT OF THE WEST UNIVERSITY OF TIMIȘOARA

Secoșan Florin

West University of Timișoara, Physics Department

The Planetarium of the West University of Timișoara has been built in 1964 and equipped with a ZKP-1 Zeiss projector. In 2022 the Physics Department took it under its supervision and refurbished it. Soon after a Barco digital projector has been also purchased and it is now being operated by SureyyaSoft, a known Planetarium software. The two projectors are used alternatively providing an excellent educational environment for both High School students and University students. **The proposed poster** underlines the most relevant activities which are the free-of-charge visits for all students, regardless of their specializations, and the free-of-charge classes of Astronomy and Astrophysics offered to all passionate students, regardless of their age, for which the Planetarium serves as a laboratory. In the last 3 years the Planetarium turned out to be a very efficient tool for **educational Physics**.

At the same time the poster encloses information about the **National Master's Degree Program in High-Energy Physics**, involving 4 Universities, University of Bucharest, "Babeș-Bolyai" University of Cluj-Napoca, "Alexandru Ioan Cuza" University of Iași and West University of Timișoara.

The connection between the two themes of this poster consists of the following fundamental questions: **"What is the matter made of at its most fundamental level? What forces shaped the Universe?"**

Keywords: Planetarium, Astronomy, Astrophysics, Educational Physics, Olympiads, High-Energy Physics Master, Fundamental questions, Universe.

EP-O03

HIGH-ENERGY PHYSICS - NATIONAL MASTER PROGRAMME

Călin Alexa^{1,2}, Paul Grăvilă³, Lázár Zsolt Iosif⁴, Daniel Radu⁵, and Roxana Zus^{1*}

¹*Faculty of Physics, University of Bucharest*

²*Particle Phys. Dept., IFIN-HH*

³*Faculty of Physics, West University of Timișoara*

⁴*Faculty of Physics, Babes-Bolyai University*

⁵*Faculty of Physics, „Alexandru Ioan Cuza” University of Iași*

*email: roxana.zus@fizica.unibuc.ro

The High-Energy Physics (HEP) master programme is a joint initiative of four physics faculties in Romania (University of Bucharest, Babes-Bolyai University, „Alexandru Ioan Cuza” University of Iași and West University of Timișoara) partnering with research groups from national R&D institutes (e.g. IFIN-HH, INCDTIM Cluj-Napoca) involved in experiments at CERN. The aim of the programme is to provide students with a strong foundation in theoretical and experimental high-energy particle physics, a field dedicated to understanding the fundamental particles and forces that govern the universe. At the heart of this global effort stands CERN, the European Organization for Nuclear Research – home to the Large Hadron Collider (LHC) and to some of the most ambitious scientific experiments in history.

The joint initiative aims to increase the number of young researchers in HEP for each university center and stimulate collaboration. Students will be involved in scientific research by participating in the realization of R&D projects and will prepare the dissertation with a specific HEP research topic, working together with scientists involved in CERN experiments.

Along with the curriculum, the structure of mobility and each partners' contribution, we present the steps and challenges in accrediting a joint national programme.

Keywords: national master programme, high-energy physics

EP-O04

SCIRESCAREER: FROM PUPILS, TO STUDENTS AND PHYSICS RESEARCHERS

Virgil Băran¹, Marius L. Matache¹, Codruța C. Popescu¹, Andreea Popescu-Cruglic (Ghinescu)¹, Roxana Zus¹

¹*SciResCareer Centre, University of Bucharest*

Research is the basis of a field's evolution and prosperity, being an essential part of our society's wellbeing itself. SciResCareer – “Regional Centre in Orientation and Counseling for Research Careers - Bucharest-Ilfov” is an organizational structure of University of Bucharest that aims to serve the entire scientific community of Bucharest and Ilfov County. The Center's aim is to help develop interest in research careers (for pupils, students), hone new skills relevant in research careers (both young and senior researchers), provide mentorship and vocational counseling, practice or job opportunities and facilitate networking inside and outside researchers' communities, both nationally and internationally.

Even though, naturally, SciResCareer addresses and supports all research domains, this presentation will highlight the benefits and services offered to physics researchers or potential researchers, spanning from outreach activities to advanced academic and research services. We have developed and adapted a multitude of activities and opportunities, tailored for each target group depending on age, interests and career level. We have brought together pupils, students and researchers, addressing a variety of modern topics, from macrocosmos, gravitation and cosmology, towards the microscale, to quantum physics and information, and even further, to the cutting-edge experiments probing and searching fundamental constituents of matter.

Acknowledgements: The SciResCareer project is funded under PNRR/C9/ Investment "I10 – Establishment and Financial Support of a National Network of Eight Regional Career Guidance Centers as Part of the ERA TALENT PLATFORM".

Keywords: SciResCareer, research, career, students.

References:

[1] <https://scirescareer.unibuc.ro/>

EP-O05

**STUDENTS' MOTIVATION AND THEIR MISCONCEPTIONS IN
STUDYING QUANTUM MECHANICS**

Andreea Popescu-Cruglic (Ghinescu)¹, Virgil Băran¹, Andreea-Mihaela Croitoru¹, Roxana
Zus¹

¹Faculty of Physics, University of Bucharest (405 Atomîștilor POB MG-11 RO-077125 Măgurele, România)

In this study we aim to explore possible correlations between several variables effecting students' motivation in studying Quantum Mechanics (QM). Moreover, we investigate the most common misconceptions students have before undertaking the bachelors' QM lecture and how they might change after undertaking the lecture.

Our study is based on an initial three-part questionnaire and a final two-part one, the first one assessing students' motivation and interest, QM intuition and background knowledge in other relevant disciplines. The second questionnaire assesses their acquired knowledge, partly addressing the same questions from questionnaire one, with the aim of understanding if and how the initial misconceptions might be resolved.

This contribution shows the results obtained from 141 responses for the initial questionnaire and 53 for the final one, collected over a period of 4 academic years (2022-2025).

Keywords: quantum mechanics, teaching, learning, misconceptions.

EP-P01

MODELING OF EXPERIMENTS AND PHYSICAL PHENOMENA STUDIED IN HIGH SCHOOL USING DIFFERENT SOFTWARE

Antoanetta Corina Lungu¹, Mihail Lungu² and Adriana-Florica Bogosel²

¹Technical College "E. Ungureanu", P-ta Iancu Huniade 3 Timisoara, Romania

²Faculty of Physics, West University of Timisoara, Blvd. V. Parvan 4, 300223 Timisoara, Romania

In teaching and learning Physics, teachers and students benefit from the existence of tools and software products that support the teaching approach, develop students' knowledge and skills around science and the digital world. Interactive physics lessons with the help of the computer present a potential that has not yet been exhausted.

Computer-assisted instruction represents, from a pedagogical point of view, a way of organizing the instructional-educational process. It is a particularly complex activity, integrating, in addition to human resources (teachers and students) and material resources (the presence of a computer and other information and communication technologies), the latter, most often minimizing the role of the human ones, namely the teacher, who becomes a moderator, a guide and an observer of the activity carried out. There are numerous applications that support the simulation and understanding of physical events, thus complementing the classical methods of laboratory experimentation. The present paper presents computer-assisted training systems, interactive with the user, attractive, which should provide support both for the teaching stage and for the assimilation and evaluation of the results of the educational process.

Keywords: assisted training, software,

References:

- [1]Anderson, J., Li, Y. Investigating the potential of integrated STEM education from an international perspective. *Integrated Approaches to STEM Education*. Springer, 1-12, 2020.
- [2]Struyf, A., De Loof, H., Boeve-de Pauw, J., Van Petegem, P., Students' engagement in different STEM learning environments: integrated STEM education as promising practice? *International Journal of Science Education*, **41**(10), 1387-1407, 2019.
- [3]Rohman, F., Fauzan, A., *Integration of technology in project based learning with tracker on practicum activities*. IOP Publishing, Journal of Physics: Conference Series, **1185**(1), 012036, 2019.

List of participants

Gheorghe Adam
Sanda Adam
Călin Alexa
Victor E Ambruş
Radu Andrei
Eugen Anitas
Željka Antić
N.M. Avram
Ionel Balcu
Stefan Balint
Aritra Bandyopadhyay
Radu Bănică
Mihai – Stefan Barhala
Virgil Băran
M.C. Belc
Alexandru Belenchuk
Izabella J. Benczik
Ioan Bica
Maria Bischin
Elena Bogdan
Adriana-Florica Bogosel
Ondrej Bošák
Dragos Bordescu
Oana Brâncoveanu
Mikhail G. Brik
R. Bucur
Andru Mihai Buga
Madalin Bunoiu
Gabriel Buşe
Sergiu Busuioc
M. Buryi
Cristian Casut
Adina Căta
Emil Cazacu
Debkumar Chakraborty
Maxim N Chernodub
Andrei Chesnokov
Vasile Chiş
Liviu Chirigiu

Jordan Ciucea
Alexandr Cliucanov
Andrea-Florina Codrean
Andreea V. Cojocaru
Denisa Colţuneac
Valentin Craciun
Andreea-Mihaela Croitoru
Cosmin Crucean
Alexandr S. Cudreaşov
Ioan Dancus
D. D. Darie
Anil Dhanda
G. Dima
Raluca Dinescu
E. Dinkov
Constantin Diplăşu
Alexandru Florin Dobrin
Andrei Dogaru
Miroslav D. Dramićanin
Ionut Dumitru
Narcis Duteanu
G. Dyankov
T. Eftimov
Geoşchun Ferat
Amalia Dariana Fodor
Monica Focşan
S. Fouzar
Grégory Gadret
Petronela Garoi
Aleksandar Gecić
Ioana Cristina Gerber
Makarand Ghangrekar
Gheorghe Ghileţchii
Petar Gladkov
Paul-Adrian Gogîţă
Anamaria-Giulia Goilean
Paul Grăvilă
Sebastian Grieninger
J. Grym

Yannick Guyot
Emese Hanolné Toldy
Sergiu-Mihai Hategan
Ioana M.C. Ienașcu
Tiana Ile
Cristian Ionescu
Mirela I. Iorga
Lázár Zsolt Iosif
Ștefan-Andrei Irimiciuc
M-G. Ivanovici
Gorakhanath Jadhav
Adam Zenon Kaczmarek
O. Y. Khyzhun
Emeric C.C. Kiss
Tomoki Koikawa
Petr Kostka
Péter Kovács
K. Krizmane
Marian Kubliha
Victor Kuncser
Moulindu Kundu
Vladimír Labaš
Sorina M.D.Laitin,
Antonina Lazăr
Antoanetta Lungu
Mihail Lungu
Corina Macarie
Mihai A. Macovei
Gabriel Majeri
Iosif Mălăescu
Maximilian Mangra
Mihai-Petru Marghitas
Cătălin Nicolae Marin
Alina Matei
Marius L. Matache
Marinela Miclău
Ilarion Mihaila
Iuliana Mihalache
Stanislav Minárik
Maria Luiza Mitu
Cătălin Pașcu Moca
Antoniou Moldovan

Richard Moncorgé
Cristina Moșoarcă
Igor Narolschi
Alexandru Nicolin-Žaczek
Valentin I. Niculescu
G.K. Nikolov
K. Nikolov
Mihai Oane
Cristina Pachiu
Oleg Palamarciuc
Vladimir Pankratov
Beatrice Paraschiv
Gabriel Pascu
Eugenia Paulescu
Marius Paulescu
Michal Piasecki
Abhishek Pitta
Alexander Platonenko
Valentin Pohoata
Maria Poienar
Mihaela Popa
Andreea Popescu-Cruglic (Ghinescu)
Alexandra Popescu
Codruța C. Popescu
Ovidiu Postelnicu
João P. Prates Ramalho
Olga Prochazkova
A. V. Racu
Diana R. Radnef-Constantin
Daniel Radu
Mircea Radulian
Mihaela-Carina Raportaru
Adina Rău
Pau G. Romeu
Cosmin Romanișan
Arthur Rotari
Andreea Sabadus
Carla Schornig
Adrian Scurtu
Ioana Andreea Scutelnicu
Florin Secoșan
Paula Sfirloaga

Oleg Shapoval
Yuiko Shimazaki
Viviana Sîrbu
Pracheta Singha
Victor Sofonea
Andrei Stan
I.M. Stanescu
Marius Ștef
Stefania Stepanov
Doru Sticlet
Laurențiu Stoleriu
Andrzej Suchocki
Dominik Szcześniak
Isao Tanaka
Adriana Tanasie
Bogdan-Ovidiu Taranu
Tina Tasheva
Dragos Tatomirescu
Vasilica Țucureanu
Nick S. Țolea
Cristian Mihail Teodorescu
Sergio Morales Tejera
Stanislav Tiagulskyi
Cătălin M. Ticoș
Dorina Ticoș
Coriolan V. Tiusan
Ionut Topala
Marina Alexandra Tudoran
Zafari Umar
Nicoleta Udrea
Daniel Ursu
Melinda Vajda
Alexandru Varzari
Elmira Vatavu
Sergiu Vatavu
Philippe Veber
Matias Velazquez
Kesavan Venkatachalam
Daniel Vizman
V. Vitola
J. Williams
Tomoyuki Yamamoto

Roman Yatskiv
Jiri Zavadil
Adam Zenon Kaczmarek
Yaroslav Zhydachevskyy
Roxana Zus